

Some pages of this thesis may have been removed for copyright restrictions.

If you have discovered material in AURA which is unlawful e.g. breaches copyright, (either yours or that of a third party) or any other law, including but not limited to those relating to patent, trademark, confidentiality, data protection, obscenity, defamation, libel, then please read our [Takedown Policy](#) and [contact the service](#) immediately

EFFECT OF DISABILITY GLARE ON VISUAL PERFORMANCE

RICHARD PATRICK TERENCE STEEN

Doctor of Philosophy

THE UNIVERSITY OF ASTON IN BIRMINGHAM

SEPTEMBER 1995

This copy of the thesis has been supplied on the condition that anyone who consults it is understood to recognise that its copyright rests with the author and that no quotation from the thesis and no information derived from it may be published without proper acknowledgement.

The University of Aston in Birmingham

EFFECT OF DISABILITY GLARE ON VISUAL PERFORMANCE

RICHARD PATRICK TERENCE STEEN

Doctor of Philosophy

1995

The object of the study was to investigate, establish and quantify the relationship between contrast sensitivity, intraocular light scatter and glare. The aim was to establish the effects on vision, in an effort to provide a more comprehensive understanding of the visual world of subjects prone to increased light scatter in the eye. Disability glare refers to the reduction in visual performance produced by a glare source. The reduction in visual performance can be explained by intraocular scattered light producing a veiling luminance which is superimposed upon the retinal image. This veiling luminance lowers contrast thus sensitivity to the stimulus declines.

The effect of glare on luminance and colour contrast sensitivity for young and elderly subjects was examined. For both age groups, disability glare was greatest for the red-green stimulus and least for the blue-yellow. The precise effect of a glare source on colour discrimination depends upon the interaction between the chromaticity of the glare source and that of the stimulus. The effect of a long wavelength pass (red) and a short wavelength pass filter (blue) on disability glare was examined. Disability glare was not significantly different with the red and blue filters, even in the presence of wavelength dependent scatter.

An equation was derived which allowed an intrinsic Light Scatter Factor (LSF) to be determined for any given glare angle (Paulsson and Sjostrand, 1980). Corrections to the formula to account for factors such as pupil size changes are unnecessary. The results confirm the suitability of measuring the LSF using contrast threshold with and without glare, provided that appropriate methods are used. Using this formula, an investigation into the amount of wavelength dependent scatter indicated that wavelength dependent scatter in normal young, elderly or cataractous eyes is of little or no significance.

Finally, it seemed desirable to investigate the effect ultraviolet (UV) radiation has on intraocular light scatter and subsequently visual performance. Overall the results indicated that the presence or absence of UV radiation has relatively little effect on visual function for the young, elderly or cataract patient.

DEDICATION

I would like to dedicate this thesis to my parents and to my fiancée Joanne Greatrex.

ACKNOWLEDGEMENTS

I thank my supervisors, Dr D. Whitaker and Dr J.M. Wild, for their guidance, encouragement and help.

I would also thank Dr J Archer-Hall for his help in providing the equipment used to measure the angular dependency of the scattered light produced by the solution of microspheres. I am grateful to all the patients and subjects who participated in the clinical studies and to the Department of Vision Sciences, Aston University, for access to its facilities.

	Page
Summary	2
Dedication	3
Acknowledgements	4
List of contents	5
List of figures	8
List of tables	13

LIST OF CONTENTS

CHAPTER 1. <u>Intraocular light scatter and glare</u>	15
1.A. Introduction	15
1.B. Sources of intraocular light scatter	16
1.B.1 Cornea	16
1.B.2 Measures of corneal intraocular light scatter	19
1.B.3 Effect of age on the cornea	21
1.B.4 Effect of oedema on the cornea	22
1.B.5 Crystalline lens	25
1.B.6 Measures of crystalline lens back-scatter	28
1.B.7 Measures of crystalline lens forward-scatter	29
1.B.8 Cataractogenesis	30
1.C. Lens fluorescence and aging	31
1.D. Theory of light scattering and transparency	37
CHAPTER 2. <u>Contrast Sensitivity</u>	44
2.A. Basic concepts of contrast sensitivity	44
2.A.1 Introduction	44
2.A.2 Psychophysical aspects of the contrast sensitivity function (CSF)	45
2.A.3 The peak of the CSF curve	46

2.A.4	High spatial frequency attenuation	47
2.A.5	Low spatial frequency attenuation	52
2.B.	Spatial frequency channels	52
2.C.	Methodology of threshold measurement	55
2.C.1	Threshold	55
2.C.2	Stimulus variables	60

CHAPTER 3. Direct and indirect measurements of intraocular

	<u>light scatter</u>	61
3.A.	Indirect method (Equivalent veiling method)	61
3.A.1	Introduction	61
3.A.2	Contrast sensitivity testing and glare testing	67
3.A.3	Cataract	70
3.A.4	Pseudophakia	72
3.B.	Direct method (Direct compensation method)	75

CHAPTER 4. Effect of glare on luminance and colour contrast

	<u>sensitivity</u>	82
4.A.	Introduction	82
4.B.	Effect of varying levels of induced intraocular light scatter on luminance contrast sensitivity at various spatial frequencies	83
4.C.	Effect of induced intraocular light scatter upon luminance contrast sensitivity compared with colour contrast sensitivity	93
4.D.	Effect of glare upon luminance contrast sensitivity and colour contrast sensitivity as a function of age	101

CHAPTER 5.	<u>Effect of filters on disability glare</u>	115
5.A.	Introduction	115
5.B.	Methods	117
5.C.	Results	127
5.D.	Discussion	135
CHAPTER 6.	<u>Confirmation of the psychophysical light scatter factor</u>	139
6.A.	Introduction	139
6.B.	Measurement of the psychophysical light scatter factor	140
6.B.1	Methods	140
6.B.2	Results	143
6.B.3	Discussion	149
6.C.	Comparison between direct stray light measures and the psychophysical light scatter factor	157
6.C.1	Introduction	157
6.C.2	Methods	157
6.C.3	Results	158
6.C.4	Discussion	159
CHAPTER 7.	<u>Measurement of the wavelength dependency of light scatter in the normal, elderly and cataractous eye</u>	161
7.A.	Introduction	161
7.B.	Methods	163
7.C.	Results	166
7.D.	Discussion	177
CHAPTER 8.	<u>Effect of ultraviolet absorbing filters on outdoor visual performance</u>	181
8.A.	Introduction	181

8.B.	Methods	182
8.C.	Results	186
8.D.	Discussion	193
CHAPTER 9. <u>Summary of results, conclusions and future work</u>		196
9.A.	Summary of results and conclusion	196
9.A.1	Luminance and colour contrast sensitivity	196
9.A.2	Effect of filters on glare	197
9.A.3	Light scatter factor	197
9.A.4	Wavelength dependency of intraocular light scatter	198
9.A.5	UV radiation	198
9.B.	Future work	199
9.B.1	Colour contrast sensitivity	199
9.B.2	Intraocular light scatter	200
9.B.3	Autofluorescence	200
REFERENCES		201
APPENDICES		
1.A.	Supporting publications	226-252

LIST OF FIGURES

Figure 1.1	Schematic diagram of corneal epithelial cells	24
Figure 1.2	Fluorescence spectra of a human lens	33
Figure 1.3	UV and visible light transmission of normal lenses as a function of age	36
Figure 2.1	The contrast sensitivity function plotted on a log/linear scale	47
Figure 2.2	The contrast sensitivity function plotted on a log/log scale	48
Figure 2.3	Contrast sensitivity as a function of retinal frequency and eccentricity	49
Figure 2.4	Threshold modulation as a function of retinal illuminance	51
Figure 2.5	Contrast sensitivity function for different temporal frequencies	53
Figure 2.6	Contrast threshold detection	56
Figure 2.7	Two-alternative, forced-choice method	57
Figure 2.8	Stimulus detection using the staircase method	59
Figure 3.1	Schematic diagram of the equivalent veil technique	63
Figure 3.2	Equivalent veiling luminance plotted against glare intensity for different glare angles	64
Figure 3.3	Glare function is plotted against glare angle	66
Figure 3.4	Spatial contrast sensitivity function	69
Figure 3.5	Stray light measurement as a function of age	79
Figure 3.6	Stray light measurement for cortical and nuclear cataract	80
Figure 4.1	Venus Visual Stimulator	84
Figure 4.2	Brightness Acuity Tester (BAT)	87

Figure 4.3	Wavelength dependency of scattered light from 500nm microspheres	89
Figure 4.4	Contrast sensitivity in the no-glare and low luminance glare conditions for different amounts of induced light scatter	90
Figure 4.5	Contrast sensitivity in the medium luminance glare and high luminance glare conditions for different amounts of induced light scatter	91
Figure 4.6	Diagram of the method used to calculate the isoluminant points	96
Figure 4.7	Bar charts of sensitivity to red-green and yellow-black gratings with and without induced light scatter	99
Figure 4.8	Bar charts of red-green, blue-yellow and luminance sensitivity	108
Figure 4.9	Bar charts of disability glare for red-green, blue-yellow and luminance stimuli	110
Figure 5.1	Schematic diagram of the equipment used to analyse the spectral characteristics of the scattered light produced by microspheres	119
Figure 5.2	Wavelength dependency of scattered light from 300nm microspheres	121
Figure 5.3	Wavelength dependency of scattered light from 750nm microspheres	122
Figure 5.4	Spectral distribution of scattered light from 300nm, 500nm and 750nm microspheres	124
Figure 5.5	Spectral transmission of the short pass filter and the long pass filter	125

Figure 5.6	Relative luminous efficiency of the glare source, alone, and combined with the short pass filter and the long pass filter	126
Figure 5.7	Disability glare plotted against the concentration of 300nm sized microspheres with no filter, the blue filter and the red filter (Observer RS)	128
Figure 5.8	Disability glare plotted against the concentration of 500nm sized microspheres with no filter, the blue filter and the red filter (Observer RS)	129
Figure 5.9	Disability glare plotted against the concentration of 750nm sized microspheres with no filter, the blue filter and the red filter (Observer RS)	130
Figure 5.10	Disability glare plotted against the concentration of 500nm sized microspheres with no filter, the blue filter and the red filter (Observer SR)	131
Figure 5.11	Disability glare plotted against the concentration of 500nm sized microspheres with no filter, the blue filter and the red filter (Observer SR)	132
Figure 5.12	Disability glare plotted against the concentration of 750nm sized microspheres with no filter, the blue filter and the red filter (Observer SR)	133
Figure 6.1	Venus Visual Stimulator and a tungsten-halogen bulb glare source	142
Figure 6.2	Contrast thresholds of observer DW as a function of ocular illuminance produced by the glare source	144
Figure 6.3	Contrast thresholds of observer RS as a function of ocular illuminance produced by the glare source	145
Figure 6.4	Contrast thresholds of observer IM as a function of ocular illuminance produced by the glare source	146

Figure 6.5	The ratio of contrast thresholds with and without glare against E/L (Observer DW)	150
Figure 6.6	The ratio of contrast thresholds with and without glare against E/L (Observer RS)	151
Figure 6.7	The ratio of contrast thresholds with and without glare against E/L (Observer IM)	152
Figure 6.8	Stray light estimated from disability glare measurements plotted against direct stray light measurements	159
Figure 7.1	LSF plotted against wavelength for different glare angles (Observer DW)	167
Figure 7.2	LSF plotted against wavelength for different glare angles (Observer RS)	168
Figure 7.3	Stray light values as a function glare angle	169
Figure 7.4	Stray light values for young and older subjects plotted as a function glare angle	171
Figure 7.5	Stray light values for two cataract subjects (AM and WH) as a function glare angle	174
Figure 7.6	Stray light values for two cataract subjects (HP and BJ) as a function glare angle	175
Figure 8.1	Spectral distribution of light emanating from the clear filter and the UV blocking filter	185
Figure 8.2	Bar charts of Log MAR visual acuity for young normals, elderly normals and cataract patients.	187
Figure 8.3	Log MAR visual acuity plotted as a function of age for normal and cataract patients for both filters	190

LIST OF TABLES

Table 4.1	Chromaticity coordinates and colour temperatures of the BAT	86
Table 4.2	Isoluminant ratios of the red-green grating for two observers (DW and RS)	97
Table 4.3	Isoluminant ratios of the red-green and blue-yellow gratings for young and elderly observers	104
Table 4.4	Contrast sensitivity of young and elderly observers to luminance, red-green and blue-yellow gratings	106
Table 4.5	Contrast sensitivity, under glare conditions, of young and elderly observers to luminance, red-green and blue-yellow gratings	107
Table 4.6	Disability glare of the young and elderly subjects to luminance, red-green and blue-yellow gratings	109
Table 6.1	Contrast thresholds for different stimulus luminances and different ocular illuminances produced by the glare source (Observers RS and IM)	147
Table 6.2	Contrast thresholds for different stimulus luminances and different ocular illuminances produced by the glare source (Observer DW)	148
Table 6.3	Ratio of contrast thresholds with and without glare for each stimulus luminance	153
Table 7.1	Age, Log MAR visual acuity, cataract type and iris pigmentation for each cataract subject	164
Table 7.2	Stray light values for the young subjects at different glare angles	172
Table 7.3	Stray light values for the elderly subjects at different glare angles	173

Table 7.4	Stray light values for the cataract subjects at different glare angles	176
Table 8.1	Log MAR visual acuity of normal observers in the presence of the clear filter and the UV absorbing filters (Data collected at Aston University)	188
Table 8.2	Log MAR visual acuity of cataract patients in the presence of the clear filter and the UV absorbing filters (Data collected at Aston University)	189
Table 8.3	Log MAR visual acuity of normal observers in the presence of the clear filter and the UV absorbing filters (Data collected at University of Waterloo)	191
Table 8.4	Log MAR visual acuity of cataract patients in the presence of the clear filter and the UV absorbing filters (Data collected at University of Waterloo)	192

CHAPTER 1 INTRAOCULAR LIGHT SCATTER AND GLARE

1.A. Introduction

One aspect of vision is concerned with discriminating the light intensity of one object as opposed to another i.e., contrast. Contrast can be affected by the refractive error of the eye and by optical aberrations in the eye. Contrast is also affected by glare. Although a scene may be sharply in focus on the retina the presence of an additional light source flooding the retina reduces the apparent contrast of the scene. Disability glare refers to the reduction in visual performance produced by a glare source. The reduction in visual performance can be explained by intraocular scattered light producing a veiling luminance which is superimposed upon the retinal image. According to Weber's law $\Delta L/L = \text{constant}$, which means that the depth of modulation of the stimulus, ΔL , has to be increased in order to retain detection. Hence, contrast sensitivity declines. Holladay (1927) published the first quantitative data on the masking effect of the visible halo around glare sources. This was expressed in terms of an equivalent veiling luminance (L_{eq}), that would produce the same masking effect. Vos and colleagues (Vos, 1962; Vos and Boogard, 1963; Vos et al, 1976) realised that the equivalent veil was a real light veil produced by intraocular light scatter and were able to quantify the equivalent veil effect using glare sources from 1° to 100° from fixation. This was used as the basis for calculation of the Light Scatter Factor (LSF) of Paulsson and Sjöstrand (1980). Studies carried out on theoretical (Hart and Farrell, 1969) and psychophysical grounds (Ben-Sira et al, 1980; Vos, 1962) and with the use of excised eyes (Demott and Boynton, 1958; Boynton and Clark, 1964) can be summarised as follows: Glare is due to light scattering in the eye and unwanted stray light is present in the normal eye. This unwanted stray light interferes with the contrast of the retinal image and increases the background light level. The main sources of light scatter within the normal eye are the cornea and

the crystalline lens and the intensity of stray light decreases with angular separation from the glare source (van den Berg, 1995).

Obviously, any abnormality of the eye e.g. retinal oedema, vitreous floaters, cataracts, aqueous flare and either epithelial or stromal oedema will dramatically increase the amount of light scattered onto the retina, due to changes in the microstructure of the eye, and thereby increase glare susceptibility. Many studies have measured disability glare in the clinical environment in order to aid the clinician in making a more accurate assessment of visual ability following surgery (Nadler et al, 1984; van der Heijde et al, 1985; Goble et al, 1994; Pfoff and Werner, 1994; Claesson et al, 1994) or in the presence of cataract (Hirsch et al, 1984a, Lasa et al, 1993) or as a result of the normal aging process (Le Claire et al, 1982).

It has been shown in early cataract that at medium and high spatial frequencies contrast sensitivity is reduced (Hess and Garner, 1977; Hess and Woo, 1978; Paulsson and Sjöstrand, 1980; Elliott et al, 1989). This reduction in sensitivity reflects the effect of narrow angle light scattering (Hemenger, 1990). Wide angle light scatter can be assessed by measuring contrast sensitivity at low spatial frequencies (Hess and Woo, 1978; Elliott et al, 1991) but is best evaluated by measuring contrast sensitivity in the presence of a peripheral glare source (Elliott et al, 1991; van den Berg, 1992).

1.B. Sources of intraocular light scatter

1.B.1 Cornea

The cells of the corneal epithelium are held together by desmosomes resulting in minimal spacing. There is normally only slight variation in refractive index between and within these cells. As a consequence, the epithelium scatters almost no light and transmits light as would a fluid. Clinically, this can be confirmed by looking at the

epithelial layer with the slit lamp. If a drop of fluorescein is added to the tear film, the optically empty layer between the green appearing tear film and the most anterior portion of the stroma is the epithelium.

The stroma constitutes 90% of the corneal thickness and gives the cornea its strength. It is remarkable for its regular structure and the absence of blood vessels, the two basic features upon which transparency rests. The stroma consists of about 200 lamellae of collagen fibrils ($n=1.555$) embedded in a matrix of mucopolysaccharides ($n=1.345$). The fibril diameters are of a regular size at any depth in the stroma; but they vary between an average of 19nm in the anterior layers and 34nm in the posterior layers in man (Jakus, 1961).

In 1957, Maurice produced an analysis of the transparency of the corneal stroma. Maurice calculated that if each collagen fibre scattered light independently of any other fibres, more than 90% of incident light would be scattered, hence the stroma would be opaque. In order to account for stromal transparency, it was necessary to take into account phases of waves scattered from each fibre. Maurice considered the position of each collagen fibre as being arranged in a perfect rectangular lattice, similar to a crystal. If the fibres were so arranged, the position of each particle would be precisely known, and the relative phases of each of the scattered waves could be computed, as could the sum of the scattered fields and the intensity. When Maurice carried out this calculation, it was concluded that the scattered light intensity would be essentially zero in all directions, if each collagen fibre was spaced from the next by a distance equivalent to, or less than, the wavelength of light.

Goldman and Benedek (1967) observed that the collagen fibres of the shark stroma were arranged in complete disorder, their axes being randomly orientated in every direction. If the fibres were to be treated as independent scatterers, the shark cornea would be opaque. Clearly, even in this disordered array, the phase relations of the

scattered waves substantially reduced the intensity of scattered light. Hart and Farrell (1969) computed detailed probability functions for the relative positions of fibres taken from photographs of cornea stroma. They concluded that the position of pairs of collagen fibres remained correlated only over two near neighbours at most, but that their precise mathematical summations of the phase of waves scattered by such a partially ordered array was in good agreement both in magnitude and in wavelength dependence with that found experimentally. Benedek (1971) simplified these complex mathematical results and obtained similar conclusions.

In 1971, Feuk and McQueen following from earlier work (Kikkawa, 1960), examined the angular dependence of light scattered from normal rabbit corneas. They estimated that the loss of intensity of the primary beam on passing through the cornea was about 10% of the incident intensity. Hence, clinically, the stroma can be seen with the beam of a slit-lamp. The authors further showed a decrease in light scattered with increasing scattering angle.

McCally and Farrell (1976) following the work of Lindstrom et al (1973) also examined normal rabbit corneas. By use of a slit-lamp, photocell and X-Y recorder, at a series of scattering angles between 20-145 degrees, they found as the scattering angle increased the amount of light decreased. It was concluded that the stromal region accounted for more than 60% of the total scattering over the range of angles studied. Lindstrom et al (1973) recorded greater than 70% of scattered light from the stromal region. Endothelial light scattering properties have never been considered in isolation; only as part of the total cornea. However, the clear visibility of the endothelium with a slit-lamp beam has been commented on (Kikkawa, 1960).

In conclusion, the corneal stroma is responsible for the vast majority of light scattering from the cornea. However, it is known that the physiological properties of

the cornea change rapidly in excised eyes, hence the in-vivo situation should be considered.

1.B.2 Measures of corneal intraocular light scatter

Allen and Vos (1967) quantified ocular scattered light in-vivo. They related an objective measure of scattered light obtained with a slit-lamp with the visual performance on a variable contrast visual acuity target. The assumption was that light back-scattered from the tissues of the eye was related to, and thus representative of, forward-scattering towards the retina. Slit-lamp photographs were recorded as an objective measure of back-scattered light at 30 degrees from the incident light. Less than 1% of incident light was found to be back-scattered. The corneal share of entopic intraocular scatter, for young observers with clear ocular media, was approximately 30% of the total intraocular scattered light (Vos and Boogaard, 1963; Vos, 1984).

Hess and Garner (1977) induced corneal oedema in subjects by the use of atmospheric induced anoxia. The effect on vision was assessed both by a conventional high contrast visual acuity chart and by contrast sensitivity measurements. For the amount of oedema that was produced, contrast thresholds were only depressed at high frequencies. A greater degree of oedema was simulated with a diffuser, where upon low spatial frequencies were also affected. Hess and Garner concluded that visual acuity measurements, alone, were inadequate to monitor visual function in corneal light scattering (Elliott et al, 1993a).

Hess and Carney (1979) in a similar study induced both corneal oedema with a tightly fitting scleral contact lens containing distilled water, and also 'distortion' (no appreciable thickness change but irregular topography change) by passing 100% oxygen over the cornea via a scleral lens. Visual function was measured by means of visual acuity and contrast sensitivity. Distortion produced contrast attenuation at high

and medium spatial frequencies whereas oedema attenuated contrast at low and medium-high frequencies. Although Hess and Carney acknowledged that it was virtually impossible to totally separate 'distortion' and oedema they felt that, in general terms, the two different effects could be shown by contrast sensitivity measurements.

Remole (1981) measured the light scattering characteristics of the cornea in-vivo after immersion in hypo and hypertonic saline solutions. Forward-scattering was monitored in terms of contrast thresholds, which are more sensitive than visual acuity measurements for this purpose (Hess and Garner, 1977; Elliott et al, 1993a). Scattering changes and contrast thresholds were recorded during an immersion period of one hour and during a recovery of 30mins. Scattering increased with hypotonicity (Polse et al, 1990). Remole concluded that individual variability prevented the method being used as an absolute index of scattering of the retinal image.

Stevenson et al (1983) in a similar method to Remole (1981), bathed the cornea in hypotonic saline solutions. Corneal thickness was measured with a pachometer and increase in light scatter was recorded by the presence and brightness of a halo. Brightness of the halo was measured by brightness matching of the halo against a comparison patch. A 9% increase in corneal thickness and maximum halo brightness was recorded with the use of distilled water. As the halo diminished and disappeared no significant decrease in corneal thickness could be monitored. Since pachometry records changes in stromal thickness it was concluded that halos were epithelial in origin (Lambert and Klyce, 1981; Lovasik and Remole, 1983).

The forward light scattering profile of excised corneas were measured by Lovasik and Remole (1983). The angular dependence of scattered intensity over a 140 degree angle was recorded. Corneas were bathed in saline ranging from 0.9% NaCl (isotonic) to 0.5% NaCl (hypotonic) and corneal thickness was also recorded. The method used

was quick and confirmed previous findings (Feuk and McQueen, 1971; Kikkawa, 1960) showing a decrease in corneal light scatter with increasing scatter angle.

1.B.3 Effect of age on the cornea

As age increases the normal cornea scatters more light, (Allen and Vos, 1967; Stocker and Moore, 1975) up to about 1% at the age of 80 years, although 10% light scattering has been cited from animal studies (Feuk and McQueen, 1971). Olsen (1982) using similar techniques to Allen and Vos (1967) found an increase in back-scatter with age and concluded that it was due to the increasing irregularity of collagen fibril spacing with aging. Boetter and Woltner (1962) showed that the spectral transmissivity dropped with age. Beems and van Best (1990) and van den Berg and Tan (1994) both found no change in corneal transmissivity with age. Whether or not the increase in light scatter and decrease in transmissivity are connected is still a subject of controversy.

The hydration of the cornea is higher than the sclera and changes in the water content alter the refractive index of both tissues (Pau, 1955). Laing et al (1979) examined the endothelial mosaic with a specular microscope. In young subjects, the cells in this unicellular layer are approximately equal in size and normally distributed around a mean of about 20 μ m. Their size increases to 30 μ m by the age of 70. In order for this to happen, either the cornea has increased hydration or, if there is no change in tissue volume, there must be cell loss (Carlson et al, 1988; Doughty and Dilts, 1994). The regular hexagonal shape of the young cells is replaced by more irregular units in the old (Malik et al, 1992). This loss of regularity could cause an increase in scatter (Weale, 1982).

The density of the corneal stroma increases with age (Savage et al, 1993). This may increase light scatter and slow down protein transport through the cornea (Maurice,

1962), which is accompanied by a reduction in permeability to much smaller ions. The increase in stromal density is preceded by a rise in corneal fluorescence (Klang, 1948). A fluorogen has been identified in the cornea (Phillips and McDonnell, 1994) and was found to be present at higher levels in diabetics (Fantaguzzi et al, 1994). Weale (1982) notes that in-vivo measurements of corneal fluorescence may be contaminated by lenticular fluorescence.

1.B.4 Effect of oedema on the cornea

Corneal epithelium

In an oedematous epithelium, fluid fills the intercellular spaces of the basal epithelium. This produces an intricate three dimensional meshwork around the cells. The average refractive index surrounding the cells is different from the refractive index of the cells. If this fluctuation in the refractive index has sufficient spatial regularity, it will serve as a diffraction grating which produces a diffraction pattern (Miller and Benedek, 1978; Finkelstein, 1952). Figure 1.1 shows a schematic representation of the appearance of the diffraction grating produced by intercellular oedema. Such an arrangement of cells distributed in the epithelium will produce a circular diffraction pattern or halo.

It is possible to estimate the angular radius of the halo produced by the epithelial cells. Finkelstein (1952) was among the first to calculate this after inducing epithelial oedema with scleral contact lenses. The index of refraction fluctuates in the manner shown in Figure 1.1. This is equivalent to a set of diffraction apertures whose spacings (d) are equal to the average cell diameter. The direction (θ) in which this line of apertures will produce diffraction maxima is given by:

$$n\lambda = d\sin\theta$$

where $n = 1, 2, \dots$
 $\lambda =$ Light wavelength
 $d =$ Cell size

The meshwork distribution of index of refraction fluctuation can be represented by a sum of plane fluctuation waves of principal wavelength equal to the cell diameter. These plane waves are orientated in all directions in the plane of the figure. The superposition of such plane waves makes up the meshwork, and the diffraction pattern produced by all the waves will produce a circular diffraction pattern whose angular radius is given by the above equation. The first order ring corresponds to $n=1$, and the second order corresponds to $n=2$. Finkelstein (1952) measured epithelial cell diameter (d) as about $10\mu\text{m}$, which is in good agreement with other authors (Miller and Benedek, 1978). Corneal epithelial haloes have been recorded as a means of monitoring corneal epithelial oedema (Stevenson et al, 1983; Remole, 1981) with obvious clinical implications particularly regarding contact lens practice.

The corneal epithelial cells with desmosomal connections are very tightly packed. Haloes will present themselves only when epithelial oedema forces fluid into the cellular interstices. Various authors have measured the diffraction maxima as angular radii; 3.18° (Finkelstein, 1952) and 2.8° (Miller and Benedek, 1978).

Corneal stroma

Maurice (1957) extended his lattice theory to account for the increased light scattering in the stroma on swelling, mechanical straining or cooling. Under such conditions, the collagen fibrils separate from each other and cease to be in the same order and straightness. This results in decreased transparency and increased light scattering (Wiegand et al, 1995).

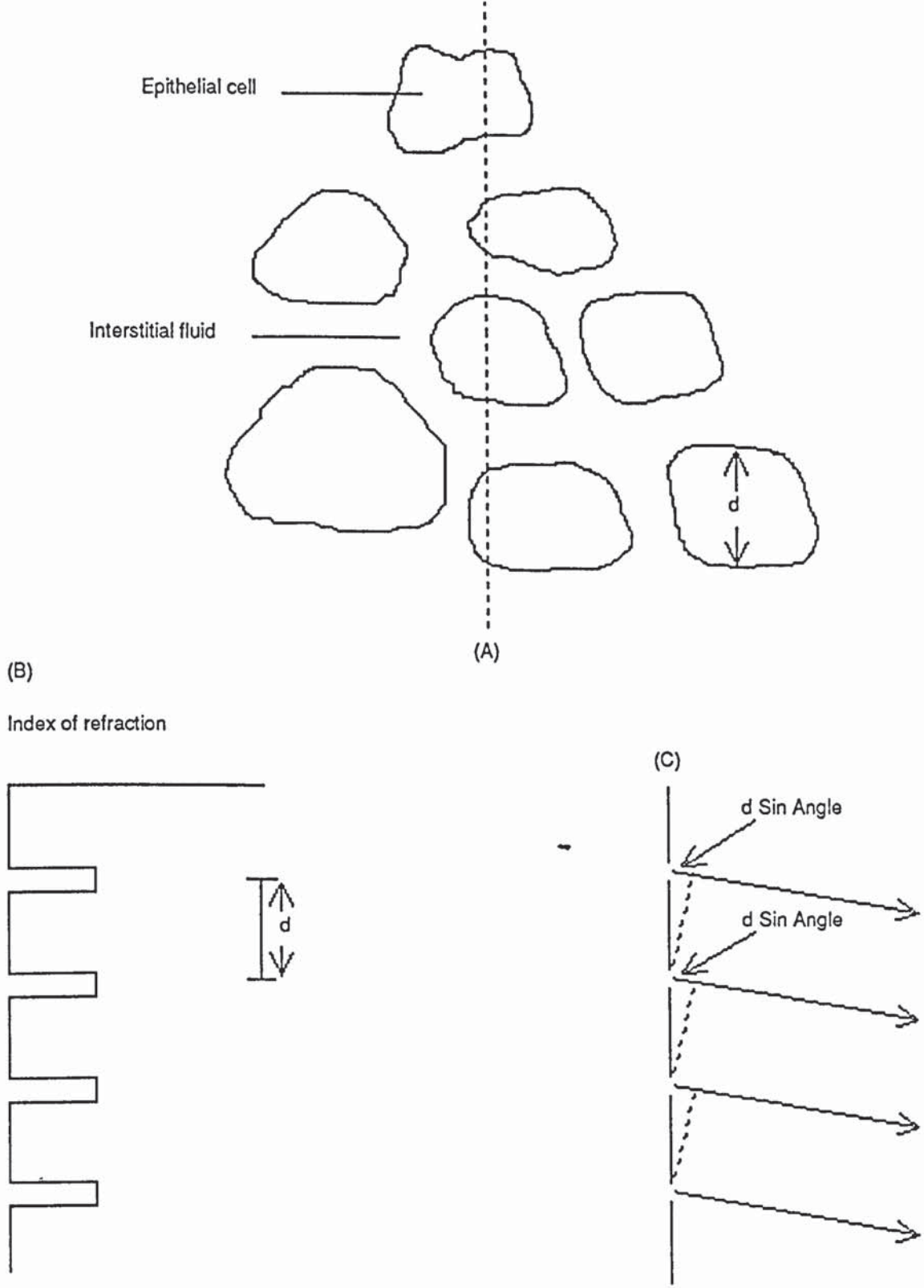


Figure 1.1 Theoretical representation. (A) A flat section of corneal epithelial cells surrounded by oedema fluid forming a diffraction grating. (B) Distribution of refractive index on traversing an oedematous corneal epithelium. (C) A typical diffraction grating (After Miller and Benedek, 1978).

Hart and Farrell (1969) reported that the ordering of collagen fibrils was short-ranged i.e., the regularity of spacing did not extend over many wavelengths in any given region. When the cornea becomes even more inhomogeneous, wavelength dependence of stromal light scatter changes from λ^3 to λ^4 . Twersky (1975) considered stromal oedematous light transmission as through correlated pairs of random distributions of small scatterers, and considered that loss of transparency was due to increased spacing between particles. This would decrease the destructive interference effect, and Twersky's model predicted a transmissivity at 500nm which was in good agreement with experiments on excised corneas swollen to 1.5 times initial thickness. Malik et al (1992) found little change in fibril diameter of swollen stromas. In between stromal fibrils, large areas called 'lakes' have been identified and these could account for increased scattering. Farrell and McCally (1975) considered two factors concerning stromal oedema, the distribution in ordering of fibrils and the increasing difference in refractive index between fibrils and the surrounding medium. They concluded that the disorientation of fibrils was the most significant effect. Although the explanation of Maurice (1957) concerning stromal transparency and its loss during swelling has subsequently been questioned, the basic principle of the ordered arrangement of collagen fibres appears to be an adequate explanation.

1.B.5 Crystalline lens

Most of the light scattering in the normal lens comes from fibre cell membranes which have a higher refractive index than the surrounding cytoplasm (Hemenger, 1992). Fibre cells are packed regularly so the light scattering gives rise to a diffraction pattern. Simpson (1953) attributed ocular halos that surround bright objects to this diffraction effect. He described many diffraction effects having their origin within the eye.

With the use of lasers, sharp diffraction patterns have been produced from thin sections of bovine lenses. These patterns show second- and third-order diffractions (Bettelheim and Vinciguerra, 1971; Vinciguerra and Bettelheim, 1971). Calculations from the laser diffraction patterns correspond well to the membrane-to-membrane distances in fibre cells observed in electron micrographs. The diffraction patterns can be observed using unpolarized light or polarized light, indicating that the membranes causing the diffraction have only periodic density fluctuations and no optical anisotropy. Similar diffraction patterns were found in thin sections of human lenses by Philipson (1973), and the calculated spacings from such patterns correspond well to the thickness of cortical fibre cells. Also using laser diffraction patterns from thin sections, fibre cells and their orientation have been investigated under stress (Bettelheim et al, 1973). Lens sections were submitted to periodic vibrations and the diffraction spots showed periodic changes in their intensities which were explained in terms of a change in the refractive index difference between membrane and surround due to the migration of water. Cortical fibre cells have a capacity to store water, possibly between two adjacent fibre cells, when subjected to stress. In the nucleus there is less of a barrier to water migration under stress than occurs in the cortex (Sanders and Larsen, 1994).

The total light scattered in the young normal lens is less than 5%. Over half of this comes from membrane scattering. This occurs in spite of the fact that the volume fraction of membrane in the lens is about 0.05. Therefore the cytoplasm is largely transparent. Trokel (1962) thought that an even distribution of lens protein within the fibre cells could account for the transparency. Benedek (1971) accounted for the transparency by proposing that in the normal lens the sizes of the spatial Fourier components are smaller than the wavelength of light. Thus, either the absence of large fluctuations in refractive index (Philipson, 1973) or the absence of scattering units comparable to the wavelength of the light provide a clear appearance (Hemenger, 1992).

Considering normal light scattering from lens cytoplasm, it has been thought that the proportion of light scattered is directly proportional to the inverse 4th power of the light wavelength. This is the type of Rayleigh scattering called the Mie (Dilute solutions) theory (Mie 1908). However, Hemenger (1982) using the data of several previous studies of light transmission through lenses (Said and Weale, 1959; Zigman et al, 1976; Ludvigh and McCarthy, 1938) concluded that the light scattered was proportional to the inverse 2nd power of the wavelength.

If the scattering particles are small compared to the light wavelength, little light scattering will occur and the lens is transparent. When the size of the scattering particles becomes very large e.g., high molecular weight proteins, comparable to the light wavelength or larger, the scattering intensity decreases with scattering angle. Particles of this size in dilute solution may be treated by the Mie theory (Mie, 1908) of scattering. Benedek (1971) predicted an increase in turbidity with an increase in high molecular weight proteins.

Another aspect of normal lens scattering is optical anisotropy, where the refractive index is a function of orientation. Light scatter may increase if the variation of refractive index orientation increases (Bettelheim, 1975).

In summary, transparency of the normal lens is accounted for by; a degree of hydration of supramolecular aggregates that minimises the refractive index difference between them and their surroundings; relative absence of high molecular weight aggregates; and very low amounts of optical anisotropy fluctuations. Consequently, any process leading to changes in the above conditions will initiate opacity and cataract formation.

1.B.6 Measures of crystalline lens back-scatter

Allen and Vos (1967) measured back-scattered light from the lens as a function of age, assuming back-scattered light is representative of forward-scattered light. An index of scatter was calculated as the percentage of light scattered out from a slit beam. They found an increase in light back-scattered from the lens with age. Glare sensitivity became more pronounced since more contrast was required to see the visual acuity target.

Siegelman et al (1974), using a slit-lamp camera in-vivo, measured back-scatter by tracing the resultant photographs with a microdensitometer. These workers examined groups of normal patients and also those with either nuclear sclerosis or senile cataracts. They found that back-scattered light from the lens increased with age. The nuclear region of the lens showed significant back-scatter; the cortical region caused some back-scatter in young lenses but there was only a slight increase with age. They found no loss of visual acuity with considerable back-scatter. Siik et al (1992) found back-scatter to increase with age and the highest amount of back-scatter was found in the cortical lens region. Yuan et al (1993) found that disability glare showed a significant correlation with objective measures of lens light back-scatter.

Ben-Sira et al (1980) repeated the work of Siegelman et al (1974) in a clinical environment using apparatus similar to that of Goldmann (1964). Their results confirmed that the cortex scatters a significant amount of light in young eyes and also that the nucleus exhibits a sharp rise in scattered light after age 40. Further improvements in this technique were elicited using rotating slit-lamp photography employing Scheimpflug principles (Lerman et al, 1981). A more quantitative clinical characterisation of lens opacity has been attempted with photography of lenses (e.g. Lens Opacities Classification System (LOCS) I, II and III systems)(Chylack, 1978; Sparrow et al, 1986; Chylack et al, 1989; Chylack et al, 1993; Karbassi et al, 1993).

1.B.7 Measures of crystalline lens forward-scatter

The studies described in the previous section examined lens back-scatter on the assumption that back-scattered light is representative of forward-scattered light. However, some studies have found little correlation between forward- and back-scatter in the aging and cataractous eye (e.g., Mitchell and Hurst, 1993). A better assessment of visual function is found by examination of forward light scatter. Wolf and Gardiner (1965) measured sensitivity to glare, the subjective result of forward light scatter, by recording the increase in contrast required to recognise Landolt 'C' rings. Good agreement was found between glare, age and scattered light in the media indicating that glare is an entopic phenomenon in its influence on visual efficiency. Up to 40 years, there was little change in glare sensitivity while above that age there was an ascending linear relationship between forward-scatter and glare sensitivity.

Hess and Woo (1978) compared contrast thresholds for a range of spatial frequencies to visual acuity tests in 10 patients with unioocular senile cataract. The main finding of this investigation was that visual loss for subjects with senile cataract could not be described by a single visual loss function because, for some subjects, vision for low frequencies was disproportionately depressed. Visual loss from all types of cataracts could not be thought of, or assessed in terms of, contrast loss from defocus, because the presence or absence of a low-frequency contrast abnormality was not correlated with the degree of visual acuity reduction. This paper was an important advance in clinical research as it firmly established the use of contrast sensitivity measurements in the in-vivo assessment of forward light scatter in the eye (Adamsons et al, 1992; Rubin et al, 1993; Williamson et al, 1992; Regan et al, 1993; Lasa et al, 1992; Lasa et al, 1993).

1.B.8 Cataractogenesis

A continuation of the aging process is eventually likely to lead to the production of cataract (Mota et al, 1992; Liang et al, 1994). There is a very fine dividing line between increased physiological scattering with age and actual cataract formation. Cinotti and Patti (1968) estimated that 65% of the normal population in the age group 50-59 years would have some form of early cataract. In comparison with normal lenses, cataractous lenses scatter significantly more light. The result of the increased light scatter is that less light will reach the retina. The net effect is increased glare sensitivity corresponding to the early stages of cataract formation and later partial or complete blockage of the passage of light, which manifests in impaired vision or complete blindness. Glare produced with different light sources seems to be independent of the wavelength, λ , of light. Moon and Spencer (1943) concluded that the scattering is not a Rayleigh type; that is, it does not have λ^4 dependence. Therefore, the scattering particles must be within the order of the wavelength $\lambda/20$ or larger. Using a reduced eye, in which all the components were reduced to a uniformly scattering field, Fry (1954) calculated the amount of scattered light reaching the fovea. He used Mie-like (Mie 1908) scatterers to predict the relation between transmitted and scattered light. However, the eye is not a uniform scatterer. The lens scatters much more light than the aqueous humour or even the vitreous. The scattering from the lens is the main contributing factor to glare, especially where cataract formation occurs. The most significant glare causing cataract is the posterior subcapsular cataract (Strong et al, 1992; Magnante et al, 1995).

There are a number of mechanisms by which cataract may form. These are aggregation processes, syneresis, microphase separation, membrane disintegration and change in the orientation of cytoskeletal elements. These mechanisms can act independently in individual cases as a sole cause, or two or three mechanisms may act simultaneously, providing a synergetic effect enhancing the development of cataracts

(Mota et al, 1992; Sen et al, 1992; Wellsknecht et al, 1993; Sanders and Larsen, 1994).

The transparency of the normal lens and, in turn, the opacification of the cataractous has a physical basis. Namely the random or non-random spatial fluctuation in density and in optical anisotropy macromolecules. When the size over which such fluctuations occur approaches the wavelength of light and when the amplitude of the fluctuations are large, significant light scatter will occur, leading to cataract formation.

1.C. Lens fluorescence and aging

When light is absorbed by a molecule it is converted from a resting state into an excited state i.e., there is an increase in the level of rotational and vibrational energy. When a photon is absorbed, an orbital electron is raised from its ground state, any remaining energy can increase the vibrational state of the molecule. Return to the ground state (de-excitation) can occur by molecular collision (dissipation as heat) or by a photon of light being re-emitted (at longer wavelength) resulting in fluorescence as the molecule returns from the excited to the ground state (Elliazy et al, 1994).

It is now generally accepted that the yellow pigmentation in the lens serves as an intraocular filter for blue light (Walls and Judd, 1933; Wald, 1952; Sen et al, 1992), which is the wavelength of the visible spectrum subject to the greatest amount of dispersion, and the yellow colour helps reduce chromatic aberration. These pigments protect the underlying vitreous and retina from UV radiation by absorbing most of the UV light (longer than 295nm) transmitted by the cornea (Weale, 1988; Liang, 1991; Sanders and Larsen, 1994). It has also been proposed that the pigments may prevent colour confusion since the receptor elements in the retina have secondary absorption maxima at 325 and 350nm. Primary maxima are 498nm for rods and 430 to 440nm

for the blue cone receptor, 540nm for the green cone receptor, and 575nm for the red cone receptor.

Before discussing the visible fluorescence of the lens, it is important to note that most proteins are endowed with an intrinsic UV fluorescence because they contain aromatic amino acids (phenylalanine, tyrosine and tryptophan)(Sen et al, 1992). Phenylalanine has the lowest fluorescence quantum yield of the three proteins. The maximal fluorescence of tryptophan is from 330 to 352 nm, depending on the type of protein (lens proteins have a λ_{max} at 332nm). Free tryptophan has a characteristic fluorescence emission at approximately 354nm, but this shifts to somewhat shorter wavelengths when tryptophan emission is measured in a protein (Yappert et al, 1992; Yappert et al, 1993).

Visible lenticular fluorescence was first described well over 100 years ago and was utilized by ophthalmic surgeons as an aid in estimating the amount of lens matter remaining in an eye following an extracapsular cataract extraction. The visible fluorescence of the lens proteins under UV illumination enabled the surgeon to determine the location and the amount of lens matter remaining within the eye.

Specific fluorescent peptides and proteins in the human and other mammalian lenses have been demonstrated by various investigators (Lerman et al, 1976; Lerman and Borkman, 1976; Lerman and Borkman, 1978a; Lerman et al, 1970; Zigman, 1971; Satoh et al, 1973; Dilley and Pirie, 1974; Spector et al, 1975; Bando et al, 1975; Larsen, 1993; Pau et al, 1993). In addition to the fluorescence due to tryptophan, these proteins contain one or more fluorescent chromophores that have been labelled fluorogens and have activation wavelengths of approximately 340 to 360nm and 420 to 435nm and emission maxima at 420 to 440nm and 500 to 520nm, respectively (Figure 1.2)(Yappert et al, 1992). This type of fluorescence has been shown to be present in the soluble, high-molecular-weight, and insoluble fractions of the human

lens and to increase with age, particularly the insoluble protein fraction (Yappert et al, 1992), and in diabetes (Sparrow et al, 1992; Larsen, 1993; Eppstein et al, 1995; Bron et al, 1993; Mota et al, 1992). These fluorogens are tightly bound to peptides derived from some of the lens proteins (Elliazy et al; 1992; Malina and Martin, 1995).

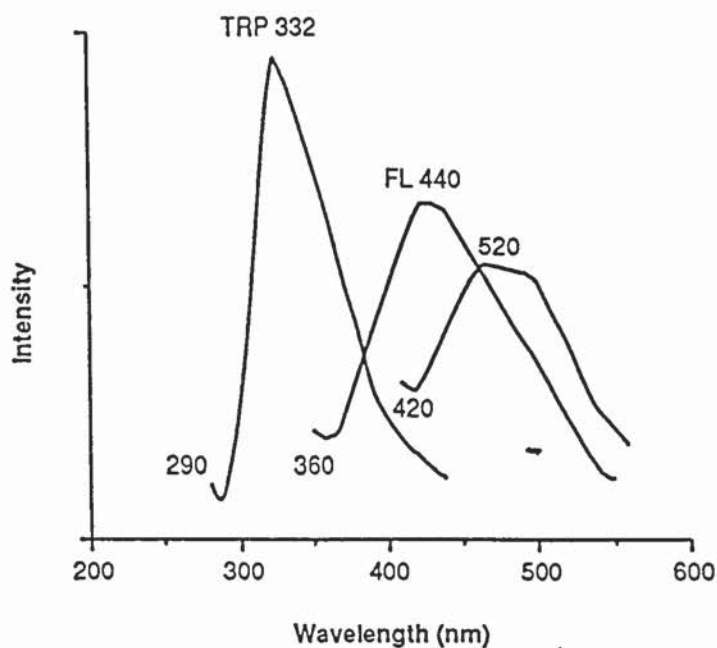


Figure 1.2 Fluorescence spectra of a 78-year normal human lens showing TRP 332 fluorescence and 440nm fluorescence. Also demonstrated is a second region that develops with excitation resulting in 520nm emission due to a second fluorescent region that develops with age (After Lerman, 1980).

Fluorescence studies on normal human lenses ranging in age from one day to 90 years have demonstrated that the 420 to 440nm fluorescence is not present to any significant extent within the first year of life (Yappert et al, 1992). It then becomes manifest and increases in intensity with age. The progressive increase in this fluorescence is paralleled by an increase in the relative concentration of the insoluble protein fraction with age (Mandal and Lerman, 1993; Yappert et al, 1992). A second fluorescent region (approximately 420 to 435nm activation and 500 to 520nm emission) becomes apparent in human lenses after the first decade of life and increases slowly as the lens ages. Although both fluorescent regions show a marked increase in intensity in the brown nuclear cataract (Yappert et al, 1993), the longer wavelength fluorogen becomes much more pronounced in the brown nuclear cataract.

It is not unreasonable to speculate that these fluorescent compounds play an important role in the development of this type of cataract (Siik et al, 1993; Pau et al, 1993, Elliazzy et al, 1994), which appears to be a form of accelerated aging. It is not yet clear whether the longer wavelength absorbing material derives from the shorter wavelength material as a photochemically induced degradation product or whether it has a separate origin. Aside from the role of the various fluorescent compounds in increasing the yellow colour of the lens core as it ages, they may also be involved in promoting polymerization and insolubilization of the previously soluble lens proteins and polypeptides (Lerman and Borkman, 1978a; Satoh et al, 1973; Dilley and Pirie, 1974; Mota et al, 1992; Mota et al, 1994).

The production of lens fluorogen is thought to be related to increased free radical activity in the lens. Photochemical studies have shown that in the presence of the compound 3-aminotriazole, lens 360/440nm fluorescence can be induced and/or markedly accelerated when it is exposed to UV radiation longer than 295nm (Lerman and Borkman 1976; Lerman and Borkman 1978a). This compound (3-aminotriazole) does not absorb UV radiation but it is thought to inhibit the enzyme catalase in the

lens cells. The inhibition of the enzyme results in a lower-than-normal concentration of glutathione in the eye. Glutathione functions as an important free radical scavenger in lenticular cells. The effect of 3-aminotriazole is to block the cell's normal defence mechanism against free radical damage. Thus, reactions that proceed by free radical mechanisms should be accelerated in the presence of 3-aminotriazole, and this was observed in the case of fluorogen production. Additional support for a free radical mechanism in lens fluorogen production comes from observations using compounds which are efficient radical scavengers and also by observing the action spectra for fluorogen production in the ocular lens.

It appears that UV radiation may exert its effect on the lens by acting on some of the protein-bound tryptophan residues. The photochemical reaction is presumably initiated by the photoionization of certain tryptophan residues. That is, tryptophan is elevated to an excited state by absorbing UV energy (over a wavelength range between 295 and 315nm in the ocular lens) and its energy must be dissipated (Sen et al, 1992; Ortwerth and Olesen, 1994; Sanders and Larsen, 1994).

In considering the role of free radical induced by the prolonged and cumulative exposure of the ocular lens to UV radiation the nucleus develops most, if not all, of the fluorogen pigmentation while the cortex remains relatively clear (Pau et al, 1993). This is due to the higher concentration of glutathione in the human lens cortex compared with the nucleus. The cortex is capable of protecting itself from UV light damage because it contains a much higher concentration of an important free radical scavenger. The presence of this free radical scavenger will abort the radical-induced photodegradation reactions and prevent the accumulation of fluorescent compounds in the cortex.

UV and visible light transmission studies on normal human lenses ranging in age from six months to 82 years show that in lenses under ten years of age over 75 percent

of UV(300 to 400nm) is transmitted, while the corresponding UV transmission in lenses above 25 years of age drops markedly to 20 percent (Figure 1.3)(Lerman, 1980). These data are consistent with the relative lack of fluorogens in the young lens and the increase in fluorogen concentration as the lens ages (Yappert et al, 1992). Accompanying the measured increase in fluorogens and the decrease in light transmission, is a concomitant increase in the yellow colour of the lens as it ages. These pigments lead to an increasing yellow colour and decreased light transmission in the aging lens (Johnson et al, 1993).

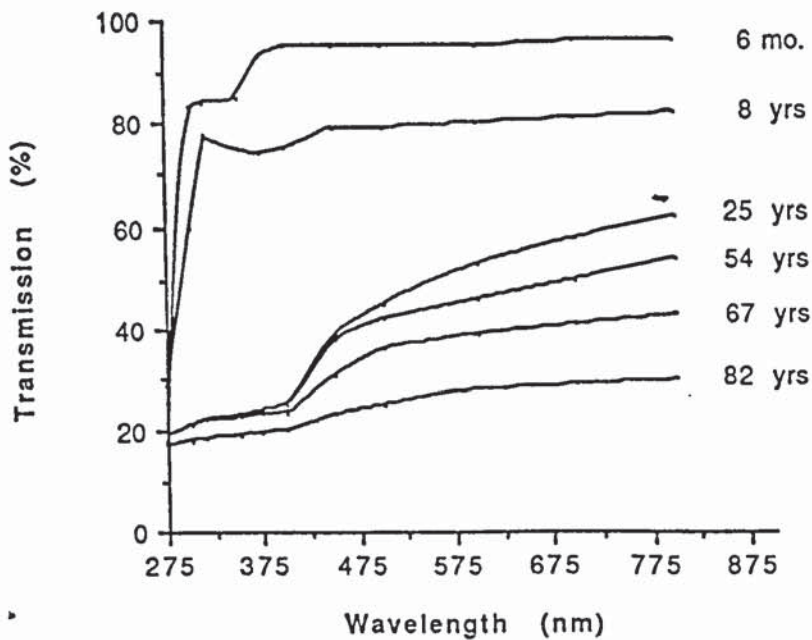


Figure 1.3 Percent UV and visible light transmission of normal lenses 6 months to 83 years of age (After Lerman and Borkman, 1976).

In conclusion, fluorescence spectroscopy can be used to measure one aging parameter in the human ocular lens and at least two fluorogens can be photochemically generated from tryptophan as a consequence of prolonged exposure of the lens to UV light longer than 295nm (Sanders and Larsen, 1994; Ortwerth and Olesen, 1994; Sen et al, 1992). This fluorescence, which has one excitation peak at 360nm (420 to 440nm emission) and a second excitation at 420 to 435nm (500 to 520nm emission), increases with age and parallels the increased concentration of water-insoluble proteins (Yappert et al, 1992). It is postulated that these fluorescent compounds are responsible for other age-related lenticular changes, including the yellow colour of the lens nucleus and nuclear cataract (Pau et al, 1993). The pigmentation is confined mainly to the lens nucleus since there is insufficient concentration of free-radical scavengers in this region to abort the photochemical reaction.

1.D. Theory of light scattering and transparency

In a perfectly transparent body the light intensity exciting the body is the same as that of the incident beam, and furthermore there is no change in the direction of the light beam. Obviously, the lens is not perfectly transparent. The diminution of the intensity of the exciting light beam may be due to absorption, refraction-reflection and scattering of light. The absorption of light is due to molecular species that have energy requirements for transition between ground and excited states that lie within the visible range of the electromagnetic radiation spectrum. In order to understand ocular transparency and turbidity it is necessary to explain some basic physical properties of light.

Light may be considered to be propagated by means of a transverse wave motion; when light interacts with a particle (i.e., light transmitted through ocular tissues or a beam of light passing through dusty air) a dipole moment is induced in the particle. This is because the particle (e.g., an atom, a molecule or an aggregate of molecules) in

the electric field is subjected to polarization (i.e., the nuclei and electrons move in opposite directions). Since electromagnetic radiation such as light carries an oscillating field, the induced dipole in the particle will also oscillate. However, an oscillating dipole is a source of electromagnetic radiation, that is, the scattered light is propagated in all directions. An observer's eye sees rays of light because of the sideways scattered light from each of the particles is detected. In the absence of scattering particles the primary light beam would be invisible to the observer. This is the principle on which a slit-lamp functions. The cornea and lens can be observed because these media scatter part of an incident beam into the objective of the microscope. As the primary beam passes through the aqueous, where scattering is very weak, nothing of the primary beam is normally seen.

A turbid medium is one that attenuates the light passing through it. Hence as a result of the scattering process the primary light beam loses energy and therefore grows progressively weaker as it passes through more of the scattering medium. The level of turbidity can serve as a characterisation of the transparency or opacity of a scattering medium. Turbidity and transparency of any medium is related to the microscopic structure of the tissues. The essence of transparency is in the superposition of the phases of scattered waves.

The review that follows is designed to summarise basic types of light scattering, turbidity and transparency, and the application to the ocular tissues.

Principles of polarization and refractive index

If a molecule is placed in an electrical field between two condenser plates, the electric field polarizes the molecule so that the positive end of the molecule aligns itself with the negative plate, and vice versa, thus the applied electrical field is reduced. The total polarization of the molecule can be measured by the dielectric constant ϵ , which is the

ratio of the capacitances of the dielectric compound in question to that of vacuum at the same geometric setting of the condenser.

$$\frac{C}{C_0} = \epsilon \quad [1.1]$$

The total molar polarization of the compound is as follows

$$P_T = P_I + P_P = \frac{4\pi N\alpha}{3} + \frac{4\pi N\mu^2}{9kT} = \frac{\epsilon - 1}{\epsilon + 2} \frac{M}{\rho} \quad [1.2]$$

where P_T is the total molar polarization; P_I is the induced molar polarization; P_P is the molar polarization due to the permanent dipole moment μ ; M is the molecular weight; ρ is the density of the compound in question; α is the polarizability of the molecule, which indicates how much distortion is induced by the field in the nuclear and electronic charge distribution; N is Avogadro's number; k is the Boltzmann constant; and T is the absolute temperature.

Two kinds of polarization can be induced by an electric field: P_A , the atomic polarization due to the displacement of the nuclei under the influence of the field, and P_E , the electronic polarization that represents the distortion of the electronic cloud induced by the field. At relatively high frequencies the contribution of P_A diminishes to zero, and the dielectric constant measured at such high frequencies is due to electronic polarization alone. When the refractive index n of a compound is measured in the visible region, the light can be considered a field of high frequency, and the Maxwell relation holds.

$$n^2 = \epsilon_{\infty} \quad [1.3]$$

where n is the refractive index measured and ϵ_{∞} is the dielectric constant at high frequencies.

Hence, in the region of interest of lens transparency,

$$P_E = \frac{4\pi N\alpha}{3} = \frac{n^2 - 1}{n^2 + 2} \frac{M}{\rho} = R \quad [1.4]$$

In using equation [1.4] in attempting to obtain a polarization value α , this value represents merely an average of the polarizabilities in various directions.

When a light passes from one isotropic medium to another (molecular weight M_1 to molecular weight M_2) both its direction and its velocity will change unless it is normal to the boundary separating M_1 from M_2 .

Light scattering

There are two types of light scattering: elastic and nonelastic (quasi-elastic). With elastic scattering (i.e., none of the energy of the incident radiation is used to put the atom or molecule in an excited-translation, rotational, vibrational or electronic-state), the frequency of the scattered light will be the same as that of the incident light. This is called Rayleigh scattering. It was Lord Rayleigh who first derived the equation for the intensity of scattered radiation in 1871:

$$\frac{I_{\theta}}{I_0} \propto \frac{\alpha^2}{\lambda^4 r^2} \quad [1.5]$$

where I_{θ} is the intensity of the scattered light at any angle θ , I_0 is the intensity of the incident beam, λ is the wavelength of the incident beam in a vacuum, r is the

distance of the observer from the scattering centre, and α is the polarizability, a molecular parameter stating how much dipole moment is induced by a unit electric field. Combination of the intensities with the distance of the observer from the scattering centre;

$$\frac{I_{\theta} r^2}{I_0 V} = R_{\theta} \quad [1.6]$$

is known as the Rayleigh ratio, which describes the intensity of the scattered light per unit volume V .

Equation [1.5] predicts that the intensity of scattered light will depend on the inverse of the fourth power of the wavelength that is scattered. Blue light will have a greater intensity than scattered red light, which accounts for the blue sky. (Bettelheim, 1985)

Scattering from each particle is produced as the electric field in the incident light wave excites electrons. Each particle radiates out an electric field in synchrony with the exciting wave. To find the resultant field at any observation point in space, the radiating fields are added together. Each of the scattered wavelets will be at a different point in an oscillation cycle at any particular observation point. The resultant electric field is the superposition of these waves and the magnitude of the result depends on whether the constituent waves interfere constructively or destructively with one another. The phase of each wave is directly proportional to the position of the scattering particle; the difference in phase between waves depends on the spacing of the scattering particles in comparison to the wavelength of light.

If two scattering particles are spaced by distances comparable to the wavelength of light, the two scattered waves may be 180° out of phase and the waves will then

cancel each other out giving no scattered light at the observation point. Conversely, if two scattering particles are spaced by distances which are small compared to the light wavelength, the phases of the two waves will be nearly the same and the scattered electric field will have an amplitude twice the amplitude of each individually, i.e. maximum light scattering. The final summation of all scattered waves will depend on the relative positions of the particles and of the light wavelength. The intensity of scattered light is proportional to the square of the total electric field. In the two examples described, scattered intensity can be four times the intensity of light scattered from each particle, or it can be zero depending on the phase of the individual waves.

Mathematical techniques have been developed to describe particle distributions from the perfectly random e.g. gases, to the perfectly ordered e.g. crystals including quasi-random distributions. Einstein (1910) and Debye (1944) recognised that the question of transparency and turbidity could be regarded as due to fluctuations in density i.e., concentration. They concluded that only a limited degree of particle correlation was needed to produce transparency. Furthermore, light scattering theories show that when light is scattered by a density fluctuation, only those Fourier components whose wavelength is larger than half the light wavelength contribute to scattering. Thus if a medium contains periodic fluctuations in density which have wavelength smaller than half the light wavelength, these will not contribute to light scattering (Hemenger, 1992).

In a gaseous medium, where the scatterers are said to be independent, there is no correlation between the relative positions of any of the scattering particles. If the density of the particles is increased to the point where the particles are comparable in size to that of the wavelength of light, then some scattering may occur. In contrast to the random position of gas molecules within a scattering volume, the atoms in a crystal are rigidly fixed in a geometric array (lattice). Since the wavelength of light is

much larger than the individual scatterers (atoms) there is always a pair of atoms (equal scatterers) which scatter out of phase from the point of view of the observer at any particular scattering angle. Thus the destructive interference of a pair of scatterers is complete and no scattered light will be observed i.e., transparency results (see 1.B.).

Scattering from pure liquids is intermediate between crystals and gases. A pair of small volume elements ($< \lambda/20$) would be independent scatterers that are out of phase, resulting in destructive interference. However, since liquids are not orderly, the packing of particles in each member of a pair of volume elements may not be the same, therefore, the intensity of the scattered light from one volume element may differ from the another volume element; destructive interference is not complete as a consequence, and some scattering will occur.

In relation to the eye, transparency of the cornea is due to an imperfect lattice arrangement, similar to a crystal. Perfect lattice periodicity is not needed theoretically, nor is it found experimentally (Goldman and Benedek, 1967) so the cornea is still essentially transparent (Beems and van Best, 1990). The lens is less transparent than the cornea (Vos and Boogard, 1963; Vos and Bouman, 1964); but in the young eye is generally regarded as a liquid in terms of its light scattering properties. The scattering molecules are not in a lattice arrangement, they produce little scattering because there are many particles within one wavelength of light and the density changes little from one region to another.

2.A. Basic concepts of contrast sensitivity

2.A.1 Introduction

Initial interest in measurement of the spatial and temporal properties of the visual system began with the early work of Schade (1956) based upon electronic principles. An electronic system's performance can be assessed by comparing the input signal with the phase and amplitude of the output. Any complex waveform can be represented as the sum of a number of sine waves of specific phase and amplitude. This is known as Fourier analysis. A black and white square wave can be made up from addition of many sine wave gratings. These gratings must be added in the correct relationship to each other. In this case the minima of harmonics must be aligned with the maximum of the fundamental. A sine wave of the same spatial frequency (the "fundamental frequency") as the square wave, has added to it a sine wave of three times the fundamental frequency and one third the amplitude of the fundamental, plus a sine wave of five times the frequency and one fifth the amplitude, and so on for all of the odd harmonics of the fundamental. In simplistic terms the visual system can be thought of as a system that adds up sine waves in a linear fashion; therefore the system's sensitivity to any two-dimensional pattern can be estimated by knowing its sensitivity to sine waves. A non-linear system will distort the wave. By examining the output form of a sine wave, a system can be shown to be either linear or non-linear (Sperling, 1964). Sine waves are therefore useful because defocus reduces the contrast of a sine wave but does not alter its form. A blurred sine wave is still a sine wave while a blurred optotype changes in appearance as well as in contrast.

The input signal can consist of a grating with a sinusoidal luminance profile when measuring the spatial properties of the visual system. The modulation of the sine wave determines the number of bars per degree of visual angle. The sinusoidal variation is superimposed on a steady luminance value. This steady luminance value determines the mean luminance of the input signal and remains constant whatever the sinusoidal modulation. This constant mean luminance ensures constant adaptation of the retina (Kelly, 1977).

Modulation is defined by the following equation which is independent of mean luminance (Campbell and Maffei, 1974),

$$\text{Modulation} = \frac{(L_{\max} - L_{\min})}{(L_{\max} + L_{\min})}$$

Where L_{\max} = The maximum luminance level

L_{\min} = The minimum luminance level.

When examining the human visual system measurement of the output signal amplitude is important and is usually determined subjectively by measurement of threshold. This threshold is the value at which the spatial and temporal modulation are just perceived, and is inversely proportional to the sensitivity of the visual system.

2.A.2. Psychophysical aspects of the Contrast Sensitivity Function (CSF)

The ability to see small targets of very high contrast is recorded by visual acuity. This measurement does not give any information on the ability to see larger objects of lower contrast. The detection of large objects of lower contrast is a more realistic assessment of the visual world. By measuring the relationship between different

values of size and contrast the CSF gives a more complete description of the visual system.

The CSF is an inverted 'U' shape with a peak at intermediate spatial frequencies (see Figure 2.1). When plotted on a linear spatial frequency axis, the extrapolation of the CSF plot to 100% contrast defines the limit of visual acuity. This is usually between 30 and 40 cpd (Arden, 1978). The CSF is more usually plotted on a log/log scale (see Figure 2.2), this will have the effect of extending the low frequency section and contracting the high frequency section. Sine wave gratings for CSF measurement can be produced on monitors or using printed gratings for clinical screening (Arden, 1978; Ginsburg, 1984; Reeves et al; 1991).

2.A.3 The peak of the CSF curve

The peak of the CSF curve is dependent on the size and position of the grating presented. Contrast sensitivity is maximum for gratings of about 4 cpd when a field size of 3° to 6° is used (Campbell and Robson, 1968; Campbell and Green, 1965; Levi and Harworth, 1977; Thomas, 1978). A peak as high as 10 cpd has been reported (Sjöstrand, 1978; Hoekstra et al, 1974) when a 1° foveal field size was used. Rovamo et al (1978) found that the peak of the CSF curve was as low as 1 cpd with an eccentric viewed target. These results indicate that the maximum contrast sensitivity value is dependent on the area of retina stimulated and upon the eccentricity (see Figure 2.3). There is also a shift of maximal contrast sensitivity to lower spatial frequencies with decreasing luminance. This shift is thought to be due to the use of larger receptive fields at lower luminance levels (Bodis-Wollner, 1980; Kulikowski, 1971).

2.A.4. High spatial frequency attenuation

Campbell and Green (1965) found that at spatial frequencies above the peak of the CSF curve, sensitivity decreases exponentially with increasing spatial frequency. Contrast sensitivity at high spatial frequencies is attenuated by optical blur. These optical blur effects can be by-passed with the use of laser interferometry to generate gratings on the retina.

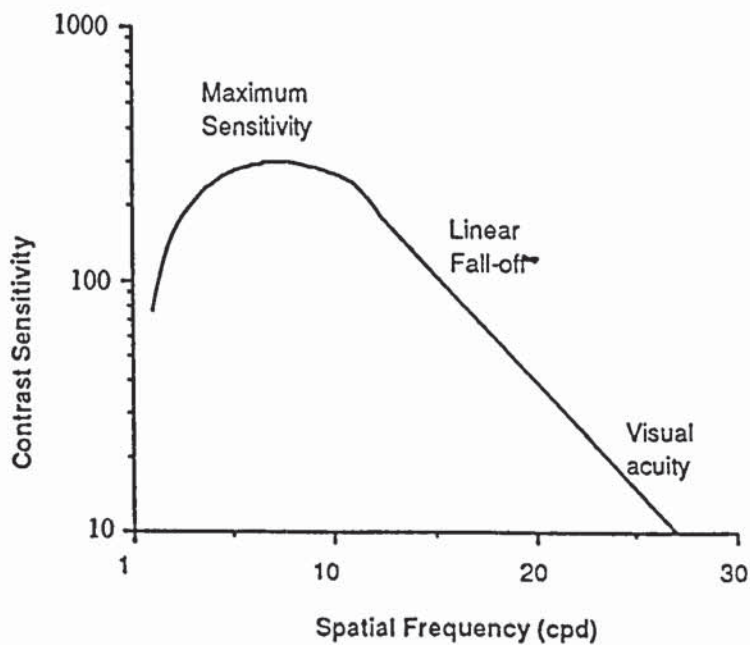


Figure 2.1 The Contrast Sensitivity Function plotted on a log/linear scale.

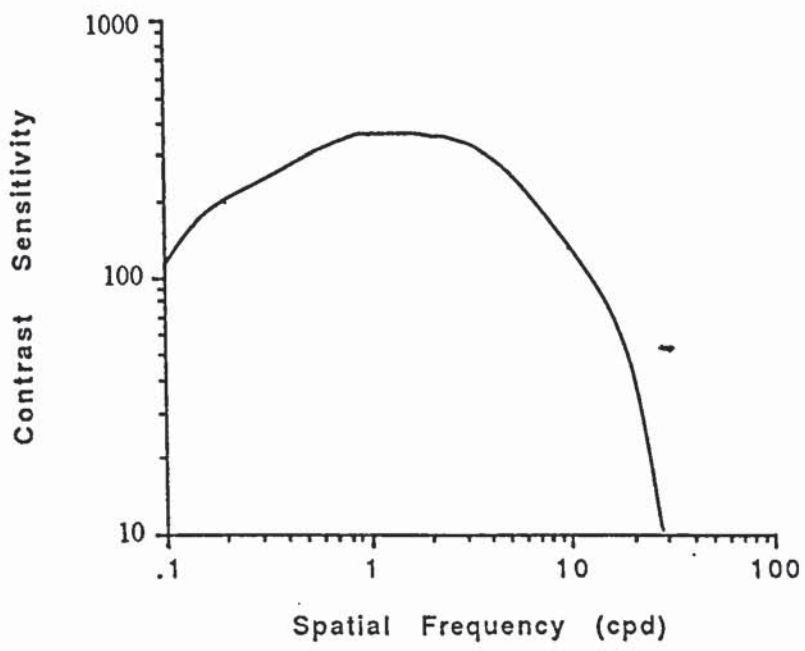


Figure 2.2 The Contrast Sensitivity Function plotted on a log/log scale.

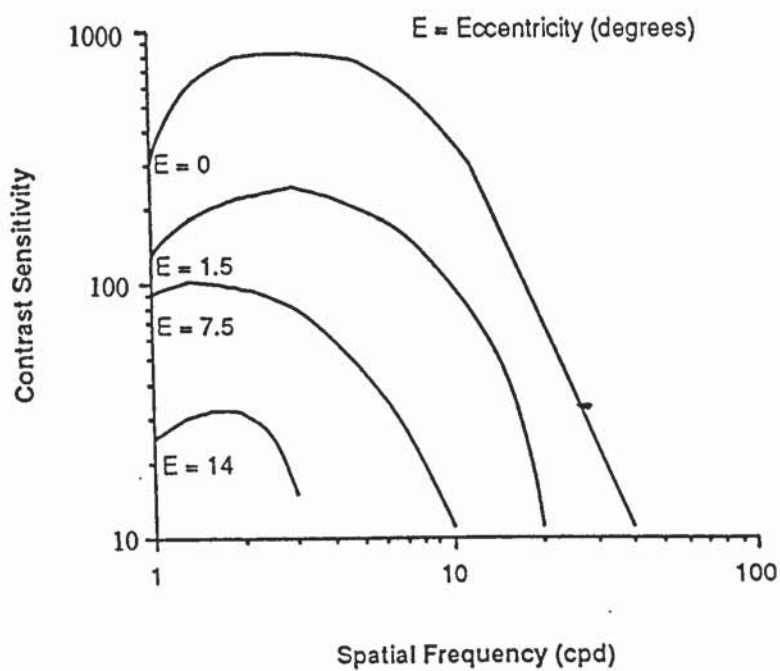


Figure 2.3 Contrast sensitivity as a function of spatial frequency and retinal eccentricity. With an increase in eccentricity there is a decrease in sensitivity and a shift in the peak to lower spatial frequencies (After Rovamo and Virsu, 1979).

The CSF measured using laser interferometry shows less high frequency attenuation. From these results it can be calculated that the eye's optics account for one third of the attenuation in the 30-40cpd range with a 2mm pupil (Campbell and Green 1965). The remaining attenuation is due to the limitations of the retinal mosaic. The level of light adaptation affects high frequency sensitivity (Bodis-Wollner 1980). High frequency sensitivity has been shown to be proportional to the square root of the average luminance. This proportionality was found only up to approximately 24 cdm⁻²; for higher luminances, contrast thresholds remained a constant fraction of the retinal illuminance (see below)(Kulikowski, 1971).

The relationship between contrast threshold and mean luminance is described by the de Vries-Rose law and the Weber-Fechner law. van Nes and Bouman (1967) showed that for retinal luminances up to 300td, contrast threshold is approximately proportional to the inverse of the square root of the mean luminance (de Vries-Rose law):

$$\Delta I \propto I^{-1/2} \quad [2.1]$$

where I is the mean luminance and ΔI the incremental contrast threshold. This could suggest that the detection of illuminance differences on the retina, corresponding to the image of bright and dark lines of the grating, is limited by only the statistical quantum fluctuations in the bright and dark portions of the image. For retinal illuminances higher than 300td, however, contrast threshold remains a constant fraction of the retinal illuminance in accordance with the Weber-Fechner law:

$$\Delta I \propto I \quad [2.2]$$

Figure 2.4 shows the dependence of contrast threshold on retinal illuminance for different spatial frequencies (van Nes and Bouman, 1967).

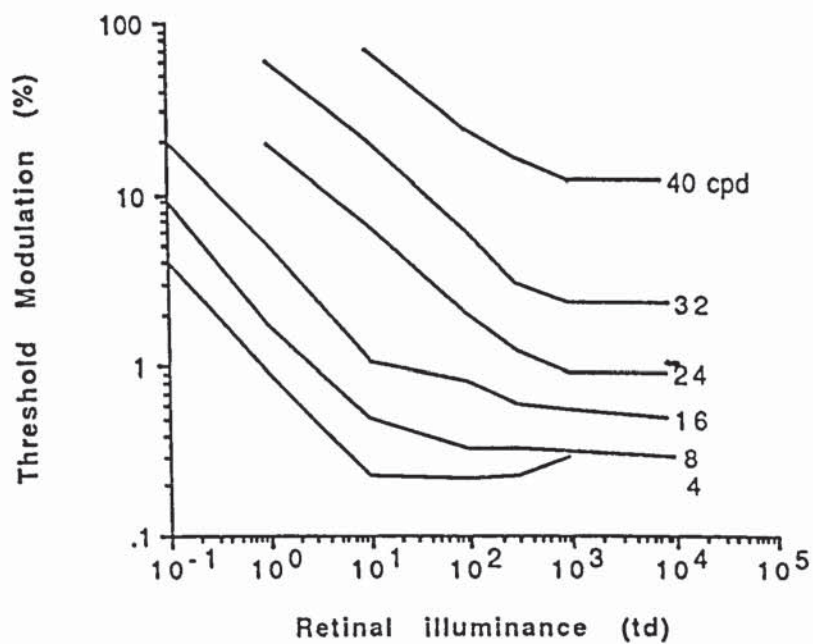


Figure 2.4 The dependence of threshold modulation on retinal illuminance for seven spatial frequencies (40, 32, 24, 16, 8 and 4 cpd). Each pair of data points represent the average values of the measured supra- and sub-threshold modulations, respectively (van Nes and Bouman, 1967).

2.A.5. Low spatial frequency attenuation

Neural properties of the visual system, such as lateral inhibition, have been thought to be responsible for low spatial frequency attenuation (Kelly, 1975; Banks and Salapatek, 1976). As the stimulus area increases, contrast sensitivity to low spatial frequency increases. This can be partly attributed to the increase in receptive field size with eccentricity. The level of low spatial frequency attenuation is also affected by the number of cycles present in the viewing field. Contrast sensitivity is dependent on the number of cycles in the viewing field (Hoekstra et al, 1974; Savoy and McCann, 1975). The critical number of cycles that must be present in the viewing field has been quoted as eight (Hoekstra et al, 1974), six (Robson, 1966), five (Savoy and McCann, 1975) and four (Campbell and Robson, 1968). Sensitivity to low spatial frequencies is also improved with increasing temporal modulation of the stimulus (Kelly, 1977; Robson, 1966). If the grating's bars are modulated in counterphase at temporal frequencies equal to or greater than 6Hz there is no low frequency attenuation (Figure 2.5).

2.B. Spatial frequency channels

It has been suggested that the visual system acts according to Fourier principles and that information about the sinusoidal components of an image is transmitted separately through neural channels called spatial frequency channels (Campbell, 1979). There have been many experimental techniques that provide evidence of a limited number of spatial frequency selective channels underlying the CSF.

Adaptation of a spatial frequency channel means that if stimulation of a channel occurs it renders that channel less sensitive to subsequent stimulation for some period of time. Adaptation of a psychophysical channel is directly analogous to adaptation of

photoreceptors to light. Adaptation of these channels can suggest how many spatial frequency channels there are underlying the human CSF.

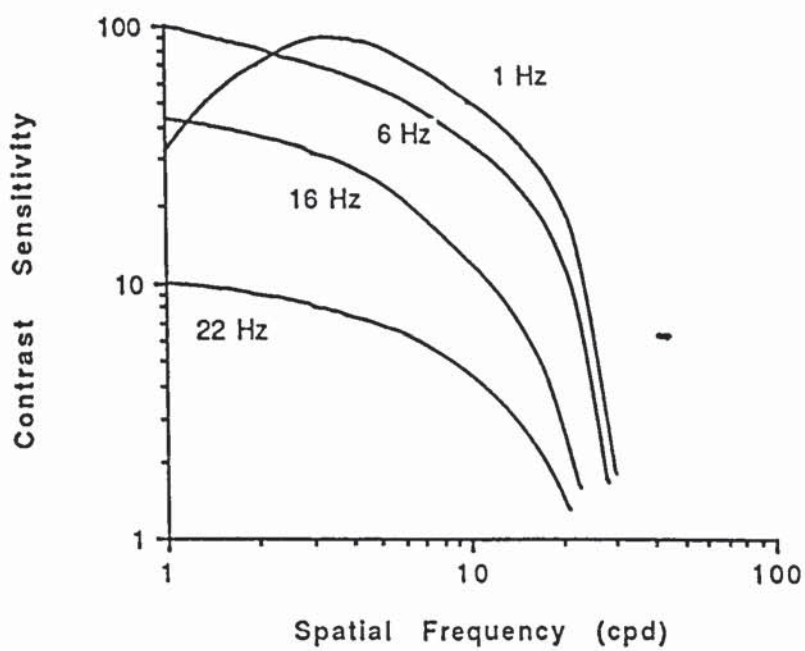


Figure 2.5 The Contrast Sensitivity Function curve for different temporal frequencies (After Robson, 1966).

If at one extreme the CSF reflected the sensitivity of a single channel, then adaptation at one spatial frequency should reduce sensitivity at all visible frequencies. At the opposite extreme adaptation at one frequency would reduce sensitivity only to that frequency. In reality adaptation to a single spatial frequency reduces sensitivity to a range of spatial frequencies surrounding the adapting frequency (Blakemore and Campbell, 1969).

By investigating the difference between numerous pairs of spatial frequencies it is possible to estimate the number and shape of the underlying spatial frequency channels. Watson and Robson (1981) used this method to obtain an estimate of seven selective mechanisms or channels.

The idea that gratings should interact if their spatial frequencies are similar enough to stimulate the same mechanisms has considerable support. Firstly, if two sinusoidal gratings are presented to the same patch of retina at subthreshold contrast, they may summate the same underlying spatial frequency channel. If the two gratings are far apart spatially they may stimulate different channels and consequently no summation will occur. Experiments using this subthreshold summation technique indicate that gratings show summation if their spatial frequencies differ by less than a 2:1 ratio (Graham and Nachmias, 1971). Frequencies that are much farther apart may inhibit each other (Olzaf and Thomas, 1981). Secondly, if the threshold for a test grating of one spatial frequency was raised by the presence of a second masking frequency that masking frequency would stimulate the same channel as the test frequency. In masking experiments, gratings mask each other when their spatial frequencies differ by less than a factor of 2. Again this method estimates the number of underlying mechanisms which are similar to those obtained by other methods (e.g., six channels (Wilson et al, 1983)).

Different studies produce different estimates of the number and shape of spatial frequency channels but the average estimate is between six to eight channels. The shape of the CSFs for these channels appears to be roughly parabolic when plotted on logarithmic coordinates. The width of these channels at half height appears to be 1 octave (i.e., a channel that responds maximally to, say, 8cpd would at 6 and 12cpd respond with half the maximal value). The set of spatial frequency channels can be thought of as filters that can selectively attenuate any component of specific frequencies. The CSF is the sum of all those filters. If the filtering of an input stimulus for any system is altered the output changes. Deviation from the normal CSF therefore would produce deviations from normal vision.

2.C. Methodology of threshold measurement

2.C.1 Threshold

To measure a contrast sensitivity function the minimum detectable contrast is determined for a variety of spatial frequencies. Sensitivity is defined as the inverse of the minimum contrast. Sensitivity plotted as a function of spatial frequency gives the contrast sensitivity function. The first difficulty is to define “minimally detectable”. It is not correct to assume that there is some contrast above which a particular stimulus is visible and below which it is not. Figure 2.6 shows hypothetical results from an experiment. Many repetitions are recorded at each contrast level and the percent of the detected stimuli is plotted as a function of contrast. Results have the characteristic sigmoid shape. The observer could give a 100% correct response simply by stating that the stimulus was present at each trial thereby rendering the method unreliable. Reliable tests of contrast sensitivity require a method to counteract the effect of guessing. Two possible stimulus locations could be presented to the observer. The observer would then be asked to state which of the two contained the stimulus. For each presentation one location would contain a grating of some contrast and the other

contain a blank grey field of the same average luminance. The two locations could be separated in space or in time. In this method the observer would be forced to make a response. Guessing will produce correct answers to 50% of the stimuli presented. Hypothetical results are shown in Figure 2.7. There is no exact threshold but a fixed criterion level can be picked (e.g., 75%). This method contains a correction for guessing and therefore more reliable comparisons can be made.

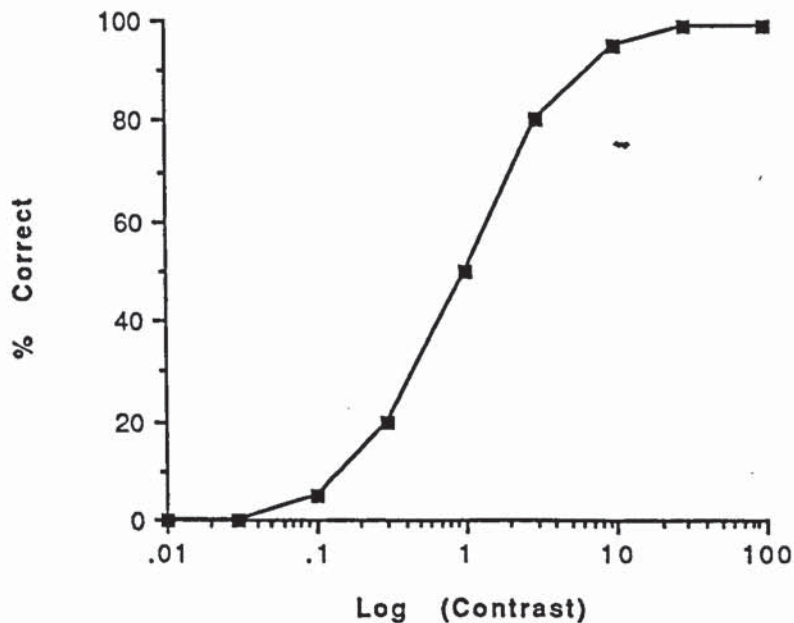


Figure 2.6 In this contrast sensitivity experiment the observers ability to detect the stimulus increases as the contrast of the stimulus increases. Contrast threshold is an arbitrary point on this function. (After Wolfe, 1990)

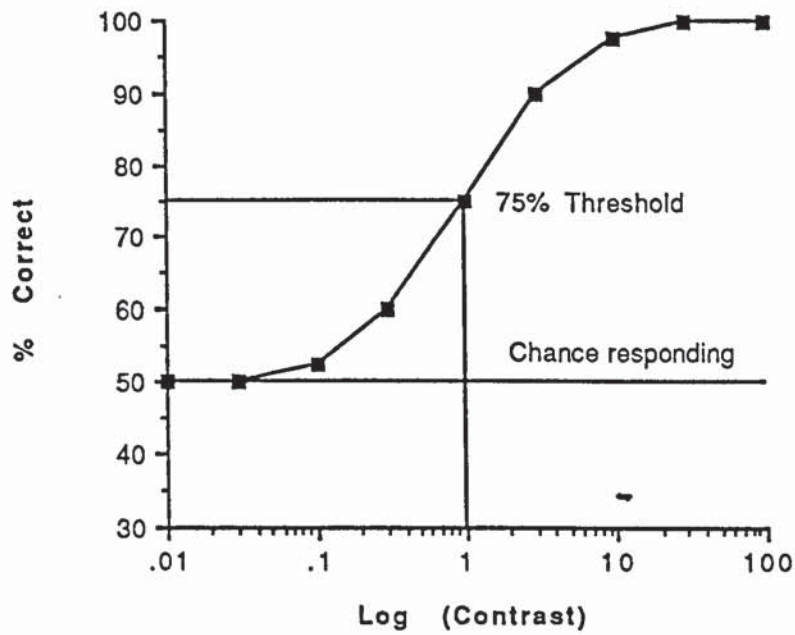


Figure 2.7 The two alternative, forced-choice method is used to measure contrast threshold. There is no exact threshold but a fixed criterion level can be chosen (e.g., 75%). This method is criterion-free and therefore more reliable comparisons can be made. (After Wolfe, 1990).

The method is known as two alternative, forced-choice method (2-AFC). The threshold could be measured at different spatial frequencies and at a range of contrasts for each frequency. Curves as shown in Figure 2.7 would be generated for each frequency, an arbitrary 75% point would be estimated, and a set of 75% points would serve as the CSF. The process, however, is very time consuming. By reducing the accuracy of the 2-AFC technique slightly, a substantial saving in time can be achieved. One such method is called the staircase method. For example, if an observer detects a stimulus in a contrast sensitivity experiment then the contrast of the stimulus is lowered by one measurement step and if the observer does not see the stimulus, the contrast is raised by one measurement step. The staircase will locate the 50% point on a function such as the one shown in Figure 2.6. This version of the staircase method is subject to errors due to guessing. The 50% point is the chance response level and is not useful. For the two alternative, forced-choice case it is better to decrease contrast if the observer makes two correct responses at a given contrast level (Heinemann 1961) and to increase contrast if the observer makes one incorrect response. For example (Figure 2.8), the contrast modulation starts at 100%. It is decreased to 30% after two correct responses, to 10% after two more, and to 3% after two more. If at 3% the observer fails to detect the stimulus the staircase goes back up to 10%, and so on. This staircase will estimate the 70.7% point on a two alternative, forced-choice function such as shown in Figure 2.7. By averaging the peaks and troughs of the function shown in Figure 2.8 the threshold estimate is obtained. It is important that the contrast steps be equal. A staircase is usually run for a fixed number of peaks and troughs (reversals). The accuracy of the threshold estimate improves with the number of reversals.

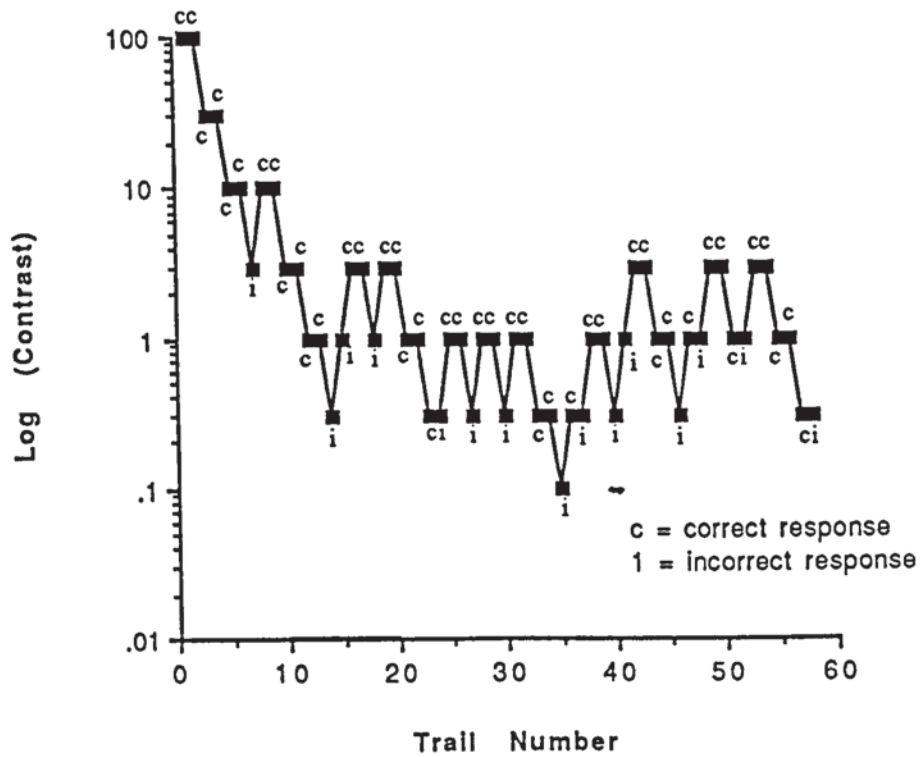


Figure 2.8 The staircase method. If the stimulus is detected on two successive occasions, the contrast of the stimulus is decreased and if the stimulus is not detected the contrast of the stimulus is increased. The staircase will eventually oscillate around the threshold. (After Wolfe, 1990).

2.C.2. Stimulus variables

It is important that stimulus variables be held constant so that contrast sensitivity measurements can be comparable one to another. Van Nes and Bouman (1967) noted that as mean luminance increased contrast sensitivity also increased. Contrast sensitivity also improved as the size of the stimulus increased (Hoekstra et al, 1974; Savoy and McCann, 1975). Acuity and contrast sensitivity for medium and high frequencies decline rapidly from the fovea to the periphery (Westheimer, 1979), therefore contrast sensitivity varies with retinal location. Acuity and contrast sensitivity also vary with the orientation of the stimuli (Zemon et al, 1983). Temporal factors affect the CSF (Henning, 1988). The timing of the onset of the stimulus may affect measurements; contrast sensitivity at a low frequency is likely to be enhanced by abrupt stimulus onset. This effect can be minimized by having the stimuli appear and disappear slowly. Contrast sensitivity is also affected by refractive state and pupil size. Defocus has a predictable effects on all frequencies (Westheimer, 1964; Mitchell and Wilkinson, 1974; Legge et al, 1987). Pupil size has two primary effects. Retinal light level varies with pupil size and large pupils introduce larger optical aberrations. Intermediate pupil size (2-5 mm) provides the best acuity and contrast sensitivity (Leibowitz, 1952; Campbell and Green, 1965).

CHAPTER 3 DIRECT AND INDIRECT MEASUREMENTS OF INTRAOCULAR LIGHT SCATTER

3.A. Indirect method (Equivalent veiling method)

3.A.1 Introduction

Intraocular light scatter corresponds to the amount of light reaching the retina that does not contribute to normal image formation. Light rays are converged by the refracting surfaces of the eye to a focal point on the retina. Some of the rays are dispersed to other areas by optical imperfections of the eye which may be multiple. This occurs especially in cataract, corneal dystrophy and when floating particles are present in the anterior or posterior chamber. The dispersed rays are distributed all over the retina, in decreasing density at distances further away from the original focal point. Because of this redistribution of light the image of a point object is no longer a point, the light is more spread and this is described by the point spread function. The image of a bright point object formed by a perfect optical system of circular aperture is not just a point but consists of a central bright circular disc (Airy disc) surrounded by alternating dark and bright rings of decreasing intensity. The size of this diffraction pattern decreases and approximates more and more to a point as the aperture of the system increases. Therefore, the explanation of the point spread function is diffraction by the pupillary aperture as well as the fact that the optical media scatter the light.

The point spread function can be divided into two components, focused light and stray light. The central part up to 10 minutes of arc has been studied optically by Campbell and Gubisch (1966) using the retinal image of a line observed ophthalmoscopically. The peripheral flanks of the point spread function are too weak to be easily studied in this way. This part can be referred to as stray light which can be quantified by means of the point spread function. The amount of stray light falling at

a given distance from the centre of the retinal image is usually specified in terms of the equivalent veiling luminance, L_{eq} . This is the luminance of veiling light which will have the same effect on the absolute threshold at that part of the retina as the stray light produced by the point source. This indirect method of measuring stray light was called the equivalent veil technique (Cobb, 1911). The technique assesses the amount of stray light falling at the fovea when the beam of light producing the stray light is at the glare angle, θ (Figure 3.1):

$$L_{eq}/E_{gl} = f(\theta) \quad [3.1]$$

Where L_{eq} is the equivalent veiling luminance and E_{gl} (lux) is the illumination on the observer's eye. If a glare source is at a given glare angle θ and the relationship between L_{eq} and E_{gl} is constant for varying values of illumination this would show that stray light is the limiting factor on the absolute threshold for that particular point on the retina. For example, doubling the amount of light reaching the eye should result in a doubling of stray light. If the proportionality between L_{eq} and E_{gl} was not constant this would indicate some type of neural input. Investigation into the relationship between L_{eq} and E_{gl} has shown that the proportionality between L_{eq} and E_{gl} is constant (Holladay, 1926; Holladay, 1927; Stiles, 1929a; Stiles and Crawford, 1937; Le Grand, 1937).

More recently there have been studies that have shown some deviation from the exact linearity between L_{eq} and E_{gl} . Vos (1962) investigated the equivalent veil technique using an experimental set up that encouraged neural interaction. The angle of the glare source from the line of vision was small (30 minutes of arc). Thresholds were measured when both the test object and the glare source were presented peripherally and also centrally. Vos (1962) found that in the peripheral retina, linearity between L_{eq} and E_{gl} held while centrally there were deviations from the exact linearity when luminance levels were low (Figure 3.2).

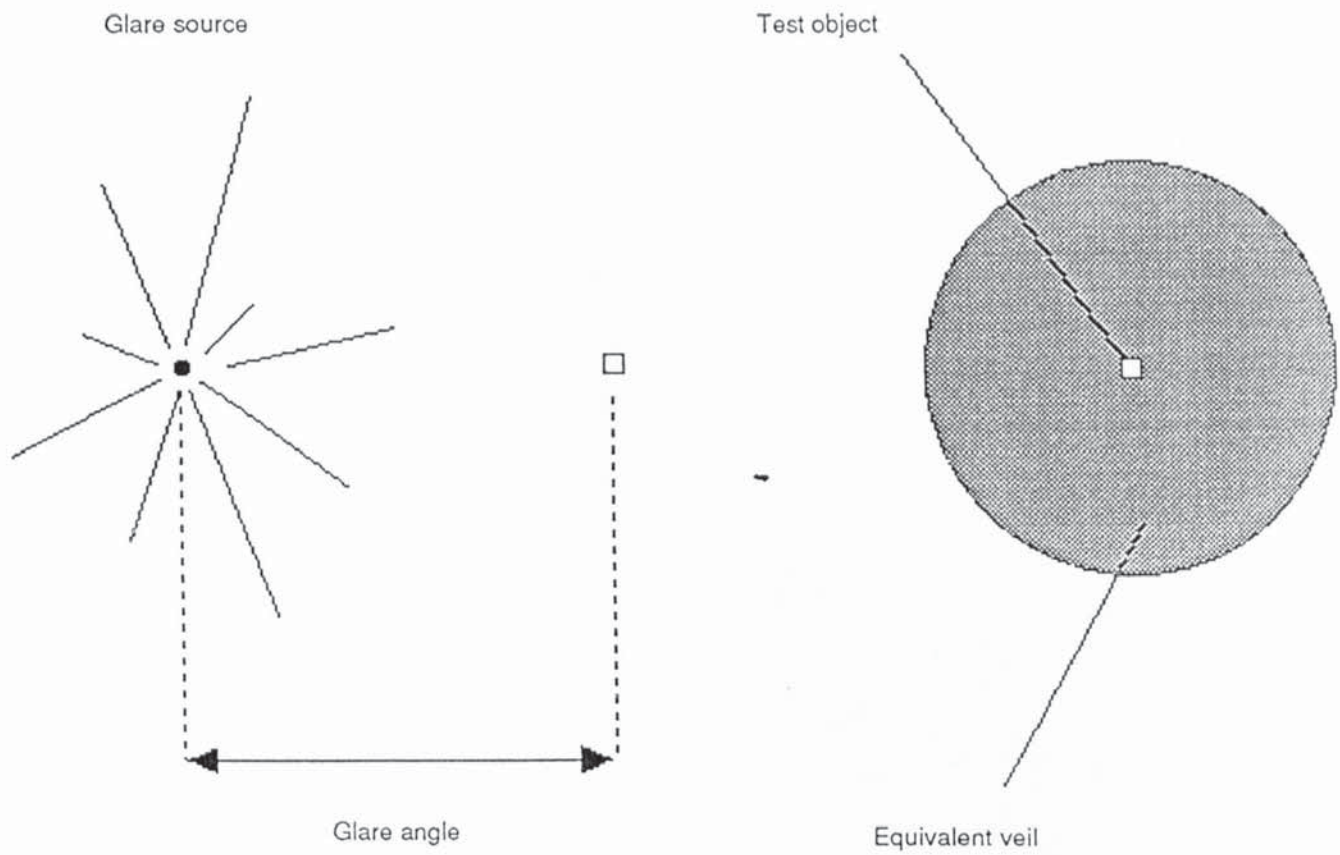


Figure 3.1 Equivalent veil technique. A comparison is shown between the effect of a glare source (left) and of a veiling luminance (right) (After Vos, 1984).

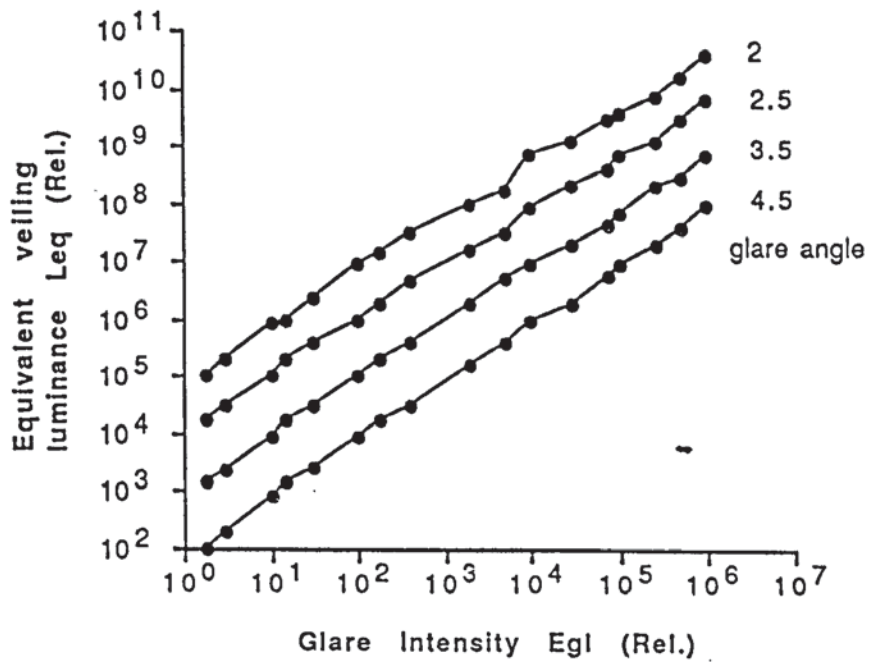


Figure 3.2 Equivalent veiling luminance against glare intensity as a function of four different glare angles (2, 2.5, 3.5 and 4.5°). Luminance and intensity units are arbitrary (After Vos, 1984).

The level of luminance where the deviation from linearity occurred coincided with the luminance levels at which retinal function changed from being mainly cone function to rod function. Vos (1984) speculated that cone sensitivity and rod sensitivity to stray light might differ and therefore, when changing from one threshold level to another changes in linearity could occur. Such studies point to the overwhelming dominance of stray light as a cause of the masking effect of glare.

As already mentioned, the value L_{eq}/E_{gl} is constant for any stated glare angle, but as the glare angle varies so does the value L_{eq}/E_{gl} . This angular dependency has been investigated and the scatter function, $f(\theta)$, has been found to be inversely proportional to the glare angle squared:

$$f(\theta) = k\theta^{-n} \quad (\theta \text{ in degrees}) \quad [3.2]$$

n = scatter index, k = stray light coefficient.
in the normal eye, $n = 2$ and $k = 10$.

This relationship is called the Stiles-Holladay formula (Holladay, 1926; Holladay, 1927; Stiles, 1929a; Stiles and Crawford, 1937). The formula does not hold for every glare angle. The equivalent veiling method is satisfactory for measuring the scatter function for values of θ greater than 2° , but is not satisfactory for smaller angles (Fry, 1965). Therefore for very small glare angles the relationship between the amount of scattered light and glare angle must change from the Stiles-Holladay formula. At $\theta = 0^\circ$; the Stiles-Holladay formula would predict an infinite amount of stray light, but the amount of light must be finite. Some experimental studies have examined the amount of light produced at these very small angles. Using direct photometry of the retinal image, Campbell and Gubisch (1966) determined the point spread function in the region between $\theta = 0^\circ$ and $\theta = 0.1^\circ$. Further studies using different techniques were able to investigate the angular dependency of stray light at small angles. Using colour induction experiments (Walraven, 1973) indicated that, at $\theta = 0.15^\circ$, the increase in steepness ceased. Vos and co-workers (Vos et al, 1976) linked together all data to one

complete function, $f(\theta)$, which can be described by the following equation (Figure 3.3):

$$L_{eq}/E_{gl} = 10/(\theta + 0.02)^2 + 10/(\theta + 0.02)^3 + 10^6/\exp(\theta/0.02)^2 \quad [3.3]$$

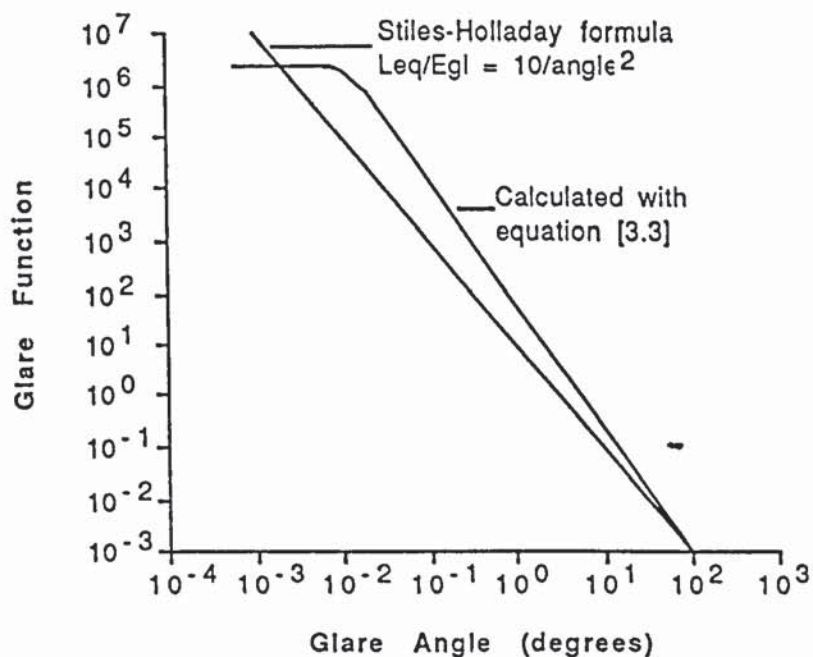


Figure 3.3 Glare function $f(\theta)$ is plotted against glare angle θ (After Vos, 1984).

3.A.2 Contrast sensitivity testing and glare testing



Although a scene may be sharply in focus on the retina the presence of an additional light source flooding the retina reduces the apparent contrast of the scene. Disability glare is the term used to describe the contrast lowering effect of intraocular scattered light on a visual scene. In 1927, Holladay published the first quantitative data on the masking effect of the visible halo around glare sources. This was expressed in terms of an equivalent veiling luminance (L_{eq}), that would produce the same masking effect. Vos (Vos, 1962; Vos and Boogard, 1963; Vos et al, 1976) realised that intraocular light scatter produced the veiling light, and by using glare sources was able to quantify the equivalent veil effect (see 3.A.1). This was used as the basis for calculation of the LSFs of Paulsson and Sjöstrand (1980). Paulsson and Sjöstrand (1980) combined contrast sensitivity measurement with a quantitative assessment of intraocular light scatter using glare lights. They derived an expression for a Light Scattering Factor (LSF) where

$$LSF = \frac{L}{E} \left(\frac{M_2}{M_1} - 1 \right) \quad [3.4]$$

where L = luminance of target screen

E = direct illuminance onto the eye of the glare light

M_2 = detection contrast threshold with glare light

M_1 = detection contrast threshold without glare light

The LSF was a direct measure of intraocular light scattering. The patient's CSF was measured using a cathode-ray tube (CRT). A bright light source was introduced into the field of vision and the resulting decrease in the CSF was measured. The LSF was then calculated from the results. Five normal controls (age 30-61 years) and six patients with posterior subcapsular cataract (age 46-68 years) were used. Results showed a loss of contrast sensitivity at low and medium spatial frequencies in patients

with cataract compared to the controls. With the addition of a glare light, the normal subjects showed no significant decrease in contrast sensitivity, whereas the CSF was markedly decreased in cataract patients. Depression in the CSF was most distinct at low and medium spatial frequencies. The LSF was a convenient measure of intraocular light scattering and was found to vary between cataract patients with the same visual acuity. Paulsson and Sjöstrand (1980) concluded that their method of measuring threshold with added glare light gave a quantitative measure of a patient's intraocular light scatter which might prove useful as a clinical vision test.

Glare is due to light scattering in the eye and unwanted stray light is present in the normal eye. This unwanted stray light interferes with the contrast of the retinal image and increases the background light level. The main source of intraocular light scatter within the normal eye is the crystalline lens and the intensity of stray light decreases with angle from the glare source.

As already stated, intraocular light scatter produces a loss of contrast. This loss of contrast is difficult to derive from tests of visual acuity. Where intraocular light scatter causes a veiling luminance, the modulation depth of the sine grating reduces. As a result the whole spatial modulation transfer function drops. Visual acuity correlates closely to the 100% contrast cut off point and this is located at the steepest part of the curve. As the whole function drops the change in visual acuity is less than the change in contrast sensitivity. In the example shown in Figure 3.4, visual acuity drops by a factor of 1.8 as opposed to a drop in contrast sensitivity by a factor of 10. Therefore visual acuity tends to underestimate the visual loss due to contrast loss. This assumes an equal loss of contrast sensitivity at all spatial frequencies.

Abnormality of the eye e.g. retinal oedema, vitreous floaters, cataracts, aqueous flare and epithelial or stromal oedema will dramatically increase the amount of light scattered onto the retina and thereby produce glare conditions.

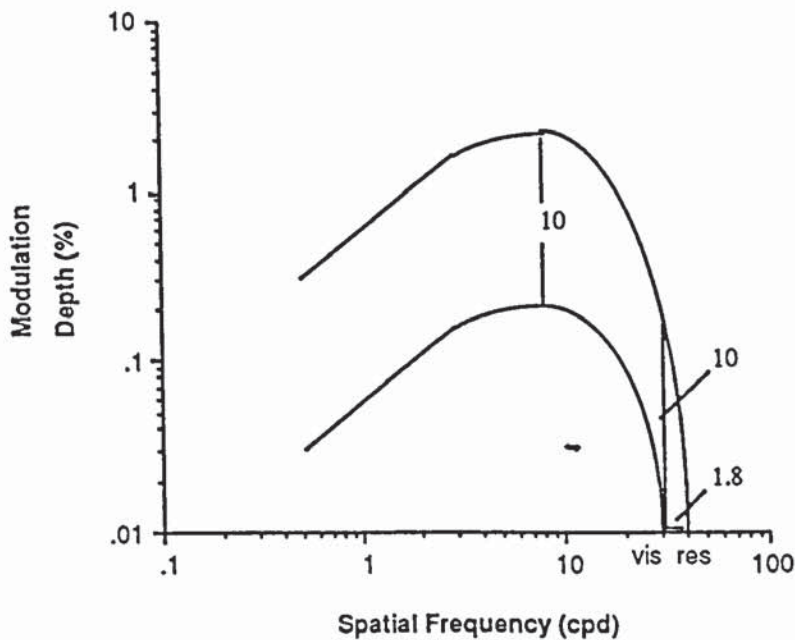


Figure 3.4 Spatial Contrast Sensitivity Function (CSF). Threshold modulation depth for sinusoidal gratings is plotted on the y-axis. Modulation depth is defined as $(I_{\max} - I_{\min}) / (I_{\max} + I_{\min})$. Along the x-axis the spatial frequency of the sinusoidal grating is plotted, defined by $1 / (\text{angular subtense of one cycle})$ in cycles per degree (cpd). The high frequency tail falls off by 4 log units per log unit of spatial frequency, which is a mean value found in literature. This Figure demonstrates that reduction in contrast sensitivity is associated with much smaller reductions of spatial resolution (visual acuity), which is determined by the intersection of the CSF with the x-axis. (After van den Berg, 1986).

3.A.3. Cataract

It has been known for some time that cataract affects the CSF (Hess and Woo, 1978). Skalka (1981) showed that, when assessing early posterior subcapsular cataracts, some patients demonstrated substantial loss of contrast sensitivity using the Arden grating test, yet these patients maintained relatively normal high-contrast visual acuity. Contrast sensitivity measurements correlate better with patients' visual complaints than does Snellen acuity (Elliott et al, 1990a). Karbissi et al (1993) showed in addition, that disability glare measurements correlate better with patients' visual complaints than contrast sensitivity measurements. Contrast sensitivity measurements can be dramatically affected by including a glare source. Paulsson and Sjöstrand (1980) demonstrated the devastating effect a glare source can have on the contrast sensitivity curve in the presence of an early cataract. Abrahamson and Sjöstrand (1986) confirmed these findings in subsequent experiments on a larger sample of cataract patients. Because of the clinical difficulties in measuring contrast sensitivity as compared to visual acuity the technique has not been incorporated into routine clinical testing.

Miller et al (1972) developed a simple glare tester for clinical settings. It consisted of a tabletop slide projector used to display a series of 35mm slides. Each slide contained a central black Landolt C ring surrounded by a grey background that was surrounded by a glare source. The luminance of the background was progressively reduced until the orientation of the ring opening was no longer detected. Luminance corresponded to the contrast threshold. Many studies have subsequently used this glare tester (Le Claire et al, 1982. Miller et al (1972) found that in normal subjects, glare sensitivity increased with age. Aphakic patients were found to be more sensitive to glare than were normal subjects. Cataract patients showed increased glare sensitivity but no correlation was found between near visual acuity and glare sensitivity (Le Claire et al, 1982; Hirsch et al, 1984(a); Hirsch et al, 1984(b); Neumann et al, 1988). Le Claire

and co-workers also found high levels of glare sensitivity in patients with subcapsular cataract. Increased glare sensitivity was also found in patients with anterior cortical spokes encroaching into the pupillary aperture. The smallest increase in glare sensitivity secondary to cataract was found in pure nuclear sclerosis. The Miller glare tester was also used to assess cataract patients' outdoor visual acuity when facing the sun; it was found that the glare tester was significantly better at predicting outdoor visual acuity than was Snellen acuity (Hirsch et al, 1984(a); Hirsch et al, 1984(b)). Neumann et al (1988) correlated the results from the Miller-Nadler tester with outdoor acuity in a sample containing a variety of types of cataract. Different types of opacity showed different levels of glare sensitivity, but some patients with pure nuclear sclerosis did not have reduced glare sensitivity although they did have poor Snellen acuity outdoors. Glare testers are sometimes an imprecise predictor of outdoor acuity in cataract patients.

The Brightness Acuity Tester (BAT) (Holladay et al, 1987) simplified glare testing for clinicians by allowing subjects to view the standard eye chart. The glare source on the BAT is an illuminated hemisphere bowl 60mm in diameter with a 12mm aperture through which the patient views the eye chart. Three luminance settings of the BAT simulate conditions of bright indoor lighting, overcast skies and bright sunlight.

The glare testers used are each slightly different and there is a lack of standardisation. Comparing results obtained using different glare testers is very difficult. The glare sensitivity of each test varies with type and size of the target and the position, brightness and type of glare source. Smith et al (1987) published a comparison of the Miller-Nadler glare tester and the Brightness Acuity Tester which illustrates the problem of comparability. When assessing the decrease in Snellen acuity for patients with cataract both devices compared well, yet when assessing patients with posterior subcapsular opacities the BAT showed a much greater glare sensitivity than the Miller-Nadler glare tester.

Other types of glare tester involve the use of a single bright light off the visual axis as a glare source; the rationale behind this choice of glare source is that it resembles a more real life environment i.e., vehicle headlights (Koch, 1988). One disadvantage with this type of glare source is that with inexperienced observers the subject may momentarily lose fixation and glance directly at the glare source. This could affect macular function resulting in decreased contrast sensitivity adding to the decrease in contrast sensitivity due to the veiling luminance thus producing an increase in disability glare measurements.

Finally one of the most common glare tests used in clinical practice to examine cataract patients is the penlight test. The examiner shines a penlight into the subject's eye off the visual axis and the subject reads the eye chart (Maltzman et al, 1988). This test is quick, inexpensive and easily understood by the patient but it lacks accuracy and reproducibility. Major factors which effect the level of disability glare measured, such as the luminance of the glare source, the distance of the glare source from the patient, the glare angle and the luminance of the target are difficult to control in this test.

3.A.4. Pseudophakia

Because of the increasing prevalence of extracapsular cataract surgery and intraocular lens implantation there has been increased interest in the effect these procedures have on visual function and on the amount of induced intraocular light scatter. Capsular opacification, intraocular lens design and malpositioned lens implants can all sometimes result in significant visual loss (Hard et al, 1993; Claesson et al, 1994; van den Berg and IJspeert, 1991; Sunderraj et al, 1992). Glare and contrast sensitivity testing could be important methods for evaluating visual complaints related to both pseudophakia and aphakia.

Miller and Lazenby (1977) using a glare tester similar to the Miller-Nadler tester found that the mode of correction for aphakia does not affect glare sensitivity and whether the patient was aphakic or not did not result in any significant difference in glare sensitivity.

Coupland and Kirkham (1981) reported that pseudophakic eyes produced 2.3 times more light scatter than normal phakic eyes. They concluded that the reason for this increase in light scatter could be due to the fact that the refractive index of the IOL (1.492) differed from that of the human lens (1.386). Also in the human lens the refractive index increases gradually from the outside of the lens to the core, reducing optical reflections. Le Claire (1982) measured glare sensitivity on normal phakic subjects, spectacle corrected aphakic patients, and patients with either Copeland-style PMMA lens implant or with the Lynell glass lens implant. Patients with corrected aphakia were all more glare sensitive than the phakic controls. Both of the lens implants were of the iris-supported type. These lens implants can sometimes demonstrate optical distortion in the pupillary area and this could have produced significant intraocular scatter.

Weatherill and Yap (1986) found no difference in contrast sensitivity attenuation among 73 patients with anterior-chamber, iris-supported or posterior-chamber intraocular lenses and concluded that contrast loss in pseudophakic eyes was likely to be independent of lens design.

Hammer et al (1986) found that the contrast sensitivity of patients with UV absorbing lens implants did not differ from that of patients with non-UV absorbing lenses. Using the Miller-Nadler glare tester, Koch et al (1986) found no measurable advantage of UV filters and no measurable differences between spheric and aspheric intraocular lens design. However, the transmission characteristics of intraocular lens implants

differ from the normal human lens and particularly in an older lens with nuclear sclerosis.

Capsular opacification in pseudophakic patients is a common cause of disability glare and/or impaired contrast sensitivity (Nadler et al, 1984). Nadler and colleagues conducted a postoperative follow-up of patients undergoing extracapsular cataract extraction and posterior chamber lens implant. A highly statistically significant association was found between glare sensitivity and degree of opacification. Mild to moderate non-uniform clouding and Elschnig pearl formation on the capsule produced more intraocular light scattering than dense fibrous plaques. The plaques mainly reduced transmission of light and were most problematic when situated within the pupillary aperture. Drill holes and edges from decentred lens implants were also shown to produce disability glare. Following YAG capsulotomies significant improvements in disability glare, contrast sensitivity and Snellen acuity have been found (Knighton et al, 1985; Claesson et al, 1994). The optimal size of a posterior capsulotomy is dependent on individual variations in pupil size across a range of luminance levels. In theory, larger capsulotomies are less problematic as they will not limit visual performance by diffraction and will allow the pupil to regulate image intensity.

Other problems are more difficult to manage compared to capsular opacification. Lens decentration presents many visual difficulties especially relating to increased glare sensitivity. Brems et al (1986) examined 75 post mortem eyes containing posterior chamber intraocular lenses. In 71% of cases, a lens edge or element of the optic was positioned either within the pupillary aperture or within 0.5 mm of the pupillary margin. Such problems could be overcome by using larger lens diameters, fewer positioning holes and a matte finish for the edge of the lens implants. Apple et al (1987) noted that even well-centred lenses can produce increased glare sensitivity when pupillary dilation occurs and portions of the lens edge and positioning holes

become exposed. It must be emphasised that defects in the capsule and exposed lens elements are not always measurable with either glare or contrast sensitivity testing. Spindle-shaped deposits of epithelial cells on the posterior capsule and distortions caused by wrinkling or thickening of the capsule can produce light streaks which produce subjective complaints but are difficult to measure objectively.

Glare testing and contrast sensitivity testing in cataract and pseudophakic patients is important as it enables the clinician to document and quantify disability when standard vision testing does not. Glare and contrast sensitivity testing can substantiate patients' visual complaints and it must be remembered that it is the impact of these visual disabilities on the patient's environment which remains the crucial factor in the decision to perform cataract surgery or laser capsulotomy.

3.B. Direct method (Direct compensation method)

A perfect optical system of circular aperture does not form a point image from a bright point object. As stated in Section 3.A.1 because of the wave nature of light, it consists of a central bright circular disc (Airy disc) surrounded by alternate dark and bright rings of decreasing intensity. Therefore the optically-ideal point spread function is the Airy disc. The presence of intraocular light scattering causes its shape to widen and especially the wide-angle part to rise, at the cost of the central part (Campbell and Gubisch, 1966).

The peripheral part of the point spread function i.e., $\theta > 1^\circ$, has been termed the 'stray light function' (van den Berg, 1986):

The normalized point spread function is approximated using the equivalent veiling luminance method L_{eq}/E_{gl} (see Equation 3.1). By introducing the Stiles-Holladay

approximation (see Equation 3.2) the resultant equation should be constant with changing glare angle:

$$\theta^2 \times \text{PSF} = \theta^2 \times L_{\text{eq}}/E_{\text{gl}} \quad [3.4]$$

The following equation is now called the stray light parameter (sm):

$$\text{sm}(\theta) = \log(L_{\text{eq}}(\theta) \times \theta^2/E_{\text{gl}}(\theta)) \quad [3.5]$$

Which is abbreviated to $L_{\text{eq}} \times \theta^2/E_{\text{gl}}$

The retinal point spread function and the optical transfer function of the eye are Fourier transforms of one another (Campbell and Gubisch, 1966), and are directly related to the contrast sensitivity function. Therefore investigations into the shape and form of the point spread function have direct relevance to studies involving the contrast sensitivity function as well as other parameters dependent on the optics of the eye.

Previously the amount of stray light was measured by matching the veiling effect produced by a bright light source located at a given angle with that of a patch of homogeneous light. Vos (1984) showed that the veiling effect produced by the light source was caused by intraocular light scatter. Different methods have been used to measure the effect of the veiling luminance (see 3.A.1). Vos (1984) used the threshold for detection of a flash of light, while Paulsson and Sjöstrand (1980) used the contrast threshold for sinusoidal grating targets. This later technique was used to measure stray light in patients (Abrahamsson and Sjöstrand, 1986; Elliott et al, 1989).

More recently some disadvantages of measuring intraocular light scatter by the equivalent veiling method have been suggested (van den Berg, 1986). One

disadvantage with the equivalent veiling method is that two threshold measurements have to be made and this could increase the amount of variance in the method. Another disadvantage involves the amount of time taken to obtain results, as many stimulus presentations are needed in this method. Thresholds may vary due to a change in the patient's criterion for detecting the threshold. Variation in the adaptation of the retina due to large variation in retinal luminance could also effect threshold values. Poor fixation could introduce relatively large uncertainties. Another method of measuring intraocular light scatter has been developed which is called the direct compensation approach. This method seems to avoid some of the above disadvantages (van den Berg, 1986; van den Berg and Spekreijse, 1987).

The direct compensation approach measures when the luminance from the stray light and the target luminance are equal. The target or equivalent patch of light and the stray light are both flickered in counterphase at a frequency which has high flicker sensitivity. The stray light source is a ring with the equivalent patch in the centre, which is fixated. When the luminance modulation of the equivalent patch is low flicker due to the stray light source can be detected. This flicker can be cancelled by varying the luminance modulation of the equivalent patch. In this way stray light is directly compensated. There is a small range of luminance values where this cancellation occurs; the luminance range depends on flicker perception threshold. The observer's task is to reduce or extinguish the flicker perception by varying the luminance of the counterphase flickering central patch of light. This luminance L_{eq} is by definition identical to the equivalent luminance describing the scatter function. With the direct comparison technique the spatial relationship between the stray light source and the test patch is unaffected by the fixation of the observer. Furthermore, changes in the sensitivity of the retina will not affect the result as long as the retina can detect flicker.

The accuracy of the direct comparison method is ± 0.05 log units (Ijspeert et al, 1990). This accuracy is adequate because the spread of stray light values in normals is 0.1 log units (Ijspeert et al, 1990), and even higher in patient populations (van den Berg et al, 1989; van den Berg, 1988; van den Berg and Boltjes, 1988).

Other important factors that affect the accuracy of the measurement of stray light using the direct comparison technique are the size of the test patch and the luminance of its surround. If the patch is too large then the target will not have a specific visual eccentricity relative to the stray light source i.e., the amount of stray light will vary across the test patch. If the patch is too small flicker sensitivity will be lost. The stray light produced does not only reach the test patch but also its surround; this decreases flicker sensitivity. By introducing a lighted surround flicker sensitivity improves but if the luminance of the surround is increased to too high a value, flicker sensitivity will decrease again.

Figure 3.5 shows the measured stray light function against the scatter angle in a Caucasian population between the ages of 25 to 75 years. The level of stray light measured in cataract patients is higher than in the normal population (van den Berg, 1986; van den Brom, 1990). Van den Brom (1990) found that the average stray light values for nuclear and cortical cataracts did not differ significantly and when plotted against the scatter angle the curve was no different from that of the normal population, except that the values lay 0.65 log units higher (Figure 3.6). Van den Brom (1990) also found a significant correlation between the reduction in contrast sensitivity due to disability glare and the stray light value in cataract patients. The direct compensation method showed that the amount of stray light measured in the normal population was not only dependent on the age of the subject but also varied with pigmentation. Ijspeert et al (1990) showed the lowest levels of stray light were found with dark-brown-irides in non-Caucasians, then brown-eyed Caucasians and the largest amount of stray light.

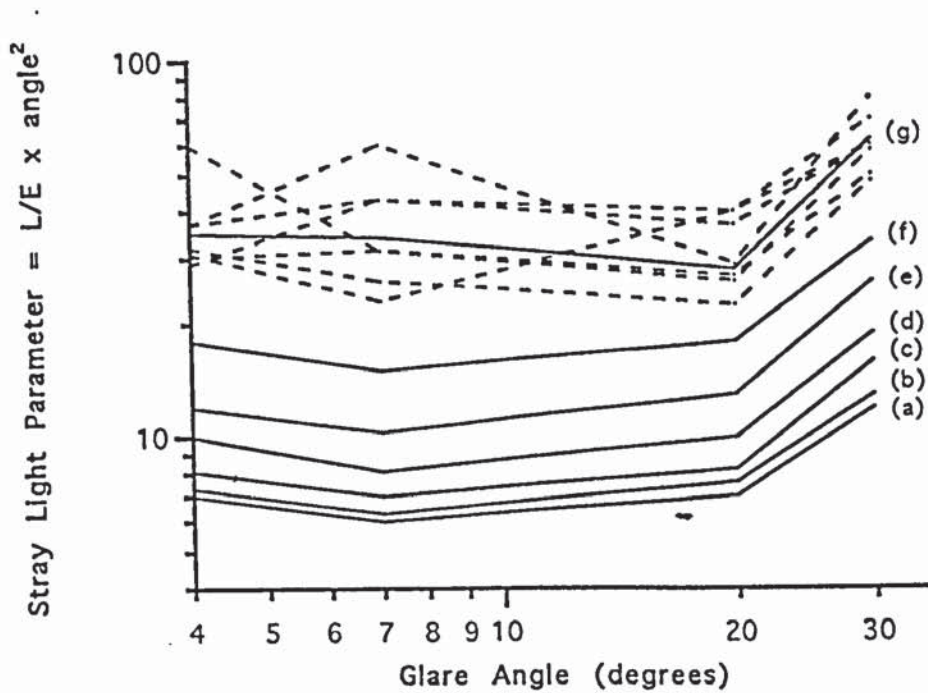


Figure 3.5 Solid lines: Caucasian population values for (a) 25 years, (b) 35 years, (c) 45 years, (d) 55 years, (e) 65 years and (F) 75 years of age. Line (g) represents a 70 year old patient with some corneal clouding due to herpes infection who was followed for one year. The solid line represents the mean of the results for each age group. Ophthalmologically the condition of the patient was stable, so the dashed lines give an impression of the reproducibility in this patient (After IJspeert et al, 1990; van den Berg, 1986).

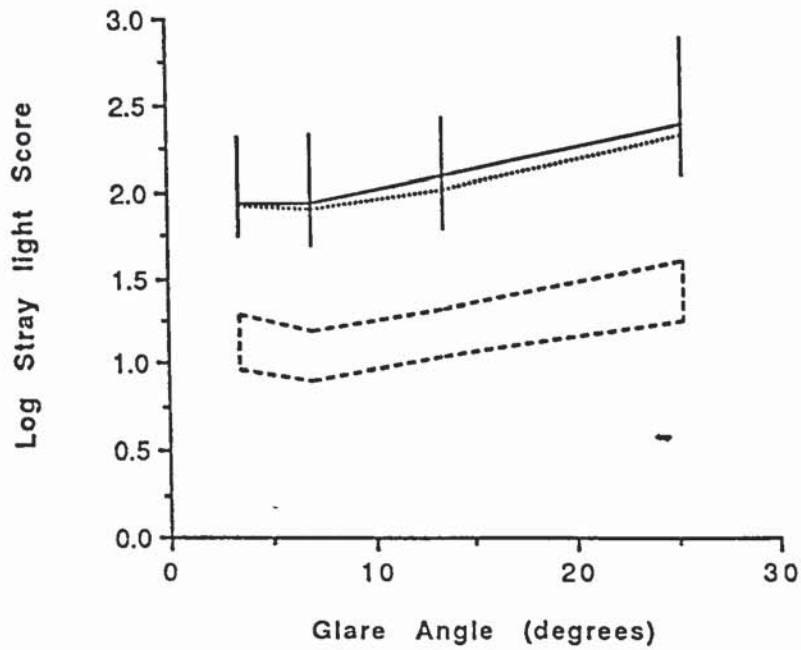


Figure 3.6 Stray light measurement for cortical (solid line) and nuclear (dotted line) cataract. The area enclosed by broken lines indicates the normal range. There is no significant difference between the cataract types. Stray light score represented as θ^2 . Vertical lines indicate one standard deviation (After van den Brom, 1990).

was measured in blue-eyed Caucasians, especially for larger angles of scattering. It is regularly accepted that the general pigmentation condition of the wall of the eye is related to the colour of the iris. As iris colour varies between subjects so does the pigmentation of the wall of the eye and thus so does the transmission of light through the wall of the eye. If the amount of transmission of light through the wall of the eye increases so will the amount of intraocular scatter.

As already stated the stray light parameter ($\theta^2 \times L/E$) should be constant with scatter angle if the Stiles-Holladay approximation is adhered to. If transmittance of the iris and the wall of the eye is important this would show up as an increase in the amount of stray light at larger angles. The reason for this is that the light transmitted through the iris and the wall of the eye, adding to the intraocular scattered light, would be effectively like a peripheral glare source producing mostly peripheral stray light. This increase in stray light was found at larger angles (Figures 3.5 and 3.6). Also this increase in stray light at larger angles was greater for more lightly pigmented eyes as compared to dark-brown eyes (Ijspeert et al, 1990). For light-blue eyes there was a significant amount of light transmitted through the iris. For the dark-brown eyes of pigmented individuals transmission through the iris is lower by two orders of magnitude (van den Berg et al, 1991). Van den Berg et al (1991) found that transmission proved to be only partly responsible for the pigmentation dependence and concluded that the other cause is probably reflection from the fundus.

CHAPTER 4 EFFECT OF GLARE ON LUMINANCE AND COLOUR CONTRAST SENSITIVITY

4.A. Introduction

The aim of this study was to investigate the effect of variable amounts of intraocular light scatter on luminance contrast sensitivity at various spatial frequencies. By artificially manipulating the amount of induced light scatter in the eye, accurate and consistent amounts of varying intraocular light scatter were achieved.

There has been very little interest in either colour identification, discrimination and sensitivity to colour variations in the presence of glare. Another aim of this study was to investigate the effect of intraocular light scatter upon colour contrast sensitivity. The amount of intraocular light scatter was artificially manipulated and the effect upon luminance contrast sensitivity was compared with the effect upon stimuli consisting of purely chromatic modulation. Also further studies were carried out to assess the effect of glare upon luminance contrast sensitivity and colour contrast sensitivity as a function of age.

In addition to the use of luminance information, the visual system is also concerned with colour variations within a visual scene. The contours and edges of objects are distinguished not only due to luminance variations relative to the background, but usually due to colour differences as well. It is of interest to consider whether the role of colour information becomes more important when luminance contrast becomes compromised, for example in the presence of disability glare. It is known that observers are quite capable of making very precise spatial judgements purely on the basis of chromatic information (Webster et al, 1990; Krauskopf and Farell, 1991). On the other hand, if chromatic sensitivity were to deteriorate markedly in the presence of

glare, it would provide an additional reason for the high level of subjective visual complaints associated with disability glare (Elliott et al, 1990a).

4.B. Effect of varying levels of induced intraocular light scatter on luminance contrast sensitivity at various spatial frequencies.

Methods

All stimuli were generated by a Venus Visual Stimulator and displayed on a standard colour cathode ray tube (CRT). The Venus Visual Stimulator (Neuroscientific Int, Farmingdale, USA) was used to generate all the stimuli used in the experiments. The equipment consists of a microcomputer coupled to a high resolution colour monitor running at 120Hz by means of which appropriate stimulus parameters are input and data is displayed. For the Venus Visual Stimulator there is a second monitor which is used to present results, stimulus information and program details. The stimuli were produced using application software written in Microsoft C by Dr. Whitaker. Figure 4.1 shows the equipment. At the viewing distance of 1.825 metres, the display subtended 5.5° square. A 4-alternative forced choice staircase technique was used to measure CS to horizontal static, black and white sinusoidal luminance gratings. The gratings were presented in one of four quadrants of the screen while the rest of the display was of the same mean luminance. The observer was required to respond as to which quadrant the grating appeared in. The observer was allowed unlimited time to respond via a keyboard. Contrast was ramped up in linear fashion and remained at a maximum until the observer responded, after which it ramped down to zero, again in a linear manner. Initial presentations were always clearly suprathreshold. A single correct response led to a reduction in contrast, whereas a single incorrect response led to an increase in contrast. The Initial step size was 0.15 log units, but this decreased to 0.075 log units after the first reversal.




Figure 4.1 The equipment used in conjunction with the Venus Visual Stimulator. The right hand monitor presents the stimuli. The observer responds by use of the keyboard.



The sequence continued in staircase fashion until seven reversals had occurred, after which the sequence terminated. Threshold was accepted as the mean of the last six reversal points. The mean luminance of the stimulus was 60 cdm^{-2} . Thresholds were measured for five spatial frequencies of 0.75, 1.5, 3, 6 and 12 cdeg^{-1} in a randomly interleaved fashion. Seven young normal experienced subjects were used (mean age 25.1 years $\text{SD}=2.1$; Gender Male (M)=3, Female (F)=4). All observers used in the experiments were visually normal with no history of ocular disease and acuities of 6/7.5 Snellen equivalent or better unless otherwise stated. Observers underwent a full ophthalmic examination before the experiment began. Exclusion criteria included systemic conditions with known ocular involvement, systemic medication with known Central Nervous System effects and past history of eye disease. Further, all had normal fundi and no lenticular opacity within the undilated pupillary area. All had intraocular pressures less than 21mmHg, normal central visual fields and ametropia below $\pm 5 \text{DS}$ and $\pm 2 \text{DC}$. Measurements were made using the dominant eye. All subjects were trained in psychophysical observation and were either students or staff of the Vision Sciences Department. Informed consent was obtained.

The commercially available Brightness Acuity Tester (BAT)(Mentor O&O Inc., Norwell, USA) (Holladay et al, 1987) was used as a glare source. This has the form of an illuminated hemispherical bowl (60mm diameter) which is placed close to the eye. It has a central aperture (12mm diameter) through which the stimulus is viewed. The glare source subtends from 5° to 50° visual angle at a vertex distance of 25mm (measured from the posterior part of the hemisphere to the cornea). The luminance of the glare source can be varied and has three levels of brightness, low luminance level, medium luminance level and the high luminance level (Table 4.1). The three glare settings representing bowl luminance values of 35, 264 and 1200 cdm^{-2} respectively were used. Different amounts of glare will have varying effect on contrast sensitivity

measurements. The chromaticity coordinates and colour temperature of the light emission at each of these luminance levels are shown in Table 4.1.

Table 4.1

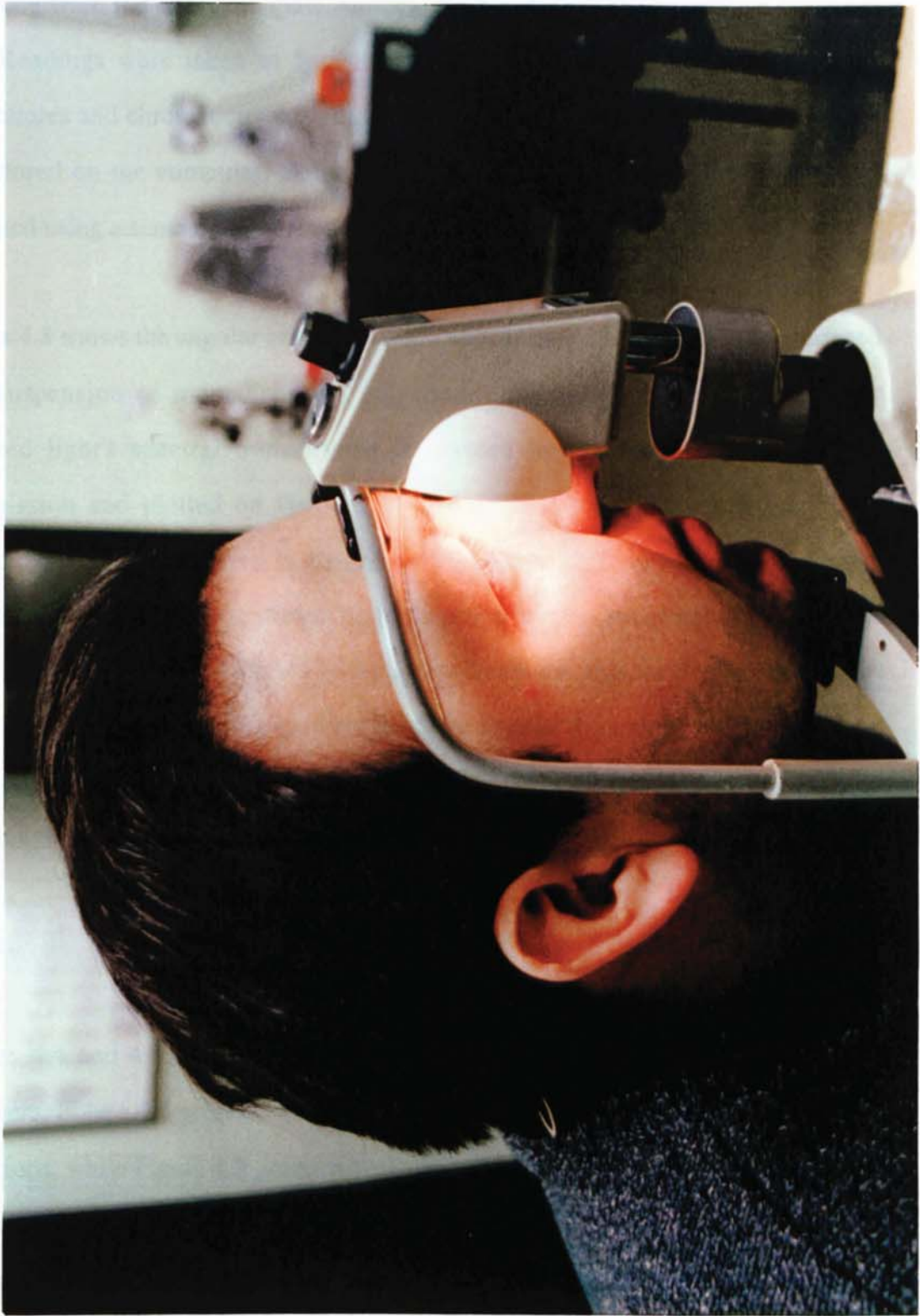
Luminance (cdm ⁻²)	CIE chromaticity co-ordinates	Correlated colour temperature
35	0.512,0.415	2139K
264	0.475,0.416	2596K
1200	0.439,0.407	2995K

The table shows the luminance in cdm⁻², its chromaticity coordinates and the colour temperature of the BAT (Figure 4.2).

Intraocular light scatter was induced artificially by placing optical cells containing suspensions of monodispersed polystyrene microspheres (Polysciences, Inc.) between the eye and the BAT. The mean diameter of the polystyrene microspheres was 500nm, which approximates to the size of scattering protein aggregates which produce significant stray light within the elderly human lens (Bettleheim, 1985). Varying amounts of stray light were produced by the use of different concentrations (0-0.16%) of the microsphere suspension and by using different glare levels. The Bentham computer controlled spectrophotometer was used to analyse the spectral characteristics of the scattered light produced by the suspensions of the monodispersed polystyrene microspheres. The methodology of this measurement is described in section 5.B.

-

Figure 4.2 The Brightness Acuity Tester (BAT). The observer views the stimulus through a central aperture (10mm diameter). The glare source subtends from 5° to 50° visual angle at a vertex distance of 25mm. The luminance of the glare source in this photograph was at the highest setting.



Throughout the following experiments a computer-controlled spectrophotometer (Bentham Instruments Ltd.) was used to measure the spectral distribution of light emanating from the CRT, the glare sources, the filters and also to analyse scattered light. Readings were taken at 5nm intervals from 300nm up to 800nm. Colour temperatures and chromaticity co-ordinates (CIE 1931) were established. The results were stored on the computer. Before each experiment the spectrophotometer was calibrated using a standard light source.

Figure 4.3 shows the angular and wavelength dependency of scattered light produced by a suspension of monodispersed polystyrene microspheres. In the graph the scattered light's spectral transmission is divided by the light source's spectral transmission and plotted on the y-axis. The angle of eccentricity at which the scattered light was measured is plotted on the x-axis. Different symbols represent selected wavelengths of scattered light recorded by the spectrophotometer. The gradient of the slope for each wavelength represents the angular dependency of the scattered light. The steeper the gradient the more angular dependent the scattered light is. The gradients of the slope were 1.28 for 380nm, 1.16 for 580nm and 1.30 for 780nm light (Figure 4.3).

Results

Figures 4.4 and 4.5 show the mean results of the first experiment for the seven observers. Figure 4.4 presents the results in the no-glare and the low luminance glare conditions, while Figure 4.5 presents the results from the medium and high luminance glare conditions (see Table 4.1). In each graph, spatial frequency is plotted along the x-axis and contrast sensitivity along the y-axis. Different symbols represent the three different concentrations of microspheres within the scatter cell (0% concentration, 0.08% concentration and 0.16% concentration).

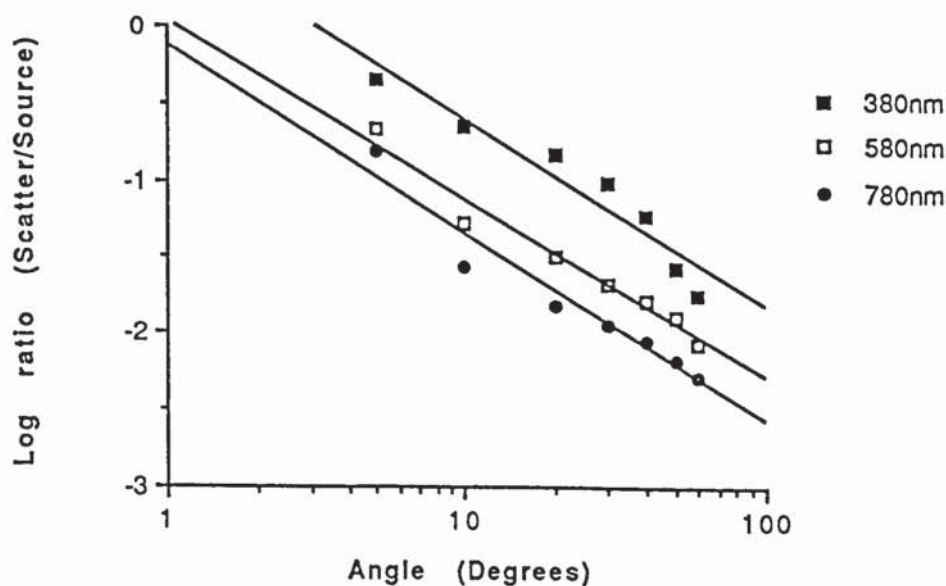


Figure 4.3 The angular and wavelength dependency of scattered light produced by a suspension of monodispersed polystyrene microspheres of mean diameter 500nm is shown. The ratio of scattered light to the light source used is plotted on the y-axis. The angle of eccentricity at which the scattered light was measured is plotted on the x-axis. Different symbols represent the different wavelengths of scattered light measured, closed square 380nm, open square 580nm and closed circle 780nm.

Different graphs represent the four different levels of glare. Two-factor Analysis of Variance (ANOVA) was used to analyse the data. In the absence of glare, the scatter cells have no significant effect upon contrast sensitivity ($F_{2,90} = 0.015$, $p > 0.1$). Similar findings have been obtained with other types of scatter cell (Miller et al, 1972; Zuckerman et al, 1973).

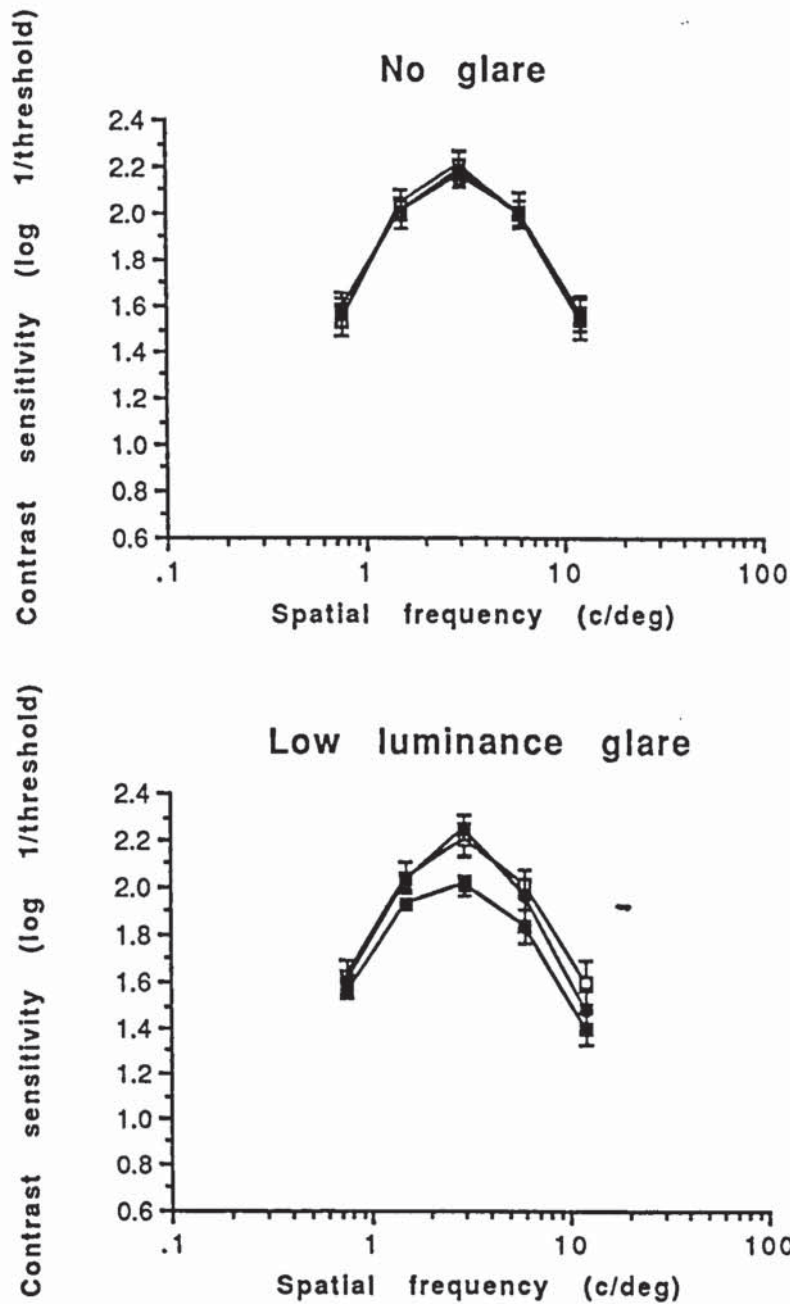


Figure 4.4 In each graph, spatial frequency is plotted along the x-axis and contrast sensitivity along the y-axis. Different symbols represent the three different concentrations of microspheres within the scatter cell (Open square; 0% concentration, closed circle; 0.08% concentration and closed square; 0.16% concentration). The top graph represents the results in the no-glare condition, while the bottom graph represents the results in the low luminance glare condition. The results shown are the mean of seven observers. One standard error is shown.

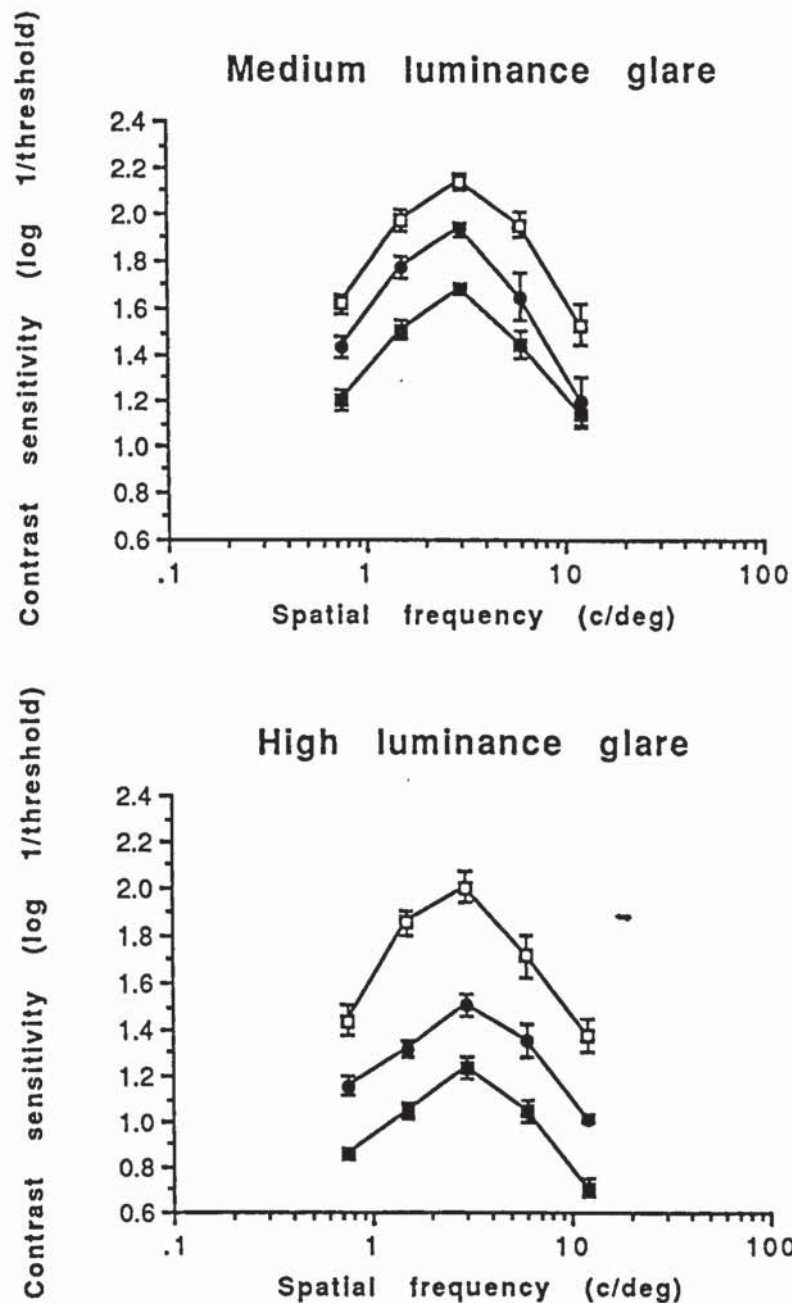


Figure 4.5 In each graph, spatial frequency is plotted along the x-axis and contrast sensitivity along the y-axis. Different symbols represent the three different concentrations of microspheres within the scatter cell (Open square; 0% concentration, closed circle; 0.08% concentration and closed square; 0.16% concentration). The top graph represents the results in the medium luminance glare condition, while the bottom graph represents the results in the high luminance glare condition. The results shown are the mean of seven observers. One standard error is shown.

However, once a glare source is introduced contrast sensitivity declines dramatically, particularly for the higher scatter concentrations. The two-factor analysis of variance (ANOVA) used to analyse the data shows that scatter had a significant effect in all three glare situations, at low ($F_{2,90} = 7.698$, $p < 0.01$), medium ($F_{2,90} = 72.013$, $p < 0.01$) and high ($F_{2,90} = 215.93$, $p < 0.01$). This highlights the fact that quality of vision can appear perfectly normal in the absence of a glare source and yet can be severely compromised once glare is introduced.

A simple quantification of disability glare is the reduction in contrast sensitivity, in logarithmic units, produced by the glare source. As might be predicted, the largest degree of disability glare occurred for the highest scatter concentration and glare level. An important point to note is that the magnitude of the disability glare appears independent of spatial frequency. This point shall be examined further in the discussion.

Discussion

The results show that increasing amounts of scattered light leads to a reduction in luminance contrast sensitivity which, in logarithmic terms, is approximately constant across spatial frequencies. Manipulation of the luminance of the glare source or of the concentration of the scatter particles both lead to this same result. The absence of a spatial frequency effect is consistent with the view that disability glare results from veiling luminance which is superimposed upon the retinal image of the stimulus. If the reduction in contrast sensitivity was not caused by a veiling luminance but by a neural effect then sensitivity reduction might vary with spatial frequency. Spatial frequency differences in disability glare could potentially arise due to the fact that the transition luminance from the DeVries-Rose (square-root) law to Weber's law is spatial frequency dependent (van Nes et al, 1967; Laming, 1991). If threshold measurements were recorded at this transition luminance, Weber's law would not operate over all the spatial frequencies producing variation in retinal sensitivity with

spatial frequency. However, the absence of such an effect suggests that Weber's law is in operation at each spatial frequency, reflecting the moderately high retinal illuminance produced by the stimulus. Another idea that may explain the lack of any spatial frequency differences could lie with the glare source used. The glare source used in this experiment subtended from 5° to 50° visual angle and this large range of glare angles covers relatively narrow and peripheral angles. If a peripheral glare source was used it may be expected to have a greater effect at lower spatial frequencies, while a narrow angle glare source would have more effect at high spatial frequencies. The location of the veiling luminance caused by the glare source relative to the retina is important as a peripheral source could affect the peripheral retina more than the fovea. Previous studies suggest that disability glare has a greater effect at low and medium spatial frequencies than at high (Paulsson and Sjöstrand, 1980; Carney and Jacobs, 1984; Abrahamsson and Sjöstrand, 1986; Elliott, 1987). However, Finlay and Wilkinson (1984) found that disability glare was spatial frequency independent.

4.C. The effect of induced intraocular light scatter upon luminance contrast sensitivity compared with its effect upon colour contrast sensitivity.

Methods

The experimental set up was the same as in section 4.B. except that the working distance was reduced to 1.625m. Two observers were used in this experiment (RS: 23 years of age, male, and DW: 30 years of age, male) and both underwent substantial training in the task before data collection began. Only two observers were used as the length of time taken to collect data was long and this was a preliminary study to assess the effect of glare on colour contrast sensitivity. Exclusion criteria are described in 4.B. The same glare source and method of inducing intraocular light scatter were used as described in 4.B.. The glare source was used at two glare levels: no-glare and the medium glare level and two concentrations of

500nm sized polystyrene microspheres used were: 0% concentration and 0.08% concentration (4.B.).

The chromatic stimulus produced for this part of the experiment was a red/green sinusoidal grating of spatial frequency 0.75cdeg^{-1} . This was created by removing the input from the blue gun of the CRT and presenting the output of the red and green guns 180 degrees out of phase. The chromaticity co-ordinates (CIE 1931) of the red and green phosphors were (0.591, 0.373) and (0.297, 0.596) respectively. The mean luminance was maintained at 10cdm^{-2} . The observer's isoluminant point was estimated using heterochromatic modulation photometry (Pokorny et al, 1989), as follows. The individual red and green constituent gratings were made to counterphase 180 degrees out of phase in a sinusoidal manner at a temporal frequency of 16Hz. Since luminance contrast sensitivity at such high temporal frequencies far exceeds chromatic sensitivity, the detection of this temporal modulation is dominated by any residual luminance information in the stimulus. Sensitivity to this stimulus was measured at seven photometrically determined red-green luminance ratios around a value of 1:1. One half of the screen contained the flickering grating, whilst the other half had the same mean luminance and chromaticity. A two-alternative forced choice staircase technique was used to determine thresholds. Incorrect identification of the flickering half of the screen led to an increase in the amplitude of modulation of the red and green (although their relative luminance remained constant), thus making the flicker more apparent. Two successive correct responses were required before a reduction in amplitude occurred. A plot of sensitivity against red-green ratio revealed a distinct minimum, and the red-green ratio at which this minimum occurred was taken to represent the observer's isoluminant point. This was repeated four times for various concentration and glare level combinations to obtain an average value. The red-green isoluminance ratio was established for each combination of scatter cell/glare source before proceeding.

The effect of various levels of glare and scatter cell concentration upon chromatic contrast sensitivity for stationary red-green gratings was then determined. A single, low spatial frequency of 0.75c/deg was used to reduce the luminance artefacts produced in chromatic gratings by transverse chromatic aberration (Mullen, 1985; Thibos et al, 1990). Having determined the isoluminant point as described above, a split-screen two-alternative forced choice staircase technique was used to determine chromatic contrast sensitivity. Again, two successive correct responses led to a decrease in contrast whilst a single incorrect response caused contrast to increase. This sequence continued until seven reversals had occurred. The threshold estimate was calculated from all but the first of these. A direct comparison was made with the effect of disability glare upon luminance contrast sensitivity by simply combining the red and green gratings in phase to produce a yellow-black luminance grating. The threshold values presented represent a mean of four threshold estimates.

Figure 4.6 shows an example of the method used to calculate the isoluminant points. Seven photometrically determined red-green luminance ratios around a value of 1:1 are plotted on the x-axis. Modulation sensitivity to the flickering stimulus at each of these ratios is plotted on the y-axis. A 4th order polynomial function is shown fitted to the data points. The minimum of this function is then accepted as an estimate of the isoluminant point. The final isoluminant point is the mean of four such estimates.

Table 4.2 shows the mean values and standard deviations of the isoluminant ratios for the red-green grating for each observers (RS and DW). The isoluminant ratios were measured for all glare and scatter combinations. The presence of the glare source and the scatter lenses resulted in little variation in the isoluminant point.

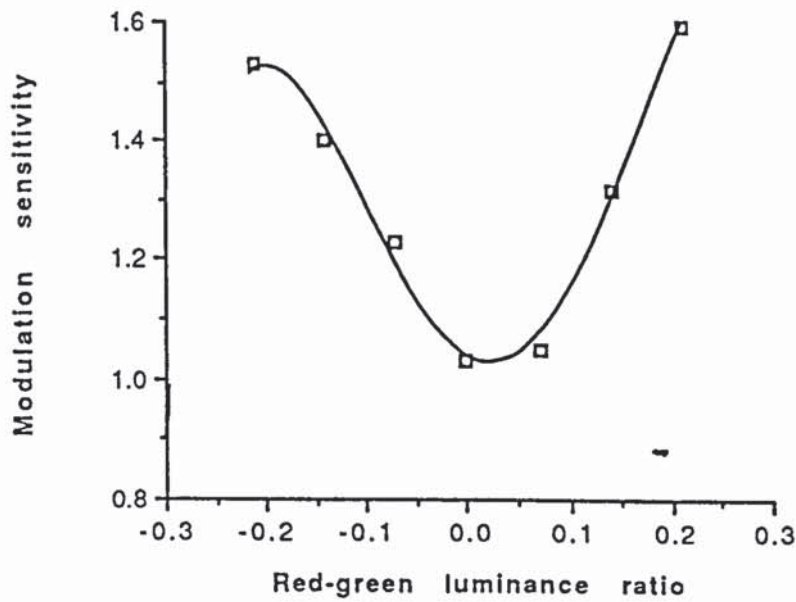


Figure 4.6 An example of the method used to calculate the isoluminant points. Red-green luminance ratios around a value of 1:1 are plotted on the x-axis. Modulation sensitivity to the flickering stimulus at each of these ratios is plotted on the y-axis. A 4th order polynomial function is shown fitted to the data points. The minimum of this function is then accepted as an estimate of the isoluminant point. The final isoluminant point is the mean of four such estimates.

	Observer (RS)		Observer (DW)	
	No Scatter	Scatter	No Scatter	Scatter
	Mean SD	Mean SD	Mean SD	Mean SD
No Glare	1.01 ± 0.02	1.02 ± 0.02	1.00 ± 0.02	0.99 ± 0.06
Low Glare	1.03 ± 0.04	1.04 ± 0.02	1.01 ± 0.04	1.07 ± 0.12
Medium Glare	1.02 ± 0.04	1.06 ± 0.06	1.01 ± 0.08	1.05 ± 0.06

Table 4.2 Mean values and standard deviations of the isoluminant ratios for the red-green grating are shown for two observers (RS and DW). Isoluminant ratios were measured at the no-glare level, low glare level and medium glare level and both with and without scatter particles (4.B.). Spatial frequency was 0.75 cpd.

Results

The effect of glare upon colour and luminance contrast sensitivity is shown in Figure 4.7 for two observers (RS and DW). For each of the glare level/scatter combinations investigated, a direct comparison is made between the red-green isoluminant condition and the yellow-black luminance grating. Measurements were made in the presence of the optical cells containing 0% (without scatter) and 0.08% (with scatter) concentration of polystyrene microspheres. Two of the three glare levels available with the BAT were used, the low luminance and medium luminance levels. The high luminance glare level was not used as the grating could not be detected. The maximum height of each bar represents sensitivity in the absence of the glare source whilst the shaded area is sensitivity in the presence of glare. Hence, the size of the unshaded part of the bar reflects the magnitude of disability glare. In the absence of scattering microspheres in the cell, the lower glare level results in a small loss of chromatic sensitivity, but no loss in luminance contrast sensitivity. Note that chromatic sensitivity is initially higher than luminance contrast sensitivity. When scatter is introduced, the loss of both chromatic and luminance sensitivity increases slightly. At the medium glare level, there is a considerably greater level of disability glare for all conditions. However, disability glare for the red-green isoluminant stimulus still exceeds that for yellow-black gratings.

Discussion

It is clear that disability glare can have a drastic effect on sensitivity to a chromatic stimulus. When a glare source was introduced the reduction in chromatic sensitivity was greater than the reduction in luminance sensitivity. The veiling luminance produced by the scattered light from the glare source has the effect of desaturating the chromatic gratings thus reducing sensitivity (Wolfe, 1992).

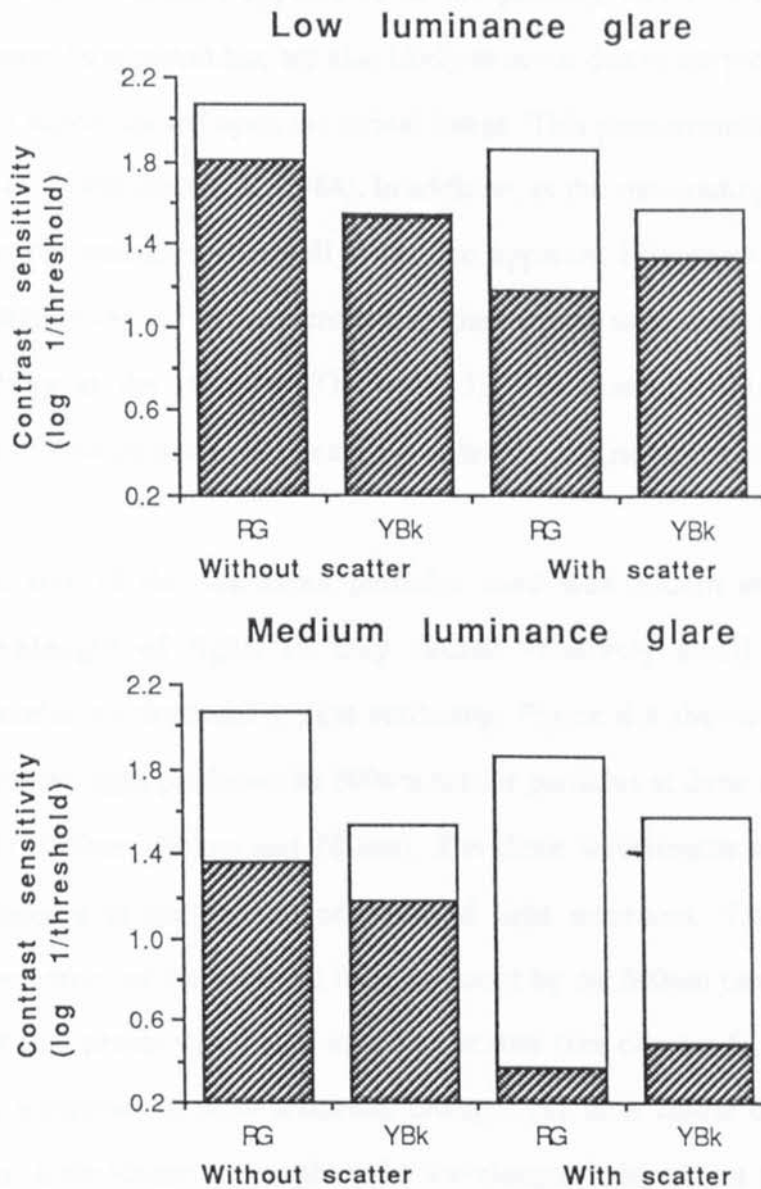


Figure 4.7 The effect of glare upon sensitivity to red-green (RG) and yellow-black (YBk) gratings. Measurements were made in the presence of the optical cells containing 0% (without scatter) and 0.08% (with scatter) concentrations of polystyrene microspheres. The top graph represents the results in the low glare condition, while the bottom graph represents the results in the medium glare condition. The maximum height of each bar represents sensitivity in the absence of the glare source whilst the shaded area is sensitivity in the presence of glare. Hence, the size of the unshaded part of the bar reflects the magnitude of disability glare. The mean standard error was 0.07 log units.

Although saturation appears to be the primary factor in determining sensitivity, changes in apparent hue are also likely to occur due to the presence of a veiling white light superimposed upon the retinal image. This phenomenon is known as the Abney effect (Kurtenbach et al, 1984). In addition, as the surrounding glare source is brighter than the stimulus, this will lower the apparent brightness of the gratings due to inhibition caused by the surrounding glare source that causes a reduction in the neural activity at the stimulus (Guth, 1973). The result of this is a decrease in hue discrimination due to the Bezold-Brucke effect (Knoblauch et al, 1987).

The size of the scattering particles used was 500nm and of the order of the wavelength of light, so they caused relatively small amounts of Rayleigh (wavelength-dependent) light scattering. Figure 4.3 shows the different amount of scattered light produced by 500nm scatter particles at three different wavelengths of light (380nm, 580nm and 780nm). The three wavelengths used showed a significant difference in the amount of scattered light measured. The amount of wavelength dependency of the scattered light produced by the 500nm particles was approximately half that produced by pure Rayleigh scatter (see chapter 5). However, in the human eye a number of other lenticular changes can alter colour discrimination. Although most light scatter is thought to be wavelength-independent (Vos, 1984; Wooten and Geri, 1987), lens absorption is dependent upon wavelength. There is a preferential absorption of short wavelength blue light which has been postulated as one of the reasons for age-related tritanopia (Verriest, 1963). One special type of light scatter which is wavelength dependent is that of fluorescence. Short wavelength fluorescence has been demonstrated at 340nm, 420nm and 510nm, with respective excitation wavelength of 290nm, 350nm and 425nm (Lerman and Borkman, 1976). This type of light scatter is known to increase with age (Weale, 1987). (see page 100a)

In conclusion, the possibility that colour information may be a useful back-up to the loss of luminance sensitivity in the presence of glare proves to be unfounded.

Another factor that could affect the perception of scattered light is the directional sensitivity of the retinal photoreceptors (Stiles-Crawford effect)(see page 178). The Stiles-Crawford effect refers to the fact that visual sensitivity is greatest for light entering near the centre of the pupil of the eye and the response falls off from this peak across the pupil. Additional elements play a role in directional sensitivity of the retina and photoreceptors optics, including the eye's lens system, the pigment orientation in the photoreceptors and the retinal pigment epithelium (for a review see, Enoch and Lakshminarayanan, 1991).

Subjectively, the colours of the chromatic grating appear 'washed out', a description often given by observers viewing a scene under glare conditions, but usually ascribed simply to the loss of luminance contrast.

4.D. Effect of glare upon luminance contrast sensitivity and colour contrast sensitivity as a function of age.

Methods

The experimental set up was the same as in section 4.B. except the viewing distance was 1.6 metres at which the display subtends 6°. Each colour grating was modulated either along a red-green (constant S-cone) axis or along a blue-yellow (tritanopic confusion) axis. The extent of colour modulation was limited by the phosphors of the monitor. At the maximum available modulation (defined arbitrarily as 100%), the red-green stimulus varied between chromaticity coordinates (CIE 1931) of (0.237, 0.379) and (0.451, 0.269) whilst the equivalent coordinates for the blue-yellow stimulus were (0.233, 0.126) and (0.417, 0.503). The point of intersection of the red-green and the blue-yellow axes was at the white point, defined by CIE chromaticity coordinates of (0.333, 0.333), where sensitivity to luminance modulation was measured. Luminance contrast was defined in conventional Michelson terms. Colour contrast of the stimuli was defined as a percentage of the maximum available modulation along each given axis. Colour contrast thresholds were defined as the smallest detectable colour modulation and were measured along both the red-green and the blue-yellow axes.

Two groups of subjects were used, one comprised of 10 young normal observers (mean age 25.4 years SD=2.6; Gender Male(M)=3, Female(F)=7) and the other 10 elderly observers (mean age 73.8 years SD=5.2; Gender M=4, F=6). The elderly observers were paid volunteers and who attended the Department weekly to provide subjects for undergraduate ophthalmic optics clinics. All the subjects used in each

experiment were colour normal on the Farnsworth-Munsell D-15 test. Exclusion criteria are described in 4.B.

Natural pupils were used throughout since variations in pupil size affect the retinal illuminance of the stimulus and the glare source equally, leaving disability glare unchanged (see section 6.B.3). Disability glare was calculated as the difference between log contrast sensitivity with and without the glare source. The glare source used was the BAT. Two glare levels were used: no-glare and the medium glare level.

Before colour contrast sensitivity measurements were made, a procedure was undertaken to ensure that luminance modulation within the stimulus was minimised so that detection of the stimulus relied on a purely chromatic discrimination. In the case of the red-green colour grating. A horizontal sinusoidal red-green grating was presented. The screen was divided into eight vertical strips of equal width. The luminance ratio (as measured photometrically) between the red and green colours comprising the grating varied between strips, and ranged from 0.3 log units below photometric isoluminance in the extreme left-hand strip (i.e. a red-green ratio of 0.5) to 0.3 log units above photometric isoluminance in the extreme right-hand strip (a red-green ratio of 2). Mean luminance, averaged across the grating, was maintained at a constant 10 cdm^{-2} . The red-green ratio in the intermediate strips was varied sequentially from left to right in equal logarithmic steps. The whole stimulus was then made to counterphase at a temporal frequency of 16Hz. At such a high temporal frequency, any residual luminance modulation within the stimulus produces a strong sense of flicker, whereas flicker is minimum or absent at subjective isoluminance. The observer was asked to report which of the eight strips of grating was flickering the least, and the red-green photometric ratio in this strip was taken to represent an estimate of the observer's subjective isoluminance point. The procedure was then repeated, but this time the range of luminance ratios was reduced to 0.15 log units either side of the newly obtained estimate of isoluminance. The luminance ratio

obtained this time was taken as the observer's isoluminance point. This was repeated and the mean of the two ratios was accepted as the observer's isoluminant point. This luminance ratio was used in all subsequent experiments. Isoluminant ratios were determined at the same spatial frequency that was used to determine contrast thresholds (1c/deg), with and without the glare source present.

A similar procedure was repeated for the blue-yellow stimulus.

Contrast thresholds were determined using a split-screen forced-choice paradigm. A single, low spatial frequency of 1 c/deg was used to reduce the luminance artefacts produced in chromatic gratings by transverse chromatic aberration (Mullen, 1985; Thibos et al, 1990). The horizontal grating was presented and the observer was required to respond as to whether the grating had appeared in the upper or lower half of the screen. Contrast was ramped up in linear fashion and remained at its maximum until the observer responded, after which it ramped down to zero, again in a linear manner. Initial presentations were always clearly suprathreshold. Two successive correct responses were required before the contrast of the subsequent presentations was reduced, whereas a single incorrect response led to an increase in contrast. Initial step size was 0.15 log units, but this decreased to 0.075 log units after the first reversal. The sequence continued in staircase fashion until five reversals had occurred, after which the sequence terminated. Threshold was accepted as the mean of the last four reversal points. Luminance and colour contrast sensitivity were measured for all observers with and without the glare source present.

Results

Table 4.3 shows the mean and standard deviation of isoluminant ratios for both the red-green and blue-yellow gratings. Measurements were taken for both the young and elderly observers with and without glare.

	Young		Elderly	
	Mean	SD	Mean	SD
Red-green/no-glare	0.96	0.10	0.86	0.09
Red-green/glare	1.04	0.07	0.95	0.16
Blue-yellow/no-glare	0.86	0.09	0.92	0.05
Blue-yellow/glare	0.80	0.04	0.92	0.13

Table 4.3 Mean values and standard deviations of the isoluminant ratios for both red-green and blue-yellow gratings are shown for young and elderly observers. (Isoluminant ratios were measured at the no-glare level and the medium glare level. Spatial frequency was 1 cpd).

The red-green isoluminant ratios decreased with age while blue-yellow isoluminant ratios increased. A repeated measures ANOVA revealed that this difference reached statistical significance for both the red-green ($F_{1,18}=4.765$, $p<0.05$) and blue-yellow ($F_{1,18}=10.680$, $p<0.01$) ratios. These findings are to be expected on the basis of the well known yellowing of the lens with age. This will result in greater absorption of the shorter wavelengths in the stimuli, leading to a higher blue-yellow ratio and a lower red-green ratio necessary to produce isoluminance. Red-green isoluminant ratios increased when a glare source was introduced ($F_{1,18}=21.933$, $p<0.01$), but no significant difference was found with the blue-yellow isoluminant ratios ($F_{1,18}=1.391$, $p>>0.05$).

Table 4.4 shows the contrast sensitivity results without the glare source and Table 4.5 shows the results with the glare source. Figure 4.8 shows the effect of age on colour and luminance contrast sensitivity in the absence of glare. The unshaded bars represent the young observers and the shaded bars represent the elderly observers. A repeated measures ANOVA revealed that age ($F_{1,36}=10.778$, $p<0.01$) and the type of stimulus ($F_{2,36}=71.215$, $p<0.01$) had a significant effect on contrast sensitivity. Also, the interaction between age and type of stimulus ($F_{2,36}=3.609$, $p<0.05$) was significant. The effect of age on sensitivity to the luminance grating (0.14 log units) ($F_{1,18}=2.676$, $p>0.1$) and red-green grating (0.15 log units) ($F_{1,18}=2.656$, $p>0.1$) was small and did not reach statistical significance. The largest reduction in sensitivity was to the blue-yellow stimulus (0.39 log units) and was highly significant ($F_{1,18}=8.543$, $p<0.01$).

-

Table 4.6 shows the disability glare results. Figure 4.9 compares disability glare values for the two age groups. Disability glare is defined as the difference in log contrast sensitivity measured with and without glare. Sensitivity of all observers to all stimuli was reduced in the glare situation. For all observers, disability glare was greatest for the red-green stimulus. Disability glare in the elderly increased (by 0.25 log units) for both red-green ($F_{1,18}=11.849$, $p<0.01$) and luminance modulated gratings ($F_{1,18}=8.911$, $p<0.01$), but not for blue-yellow ($F_{1,18}=0.239$, $p>>0.1$).

Young Group

Name	Sex(M/F)	Age	Contrast sensitivity (log1/threshold)		
			Luminance	Red-green	Blue-yellow
JG	F	20	2.06	1.97	1.56
RS	M	24	2.10	2.04	1.75
KL	F	24	2.19	2.06	1.76
NH	F	25	2.34	2.21	1.67
NE	F	25	2.19	1.97	1.96
GR	F	26	1.94	1.98	1.63
GB	M	26	2.00	1.76	1.54
F	F	27	2.27	2.49	1.76
RD	F	27	2.24	2.34	1.63
DW	M	30	2.15	2.27	1.85

Elderly Group

Name	Sex(M/F)	Age	Contrast sensitivity (log1/threshold)		
			Luminance	Red-green	Blue-yellow
ASP	F	65	2.05	1.98	1.29
WS	F	69	2.31	2.32	1.83
NM	F	70	2.15	1.96	1.47
ES	M	72	1.98	2.02	1.35
AM	M	73	1.52	2.10	1.49
DSP	M	73	1.78	1.68	1.39
TD	M	77	2.17	2.15	0.99
MJ	F	78	2.13	1.86	1.38
RD	F	79	1.91	1.70	0.79
WH	F	82	2.10	1.81	1.26

Table 4.4 Contrast sensitivity, without glare, for the young (Top) and elderly (Bottom) groups to a luminance grating, a red-green grating and a blue-yellow grating.

Young Group

Name	Sex(M/F)	Age	Contrast sensitivity (log1/threshold)		
			Luminance	Red-green	Blue-yellow
JG	F	20	1.76	1.97	1.56
RS	M	24	1.87	1.30	1.47
KL	F	24	2.07	1.52	1.42
NH	F	25	1.98	1.67	1.49
NE	F	25	1.95	1.39	1.69
GR	F	26	1.69	1.56	1.52
GB	M	26	1.52	1.55	1.31
FF	F	27	1.97	1.53	1.53
RD	F	27	1.89	1.55	1.44
DW	M	30	1.67	1.46	1.50

Elderly Group

Name	Sex(M/F)	Age	Contrast sensitivity (log1/threshold)		
			Luminance	Red-green	Blue-yellow
ASP	F	65	1.62	1.33	1.18
WS	F	69	1.81	1.34	1.63
NM	F	70	1.47	1.07	1.21
ES	M	72	1.65	1.25	1.20
AM	M	73	1.30	1.39	1.31
DSP	M	73	1.62	0.89	0.98
TD	M	77	1.26	1.07	0.84
MJ	F	78	1.42	1.09	1.05
RD	F	79	1.29	0.54	0.50
WH	F	82	1.38	0.79	0.84

Table 4.5 Contrast sensitivity, with glare, of the young (Top) and elderly (Bottom) groups to a luminance grating, a red-green grating and a blue-yellow grating.

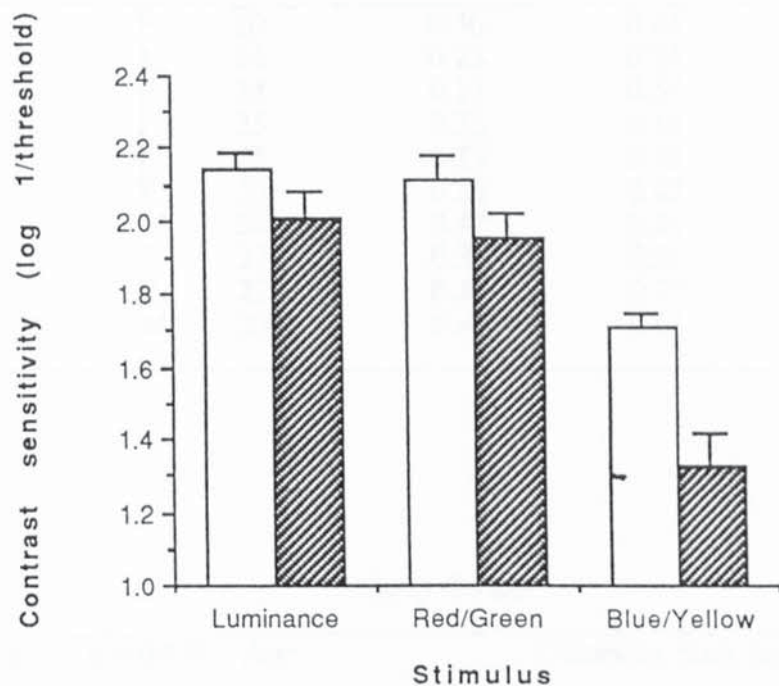


Figure 4.8 A comparison of isoluminant red-green chromatic sensitivity, isoluminant blue-yellow chromatic sensitivity and luminance contrast sensitivity is shown. The unshaded bars represent the mean for the 10 young observers whilst the shaded bars represent the mean for the 10 elderly observers. Error bars show one standard error of the mean.

Young Group

Name	Sex(M/F)	Age	Disability glare (log units)		
			Luminance	Red-green	Blue-yellow
JG	F	20	0.30	0.44	0.21
RS	M	24	0.23	0.74	0.28
KL	F	24	0.12	0.54	0.33
NH	F	25	0.36	0.54	0.19
NE	F	25	0.23	0.58	0.28
GR	F	26	0.26	0.42	0.11
GB	M	26	0.47	0.21	0.23
FF	F	27	0.30	0.96	0.26
RD	F	27	0.36	0.79	0.19
DW	M	30	0.49	0.61	0.34

Elderly Group

Name	Sex(M/F)	Age	Disability glare (log units)		
			Luminance	Red-green	Blue-yellow
ASP	F	65	0.44	0.65	0.12
WS	F	69	0.50	0.98	0.20
NM	F	70	0.68	0.89	0.25
ES	M	72	0.33	0.78	0.15
AM	M	73	0.22	0.71	0.18
DSP	M	73	0.33	0.78	0.41
TD	M	77	0.91	1.08	0.16
MJ	F	78	0.71	0.78	0.33
RD	F	79	0.62	1.16	0.29
WH	F	82	0.73	1.02	0.42

Table 4.6 Disability glare for the young (Top) and elderly (Bottom) groups to a luminance grating, a red-green grating and a blue-yellow grating.

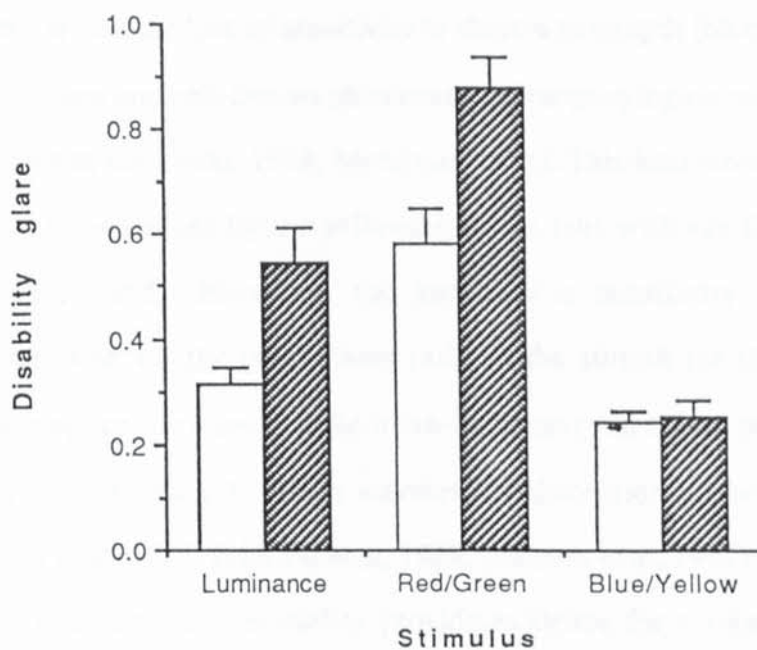


Figure 4.9 Disability glare is plotted along the y-axis and the type of stimulus used, luminance, red-green or blue-yellow, is plotted along the x-axis. Disability glare is defined as the difference in log contrast sensitivity measured with and without a glare source. The unshaded bars represent the mean for the 10 young observers whilst the shaded bars represent the mean for the 10 elderly observers. Error bars show one standard error of the mean.

Discussion

The results show, at the low spatial frequency used, the only significant change in contrast sensitivity with age was the reduction in sensitivity to the blue-yellow grating. The absence of a significant age-related loss in luminance contrast sensitivity at low spatial frequencies agrees with many previous studies (e.g., Elliott et al, 1990b). Whilst the loss of sensitivity to short-wavelength (blue) light and blue-yellow colour vision are well-known phenomena accompanying normal human aging (Elliott et al, 1990b; Lakowski, 1958; Moreland, 1971). This later reduction of sensitivity was thought to be caused by the yellowing of the lens with age (Said and Weale, 1959; Ruddock, 1965). However, the fact that a sensitivity loss remains despite compensation for the isoluminant ratio of the stimuli for the selective absorption effect supports the view that the tritan-like change-in colour perception in the elderly is not caused solely by short wavelength absorption in the media (Haegerstrom-Porknoy et al, 1989; Johnson et al, 1988; Scheffrin et al, 1992). However, evidence for this is equivocal. Some studies provide evidence for a significant selective short-wavelength-sensitive (SWS) cone loss with age (Scheffrin et al, 1992; Haegerstrom-Porknoy et al, 1989), whereas in others the effect is slight (Johnson et al, 1988), or even absent in that the sensitivities of all cone types decrease at the same rate as a function of age (Werner and Steele, 1988). Scheffrin et al (1992) attempted to differentiate the effects of age-related changes at a receptor level from other neural changes in the S-cone pathway and preretinal changes due to ocular media. Measurements of age-related threshold and ocular media density changes were taken and compared to hypothesized losses in cone sensitivities. Scheffrin et al (1992) found that changes in ocular media reduced the average log difference in the thresholds between the young and older subjects by 0.12 log units (21%) and the inclusion of hypothesized losses in cone sensitivities reduced the average difference by 0.43 log units (72%). They concluded that the reduced cone receptor activity can account for

much of the age-related sensitivity losses. Additional neural changes within an S-cone pathway may account for the remainder. The results could be explained by a selective loss of macular sensitivity for pathways carrying signals from SWS cones as a function of increasing age. Johnson et al (1988) found a small yet consistent loss in SWS cone pathway sensitivity with increasing age. After correction for changes in age-related changes in ocular transmission there is a residual SWS cone pathway sensitivity loss of 0.09 log units per decade of age as opposed to a sensitivity loss of 0.06 log units per decade of age for MWS and LWS cone pathways. Werner and Steele (1988) found that despite an age-related increase in ocular media density that was selective for short wavelengths, there was an approximately parallel decline in sensitivity of all three colour mechanisms (SWS, medium-wavelength-sensitive (MWS) and long-wavelength-sensitive (LWS)) with age. The short-wavelength mechanism decline was partially attributable to ocular media changes and to changes in the SWS cone receptors and/or pathways. The decline in sensitivity of middle- and long-wavelength mechanisms appears primarily at the receptor level and/or at the postreceptoral pathways of an achromatic channel.

It is perhaps of interest that tritan-like colour defects can be induced by a reduction in mean luminance (Knoblauch et al, 1987). Whilst the effect of reduced retinal illuminance upon luminance contrast sensitivity is known (van Nes et al, 1987), the corresponding effect of quantal noise upon colour contrast sensitivity is, as yet, unknown. This information is needed before it is known whether some or all of the age-related blue-yellow contrast sensitivity defect could be explained in terms of the reduced transmission and senile miosis which occur in the elderly eye.

The results show that disability glare in the elderly increased for both red-green and luminance modulated gratings, but not for blue-yellow. This means that the reduction in blue-yellow sensitivity produced by the glare source was relatively small. A likely explanation for this is that the chromaticity of the glare source used in the experiment

is weighted towards long wavelengths. When the glare source was introduced the mean chromaticity coordinates of the retinal image changed, the blue-yellow grating having relatively less blue light thus reducing SWS cone excitation, whilst the red-green grating had relatively more red light thus increasing long-wavelength-sensitive (LWS) cone excitation. This change in the relative level of cone excitation could affect colour contrast sensitivity. Boynton and Kambe (1980), by using additional light sources, were able to measure chromatic discrimination at various cone excitation levels. For discriminations mediated by SWS cones measured along lines of constant LWS cone and medium-wavelength-sensitive (MWS) cone excitation, they found that the higher the initial level of SWS cone activation, the greater the increment of additional excitation required for a threshold change. For discrimination mediated by LWS and MWS cones, measured along lines of constant SWS cone excitation, they found that the discrimination step ΔL was minimal at a chromatic balance point. Discrimination steps were larger as LWS-cone activation increased or decreased. Similar findings were reported by Nagy et al (1987) and, more recently, by Miyahara et al (1993) and Yeh et al (1993). These studies indicate that when cone excitation levels are varied, colour discrimination thresholds also change. The veiling luminance from the glare source used in this study altered the colour distribution of the B-Y grating, reducing SWS cone excitation which thereby improved colour discrimination. This increase in blue-yellow sensitivity partially offset the effect of increased light scatter due to the glare source. For the red-green, the opposite effect occurs. Therefore, disability glare for blue-yellow gratings was not as great as for red-green.

In certain circumstances such as for the red-green stimulus, chromatic discrimination ability is dramatically reduced. It seems that the precise effect of a glare source on colour discrimination depends upon a complex interaction between the chromaticity of the glare source and that of the stimulus. This finding has ergonomic implications concerning the presentation of visual information. Many decisions are made using chromatic information, particularly in driving environments. This emphasizes the

need to devise methods of conveying visual information which are relatively immune to the effects of disability glare. Clinicians should therefore be aware not only of the reduced luminance discrimination in patients suffering from disability glare, but also of a possible marked reduction in chromatic sensitivity. This is likely to further compromise a patient's ability to function adequately in visual environments which contain glare sources.

Another important factor in chromatic discrimination and sensitivity is macular pigment. Not only does the yellowing in the crystalline lens affect the spectral distribution of light reaching the photoreceptors, but also the yellow pigment which covers the macular region of the retina. This yellow pigment absorbs short-wavelength light, with maximum absorption between 450nm and 490nm (Ruddock, 1972). The optical density of the macular pigment varies considerably from person to person, but remains constant with age (Werner et al, 1987).

The absorption of short-wavelength light by macular pigment can reduce blue-yellow colour discrimination and thresholds for short-wavelength stimuli. It may be possible to estimate the absorption of macular pigment by using spectral sensitivity measurements (Werner et al, 1987).

CHAPTER 5 EFFECT OF FILTERS ON DISABILITY GLARE

5.A. Introduction

The aim of this study was to examine whether or not the introduction of a filter reduces the amount of disability glare. Filters act by varying the amount and spectral distribution of transmitted light and are often prescribed by clinicians on the assumption that they provide some improvement in visual performance, especially in the presence of glare. Filters have been thought to improve visual performance by either reducing the luminance of the glare source or by selectively absorbing wavelengths which are scattered preferentially in the eye. Another possible reason for why filters could improve visual performance is that the filter can absorb ultraviolet light and thus reduce lenticular fluorescence.

The choice of filter type is usually made on a somewhat arbitrary basis. However, as the following argument demonstrates, it is important to realise that the use of filters does not directly predict a reduction in disability glare. From the definition of Michelson contrast a formula can be produced for disability glare relating the veiling luminance produced as a result of the glare source, L_v , and the mean luminance of the stimulus, L_s . In the absence of a veiling luminance contrast sensitivity equals $(2L_s/\Delta L_s)$ where ΔL_s is the amplitude of luminance modulation which is just detectable. In the presence of a veiling luminance, L_v , the amplitude of modulation must increase to ΔL_v in order to keep retinal contrast the same so that

$$\Delta L_s / 2L_s = \Delta L_v / 2(L_s + L_v)$$

Therefore

$$\Delta L_v / \Delta L_s = (L_s + L_v) / L_s = 1 + L_v / L_s \quad [5.1]$$

Disability glare (DG) is defined as the difference between contrast sensitivity without and with the veiling glare, i.e.

$$DG = [\log (2L_S / \Delta L_S)] - [\log (2L_S / \Delta L_V)]$$

Therefore

$$DG = \log (2L_S \cdot \Delta L_V / \Delta L_S \cdot 2L_S)$$

which equals

$$DG = \log (\Delta L_V / \Delta L_S)$$

Substituting from [5.1], disability glare becomes

$$DG = \log (1 + L_V / L_S) \quad [5.2]$$

One prediction of this equation is that when $L_V=0$, no disability glare is present. The equation also demonstrates why there should be no reduction in disability glare in the presence of a filter. Not only does the filter have the advantage of reducing the veiling luminance due to the glare source (L_V), it also has the disadvantage of reducing the stimulus luminance (L_S) by the same proportion. Because of this, disability glare would be expected to remain unchanged. The aim of the study was to provide experimental evidence in confirmation of the above equation as there does not appear to be any study which confirms the above prediction.

Consideration should also be given to the spectral transmission characteristics of filters. It is often stated that intraocular scatter involves a significant amount of wavelength dependency, with shorter wavelengths being scattered more (Rosenberg, 1984; Leat et al, 1990; Zigman, 1990; Rutkowsky, 1987). Indeed, early

studies of intraocular light scatter assumed a considerable extent of wavelength dependency in the normal eye (Stiles, 1929b; Holladay, 1926), and this has received some experimental support (Ivanoff, 1947; Boettner and Wolter, 1962; Le Grand, 1937). On this basis, filters which remove short wavelengths before entering the eye might be expected to result in improved visual performance. However, more recent studies suggest that scatter is largely independent of wavelength in normal, healthy eyes (Wooten and Geri, 1987; van den Berg, 1991; Vos, 1984). Whether light scatter is wavelength dependent in the presence of abnormal ocular conditions such as cataract, for example, is not well established.

This study therefore seeks to investigate both the relative and absolute efficacy of two types of filters (long wavelength pass (red) and short wavelength pass (blue)) in the presence of glare. This is achieved by measuring contrast sensitivity with and without each filter in the presence of controlled amounts of wavelength dependent stray light. Different levels of wavelength dependent stray light will be used to assess whether any level of wavelength dependent scatter will produce a difference in disability glare between the two filters.

5.B. Methods

The experimental set up was the same as in section 4.B. Contrast sensitivity for horizontal sinusoidal luminance gratings of spatial frequency 0.75cdeg^{-1} was measured using a four forced-choice staircase technique. The gratings were presented in one of four quadrants of the screen while the other three quadrants were of the same mean luminance 23cdm^{-2} . The contrast of the gratings was ramped up in linear fashion and remained at its maximum until the observer responded, after which it ramped down to zero, again in a linear manner. Initial presentations were always clearly suprathreshold. A single correct response led to a reduction in contrast of the next presentation, whereas a single incorrect response led to an increase. Step size

was maintained at 20% of the current contrast level. The medium glare setting on the BAT was used and its luminance was equal to 264cdm^{-2} . Two observers were used in this experiment (Age years RS=24 and SR=25; Gender M=2)) and both underwent substantial training in the task before data collection began. Only two observers were used as substantial amounts of data were needed for each observer. Exclusion criteria are described in 4.B.

Light scatter was induced using the method described in 4.B. Two more sizes of the microsphere particles were used, one with a mean diameter of 300nm and the other 750nm to produce different degrees of wavelength dependency, with smaller particle sizes resulting in a progressively greater predominance of short wavelength scatter.

The Bentham computer controlled spectrophotometer was used to analyse the spectral characteristics of the scattered light produced by the suspensions of the monodispersed polystyrene microspheres. Three different sizes of scatter particles were investigated, with mean diameters of 500nm (used in experiments 4.B. and 4.C.) and 300nm and 750nm. As a light source a Tungsten filament lamp powered by a ten volt stabilized power supply was used. In front of the light source an achromatic lens (40mm diameter) was used to focus the light to approximate infinity. The scatter cell was placed directly in front of the lens and an aperture of 30mm diameter was placed between the lens and the scatter cell. The light source, the achromatic lens, the aperture and the scatter cell were all placed on a turn-table which could be rotated from 0 to 60° relative to the spectrophotometer. The Bentham spectrophotometer was placed 2 meters away from the light source and aligned on the zero degrees axis (Figure 5.1)

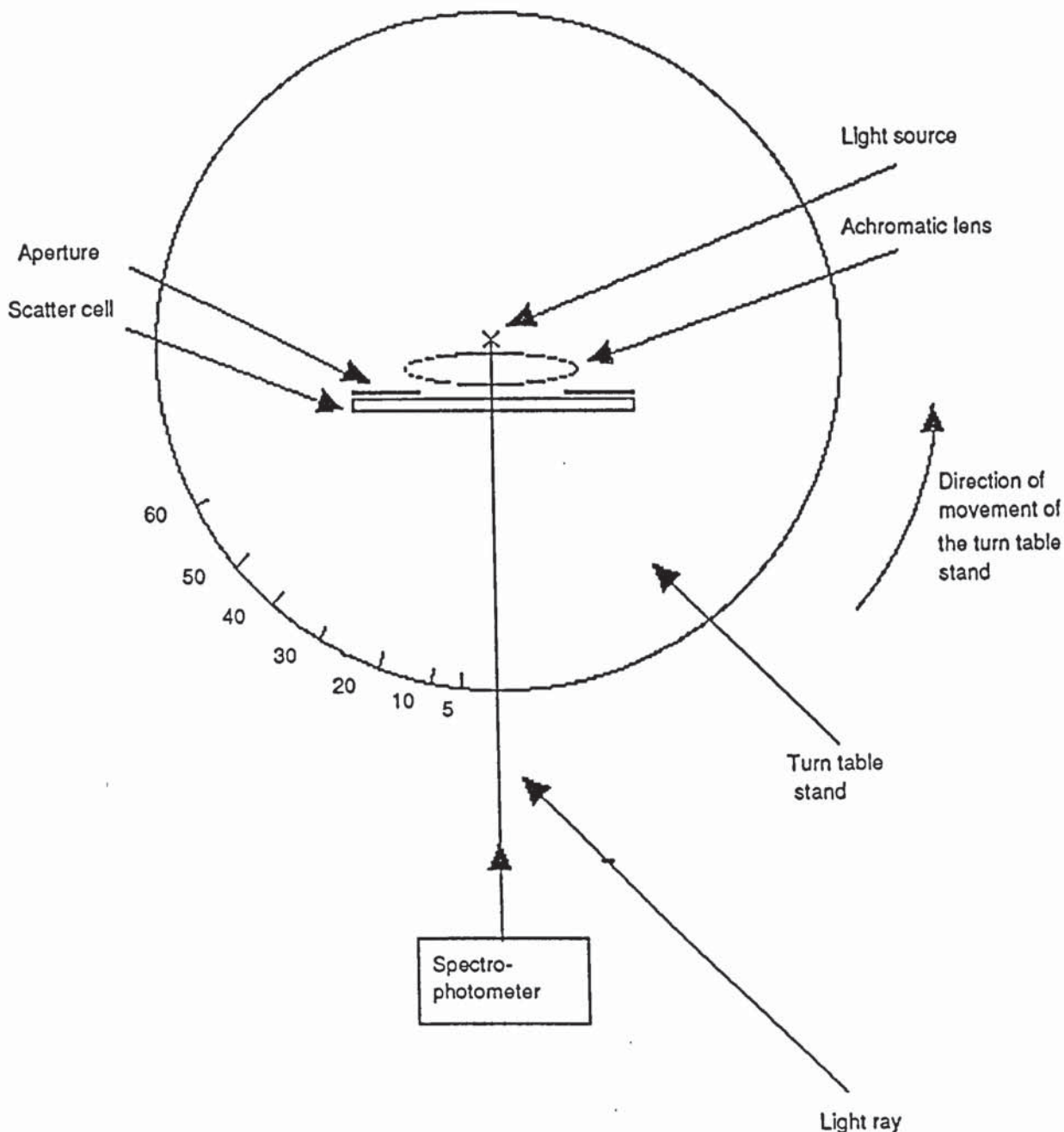


Figure 5.1 Diagram of the equipment used to analyse the spectral characteristics of the scattered light produced by suspensions of polystyrene microspheres. A Tungsten filament lamp was used as a light source and the achromatic lens focused the light to approximate infinity. The cell containing the scatter particles was placed in front of the achromatic lens. The turn table stand was rotated in the direction shown from 0 to 60 degrees relative to the spectrophotometer to measure the angular dependency of the scattered light.

As the scattering source was large (30mm) the results were dependent partially on the size of the acceptance angle at the spectrophotometer.

The first measurement was taken at zero degrees without the scatter lens in place. This was done in order to characterise the spectral characteristics of the source. This measurement was taken using an indirect method by reflecting light from the Tungsten lamp off a magnesium oxide block, since the luminance of direct light was extremely high and could have damaged the spectrophotometer. The reflectance of the magnesium block was constant (98%) across wavelength. After recording the spectral characteristics of the light source then the spectral characteristics of the scattered light at 5, 10, 20, 30, 40, 50 and 60° were measured. These readings were divided by the spectral radiance of the Tungsten lamp to obtain the relative transmission of the scattered light across the spectrum.

Figures 5.2 and 5.3 shows the angular and wavelength dependency of scattered light produced by a suspension of monodispersed polystyrene microspheres of mean diameter 300nm and 750nm respectively. Figure 4.3 showed the angular and wavelength dependency of scattered light produced by microspheres of mean diameter 500nm. In each graph the scattered light's spectral transmission is divided by the light source's spectral transmission and plotted on the y-axis. The angle of eccentricity at which the scattered light was measured is plotted on the x-axis. Different symbols represent selected wavelengths of scattered light recorded by the spectrophotometer. The gradient of the slope for each wavelength represents the angular dependency of the scattered light. The steeper the gradient the more angular dependent the scattered light is. When 300nm scattering particles were used the gradient of the slope was 1.26 for 380nm light, 1.63 for 580nm light and 1.78 for the 780nm light (Figure 5.2). The gradient of the slope when the 500nm particles were used were 1.28 for 380nm, 1.16 for 580nm and 1.30 for 780nm light (Figure 4.3). When the 750nm particles were used the gradients were 1.89 for the 380nm light, 1.81 for the 580nm light and 1.55 for the 780nm light (Figure 5.3). This implies that the light scattered by the 750nm sized particles was more angular dependent than either the 300 or 500nm particles.

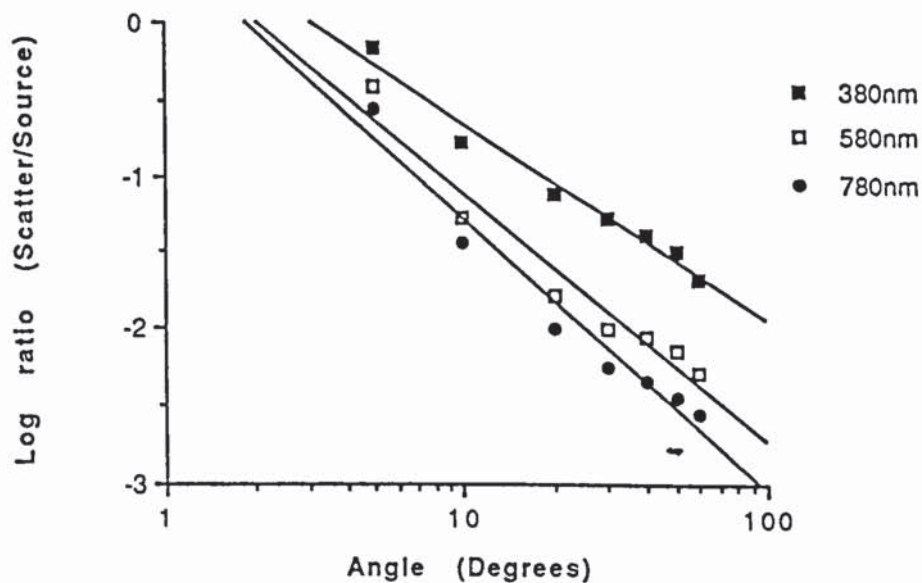


Figure 5.2 The angular and wavelength dependency of scattered light produced by a suspension of monodispersed polystyrene microspheres of mean diameter 300nm is shown. The ratio of scattered light to the light source used is plotted on the y-axis. The angle of eccentricity at which the scattered light was measured is plotted on the x-axis. Different symbols represent the different wavelengths of scattered light measured, closed square 380nm, open square 580nm and closed circle 780nm.

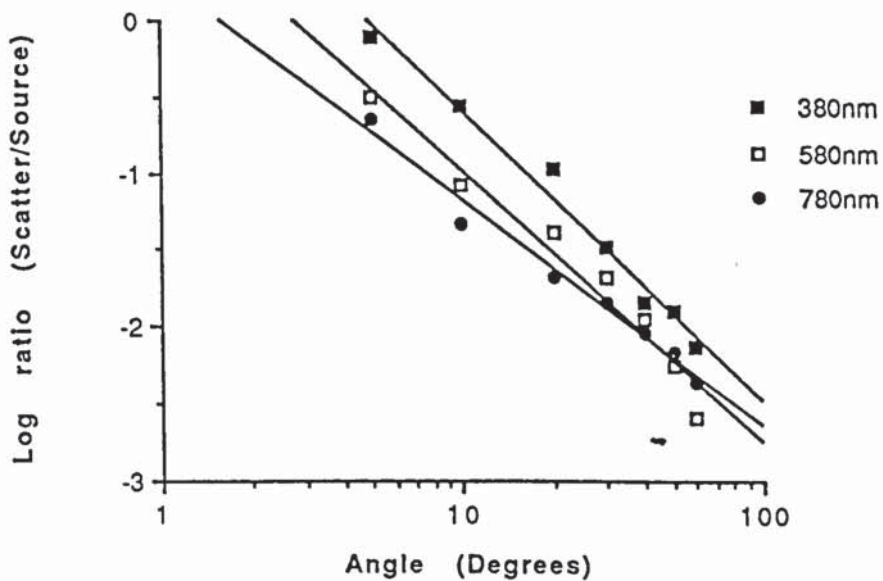


Figure 5.3 The angular and wavelength dependency of scattered light produced by a suspension of monodispersed polystyrene microspheres of mean diameter 750nm is shown. The ratio of scattered light to the light source used is plotted on the y-axis. The angle of eccentricity at which the scattered light was measured is plotted on the x-axis. Different symbols represent the different wavelengths of scattered light measured, closed square 380nm, open square 580nm and closed circle 780nm.

The separation between the lines for the three different wavelengths of scattered light shown in each graph (Figures 5.2, 5.3 and 4.3) gives an estimate of the wavelength dependency of the scattered light. The separation between the different wavelengths of light was least for the 750nm particles, which means that the 750nm sized particles scatter light less wavelength dependently than the other scatter particles.

The spectrophotometer also measured the total amount of light scattered from the BAT by the cells containing three different particle sizes (300, 500 and 750nm). Figure 5.4 shows the ratio of light from the cell to that from the glare source as a function of wavelength for the three different particle sizes. Each cell contains the same concentration (0.16%) of particles. A horizontal line would indicate that the cell scattered light independently of wavelength. However, all particle sizes produce some wavelength dependent scatter and this is greatest for the smallest particle size. The curves shown fitted to the data points represent best fitting curves of the form $\text{Ratio} \propto \lambda^{-n}$, where $n = 1.2, 1.8$ and 2.9 for particle sizes 750, 500, and 300nm respectively. Also shown is the curve representing complete Rayleigh scattering, where the exponent n has a value of 4. Therefore, 300nm particles scatter light in a more wavelength dependent fashion than 750nm sized particles. It is also apparent that, across all wavelengths, the 750nm sized particles tend to scatter more light than those of 300nm.

The filters used in the experiment were placed between the glare source and the scatter cell. One had significant short wavelength transmission in the visible spectrum (blue) and the other had predominantly long wavelength transmission (red). The transmission curve of each filter is shown in Figure 5.5 and represent typical examples of short- and long-pass spectacle filters. These two filters were chosen from a range of available filters on the basis that the luminous transmission of both lenses was equal (22%) relative to the glare source. Figure 5.6 shows the relative luminous efficiency of the glare source alone, and in the presence of each filter.

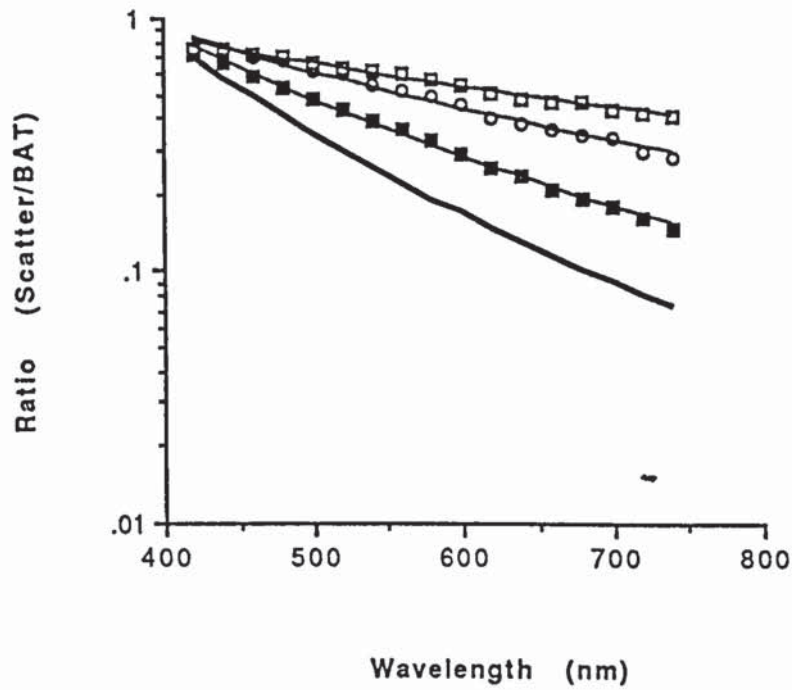


Figure 5.4 Ratio of spectral distribution of scattered light to that of the glare source (BAT) for scatter particles sizes of 750nm (open squares), 500nm (open circles) and 300nm (solid square). Light scatter at each wavelength, λ , was proportional to λ^{-n} where $n=1.2, 1.8$ and 2.9 for particle sizes of 750, 500 and 300nm respectively. The solid line represents λ^{-4} .

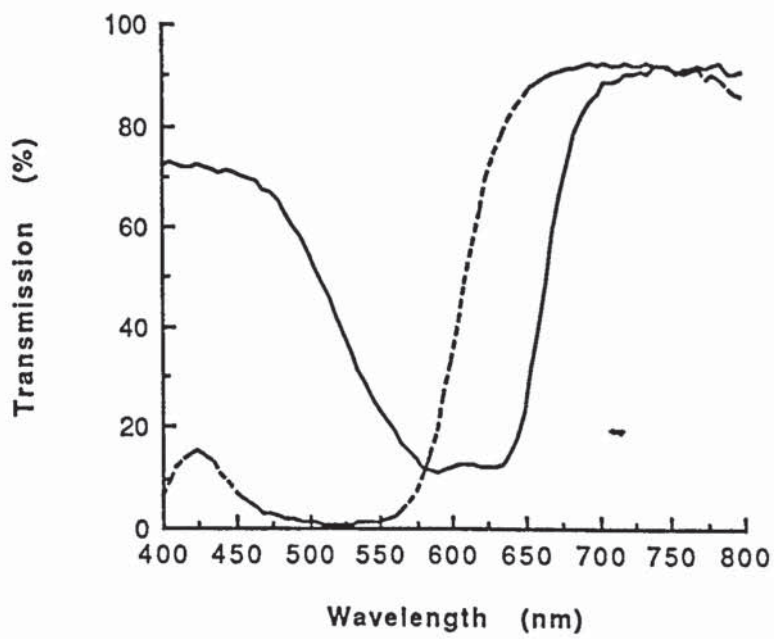


Figure 5.5 Spectral transmission of the two filters used. Short pass filter (blue) is represented by the solid line and the long pass filter (red) is represented by the dashed line.

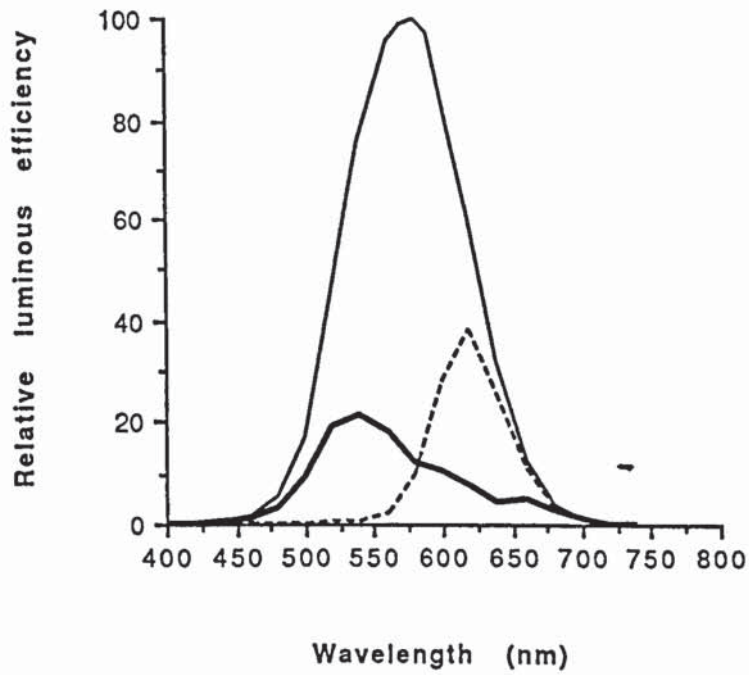


Figure 5.6 Relative luminous output of the glare source (thin solid line), and of the glare source combined with the short pass filter (thick solid line) or the long pass filter (dashed line). The graph has been normalized to 100 at the highest luminous efficiency.

The graph has been normalised to a value of 100 at the highest luminous efficiency. In addition, the spectral distribution of the contrast sensitivity stimulus was varied by appropriate software-modified combination of the red, green and blue outputs of the monitor so that the two filters also had the same 22% luminous transmission relative to the stimulus. The resulting CIE chromaticity co-ordinates of the stimulus were 0.398, 0.444. The need for matching these characteristics of the filters cannot be over-emphasized. It is obviously irrelevant to directly compare two filters which transmit different amounts of light from the glare source. Similarly, if the stimulus has a higher luminance when viewed through one filter compared to the other, a difference in performance when using the two filters would not be surprising.

In order to obtain a measure of the reliability of the technique, a single measurement of disability glare was made on two occasions separated by 1 week using a sample of 10 normal volunteers (mean age 25.4 years SD=2.6, Gender M=3, F=7). Using these results the coefficient of repeatability (COR) for the test was calculated. The COR describes the 95% confidence limits for any discrepancy between test and retest data. For normally distributed data, the COR is 1.96 multiplied by the standard deviation of the discrepancy (Elliott and Bullimore, 1993). The COR of the test was found to be 0.28 log contrast sensitivity units. This value compares favourably with other methods of disability glare measurement using contrast sensitivity measurements (Elliott and Bullimore, 1993).

5.C. Results

Figures 5.7, 5.8 and 5.9 show the results of the first experiment for observer RS, while Figures 5.10, 5.11 and 5.12 show the results for observer SR. Each graph shows disability glare plotted against the concentration of the scatter particles in the cell. Each graph shows results with either the red or blue filter in place and also for the no-filter condition. Different graphs represent each of the three particle sizes used.

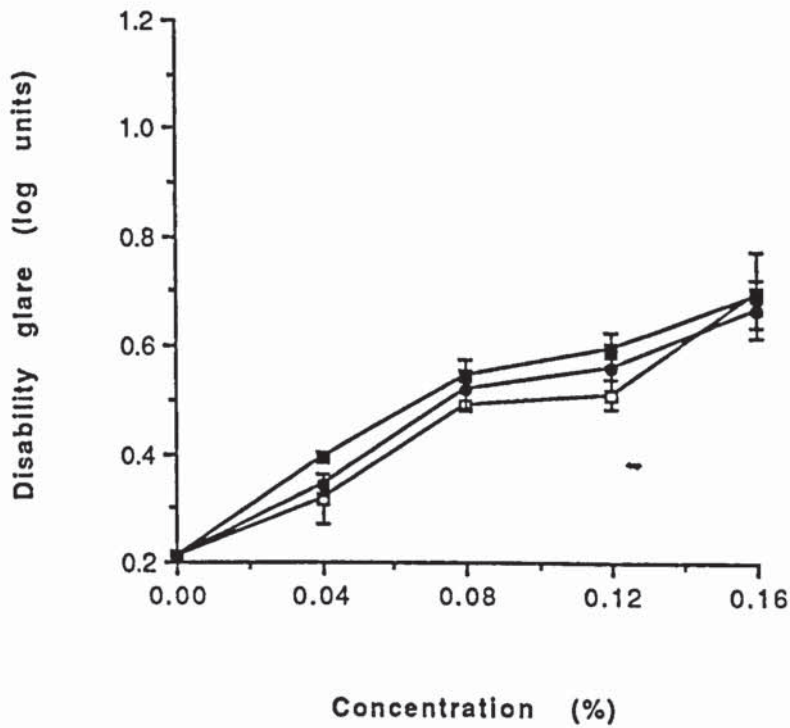


Figure 5.7 The size of the microsphere particle is 300nm. Concentration of the particles is plotted along the x-axis, disability glare along the y-axis. Standard errors are shown. Different symbols represent the filters used: solid square, no filter; open square, blue filter; solid circle, red filter. Observer RS.

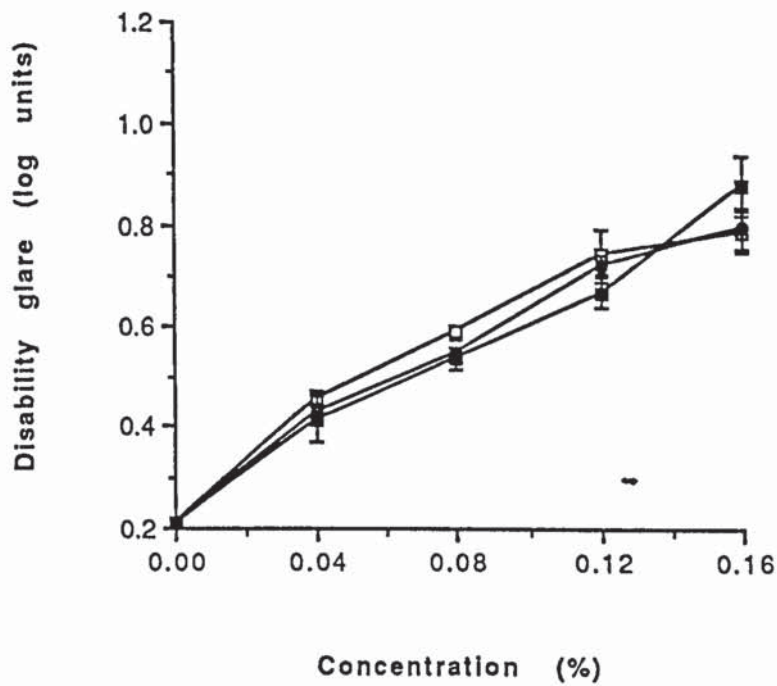


Figure 5.8 The size of the microsphere particle is 500nm. Concentration of the particles is plotted along the x-axis, disability glare along the y-axis. Standard errors are shown. Different symbols represent the filters used: solid square, no filter; open square, blue filter; solid circle, red filter. Observer RS.

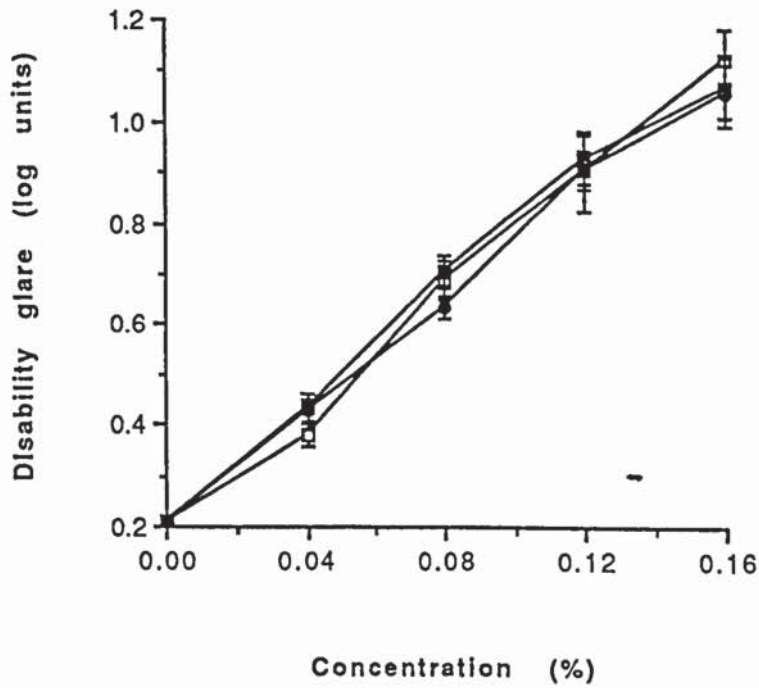


Figure 5.9 The size of the microsphere particle is 750nm. Concentration of the particles is plotted along the x-axis, disability glare along the y-axis. Standard errors are shown. Different symbols represent the filters used: solid square, no filter; open square, blue filter; solid circle, red filter. Observer RS.

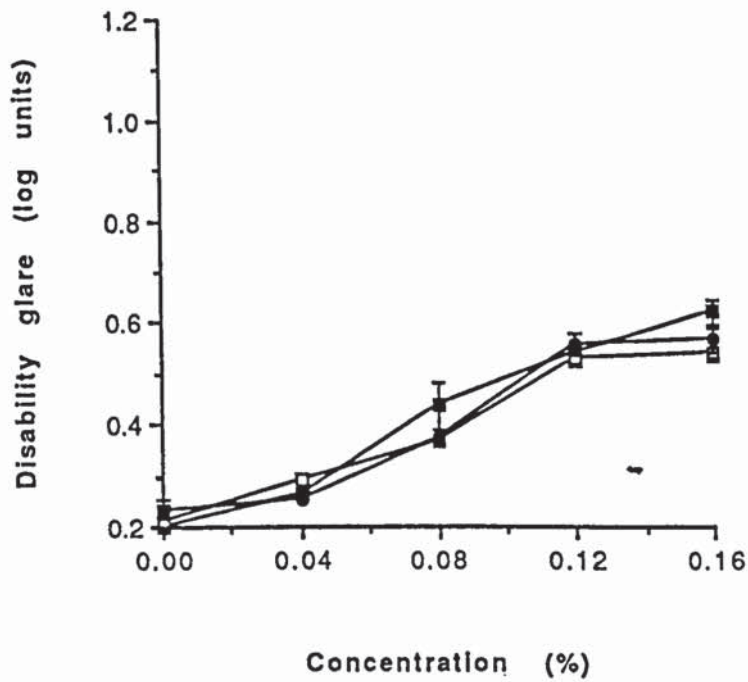


Figure 5.10 The size of the microsphere particle is 300nm. Concentration of the particles is plotted along the x-axis, disability glare along the y-axis. Standard errors are shown. Different symbols represent the filters used: solid square, no filter; open square, blue filter; solid circle, red filter. Observer SR.

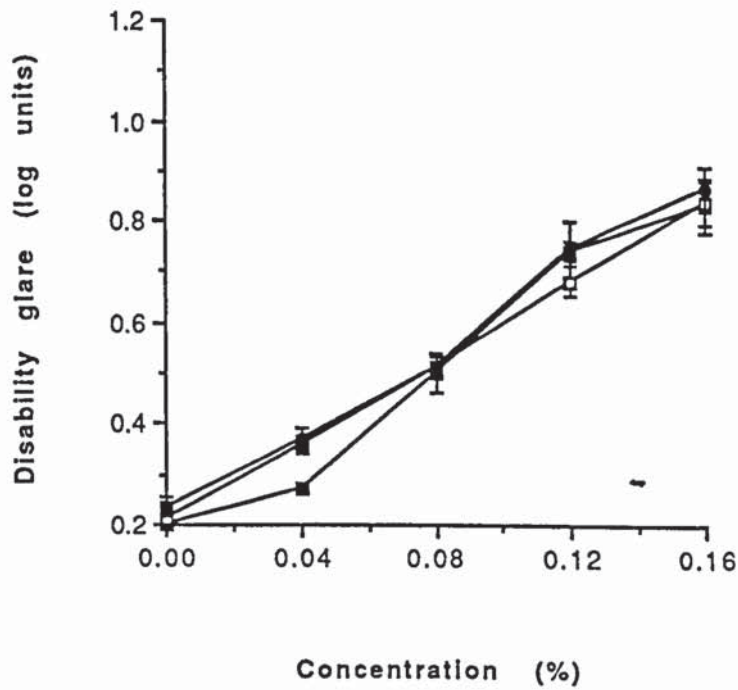


Figure 5.11 The size of the microsphere particle is 500nm. Concentration of the particles is plotted along the x-axis, disability glare along the y-axis. Standard errors are shown. Different symbols represent the filters used: solid square, no filter; open square, blue filter; solid circle, red filter. Observer SR.

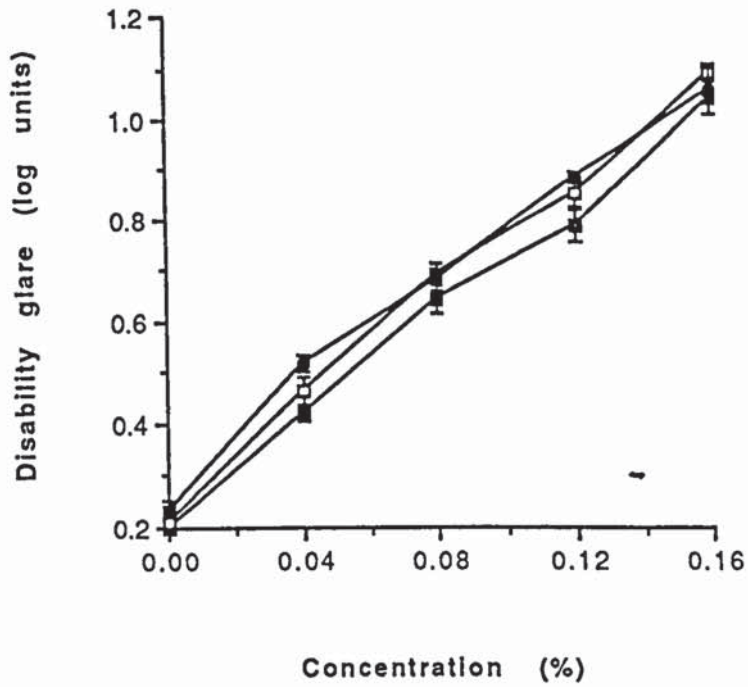


Figure 5.12 The size of the microsphere particle is 750nm. Concentration of the particles is plotted along the x-axis, disability glare along the y-axis. Standard errors are shown. Different symbols represent the filters used: solid square, no filter; open square, blue filter; solid circle, red filter. Observer SR.

Disability glare increases approximately linearly with microsphere concentration. The rate of increase of disability glare with increasing microsphere concentration varied with microsphere size; the largest increase was found with the largest size scatter particle. The graphs suggest that disability glare in the no-filter condition is no greater than with either the red or the blue filter present. This was confirmed by a split plot analysis of variance (df 2,30; $p>0.1$ for each observer and each particle size). Neither were there any significant interaction effects between filter condition and scatter cell concentration in any of the conditions (df 8,30; $p>0.1$). This confirms the prediction of equation [5.2] that disability glare is not affected by the presence of a filter since not only do filters reduce the amount of veiling luminance from the glare source, but they also reduce the luminance of the stimulus.

Despite the observation that a greater proportion of short wavelength light was present in the veiling luminance from the cells (Figure 5.4), the analysis of variance confirmed that disability glare with the short and long wavelength pass filters was not significantly different for either observer (df 2,30; $p>0.1$). This appears rather puzzling until one calculates the anticipated difference in disability glare arising from the wavelength dependency. For the 300nm sized particles the relative effect of the filters was that 33.8% more scattered light was present in the blue filter condition than in the red. Even at the highest disability glare level produced by this size of particle (approximately 0.6 log units), this scatter difference would only be expected to account for approximately 0.09 log units difference in disability glare between the two filter conditions. In addition, at least part of the 0.6 log units arises from scatter within the eye itself, which is presumably relatively wavelength-independent. Similar calculations for the 500nm particle size (which resulted in 19.6% more scattered light in the blue filter condition) reveal a maximum expected disability glare difference of 0.07 log units. For the 750nm particle size (10.6% more scattered light using the blue filter) the maximum difference is 0.04 log units. These values are all less than the average standard deviation of the data points at the highest disability glare level.

5.D. Discussion

Filters which affect the spectral distribution of transmitted visible light have little value in reducing disability glare in the presence of stray light. The reason behind this is evident from equation [5.2] which demonstrates that it is not the absolute level of stray light arising from the glare source which determines performance, but rather the ratio of stray light to stimulus luminance. Although filters do reduce the amount of stray light they also reduce the visibility of the stimulus. Therefore, the concept that tinted lenses automatically reduce disability glare is erroneous. The optimum method by which disability glare may be alleviated is to reduce stray light reaching the eye from a glare source without affecting the object of interest. This is the logic behind the use of horizontally louvered spectacles (Cohen and Waiss, 1991), pinhole glasses (Miller and Benedek, 1978) or honeycombs (Miller et al, 1976). These devices are successful in reducing disability glare by way of eliminating peripheral glare sources but the limited field of view restricts their general application. A similar effect is achieved by the use of visors or broad brimmed hats (Sliney, 1983), and also the tendency to squint in bright sunlight, although these tactics are often considered purely as methods to combat discomfort glare. Graduated tinted lenses, which selectively block glare from above, work along the same principles, but are usually prescribed on a cosmetic rather than a functional basis. Perhaps their value in individuals susceptible to intraocular stray light should be re-evaluated. Another example of selective attenuation of glare is in the use of polarising filters which preferentially absorb light which has been polarised by surface reflection.

(see page 135a).

Another potential method for reducing disability glare is evaluated in this study (5.A.). This involves choosing the spectral characteristics of a tint to selectively absorb wavelengths which are scattered preferentially. However, the present data argue against this methodology since its effect is minimal. Even in the presence of

The amount of light entering the eye not only causes disability glare but also discomfort glare. Discomfort glare causes irritating sensations without necessarily reducing visibility, because of light sources with a high luminance or an uneven distribution of light sources in the visual field. The cause of this type of glare is not well known, but may be related to pupil activity. The factors affecting discomfort glare are size, luminance and number of glare sources, their position in the field of vision and the background luminance. Discomfort glare measured both subjectively and objectively has been shown to decrease with reduction in luminance of the glare source (Berman et al, 1994). This correlates with the reduced amount of disability glare when glare luminance is reduced.

significant amounts of wavelength dependent stray light the calculated difference in disability glare between long and short wavelength pass filters is extremely modest. Indeed, using this method no difference was detected, despite the good reliability of the technique. The primary reason for the lack of demonstrable effect arises from the rather broad band nature of spectacle filters. Filters which possess quite different transmission characteristics (Figure 5.5) may have luminous efficiency curves which demonstrate considerable overlap as a function of wavelength (Figure 5.6). Of course, if the investigation had continued to much higher levels of disability glare (higher scatter cell concentrations), it seems certain that some measurable difference between the two filter conditions would have been found. To reinforce the view that the spectral characteristics of filters are of little importance it should be remembered that there appears to be little wavelength dependent scatter in the normal human eye (Boettner and Wolter, 1962)(see Chapter 7).

-

The topic of visual performance and tinted lenses is complex and often controversial. Very few studies have investigated the effect of filters upon visual performance under conditions of glare. Tupper et al (1985) present data to suggest that many cataract patients show considerable improvements in acuity under conditions of glare when an appropriate filter is introduced. However, their use of an acuity chart consisting of coloured letters on a complementary coloured background means that their results are difficult to interpret due to changes in the contrast of the letters with and without the coloured filter. Leat et al (1990) measured grating acuity with and without glare for a wide range of ocular diseases and examined the effect of different filters. Seventy-three percent of the total number of observers showed some improvement in performance in the presence of a filter either with or without glare. Of these patients, 58% showed an improvement in performance in both conditions, which means that disability glare remained approximately the same with or without the filter. The remaining 42% were equally split into those who improved under conditions of glare but not in normal viewing (reduced disability glare) and those who improved in

normal viewing but not with glare (increased disability glare). Hence, these data support the premise that the use of filters results in little overall change in disability glare levels.

The data presented here is consistent with studies in which contrast thresholds have been measured with yellow and luminance-matched neutral lenses and found not to differ (Sliney, 1983; Clark, 1969; Kelly et al, 1984). Wyszecki attempted to explain the popularity of filters on the basis of increased visibility but concluded that no specific filter would improve detection (Wyszecki, 1956). Clark surveyed nearly 100 studies of tinted lenses and concluded that there was no advantage of any coloured lens relative to neutral tints (Clark, 1969). Despite this, several studies report increased contrast performance (Leat et al, 1990; Zigman, 1990; Zigman, 1992; Rieger, 1992; Yap, 1982) and increased visual acuity (Zigman, 1990; Tupper et al, 1985) in the presence of filters. One possible reason for these observations lies in the efficacy of certain tints to absorb UV light. Specific wavelengths outside the visible spectrum can produce fluorescence of chromophore containing proteins within the human lens. The visible light produced by this fluorescence acts in the same way as a veiling luminance arising from a glare source. These 'fluorophores' have activation wavelengths of approximately 350nm and 430nm, the latter resulting in emission wavelengths well within the visible spectrum, between 500 and 520nm (Lerman and Borkman, 1976). The degree of fluorescence within the lens is known to increase with age. UV-induced ocular fluorescence has been shown to have a significant effect upon visual function (Elliott et al, 1993b), although the effect was rather small, probably due to the low levels of radiation which can safely be used in such studies. Filters which demonstrate negligible transmission at the activation wavelengths of fluorophores within the lens may therefore result in increased visual performance in environments containing moderate to high levels of UV light.

To conclude, neither the presence of a filter nor its type of wavelength selective absorption in the visible spectrum are likely to be of any benefit in alleviating disability glare. However, the extent of veiling stray light due to fluorescence in the real eye under everyday visual conditions needs to be considered before the efficacy of wavelength selective filters can be completely evaluated. The most successful means of reducing disability glare resides in methods which selectively attenuate peripheral sources of glare without affecting foveal vision.

CHAPTER 6. CONFIRMATION OF THE PSYCHOPHYSICAL LIGHT SCATTERING FACTOR

6.A. Introduction

This aim of the experiment was to re-evaluate the validity of Paulsson and Sjöstrand's LSF calculation by firstly assessing the consistency of LSFs measured with three glare luminances at each of three stimulus luminance levels, and secondly to compare direct stray light values with values obtained using the Paulsson and Sjöstrand's LSF calculation for a number of normal young subjects, elderly subjects and also subjects with cataract.

A measure of the quality of the ocular media may be obtained by determining the proportion of illuminance arriving at the eye from a peripheral glare source (E_{gl}), which is subsequently scattered to the fovea. This has the same effect as an equivalent veiling luminance, L_{eq} , superimposed upon the stimulus itself. The light scattering factor (LSF) of the eye can be defined as (see 3.A.1)

$$LSF = L_{eq}/E_{gl} \quad [6.1]$$

The veiling luminance reduces stimulus contrast by a factor $L/(L + L_{eq})$, where L represents mean stimulus luminance. Therefore, the ratio of contrast thresholds measured with and without the presence of a glare source (M_2 and M_1 , respectively) is given by

$$M_2/M_1 = (L + L_{eq})/L = 1 + L_{eq}/L$$

thus,

$$L_{eq} = [(M_2/M_1) - 1] L$$

substituting into [6.1],

$$\text{LSF} = (L/E) \cdot (M_2/M_1 - 1) \quad [6.2]$$

This equation allows an intrinsic LSF to be determined for any given glare angle (Paulsson and Sjöstrand, 1980). In addition, the LSF calculated in this way should remain independent of the precise stimulus conditions used for its determination, because any variation in L and E should be cancelled out by the corresponding variations in contrast thresholds.

In a recent study the validity of this approach to calculating a LSF has been questioned (Yager et al, 1992). This study did not find the expected constancy in LSF when two different values of L/E were used. Other authors have used Yager's study to question the validity of the formula and therefore the method of assessing light scatter using contrast thresholds with and without glare (de Waard et al, 1992; van den Berg, 1991).

6.B. Measurement of the psychophysical Light Scattering Factor

6.B.1 Methods

Contrast thresholds for the detection of 1.87 Hz sinusoidal uniform field flicker of a 50 minute arc circular target on a 5° square background of identical mean luminance were measured with and without the presence of glare. The stimulus was presented on the face of a CRT at a viewing distance of 2 m and was controlled by the Venus Visual Stimulator (4.B.). This localized target was used because visual eccentricity can be accurately specified relative to the glare source. This is not true for wide-field grating stimuli in which different parts of the stimulus lie at different angular distances to the glare source. This results in an uneven distribution of veiling luminance across the

stimulus. In addition, the equal mean luminance of the background field reduces potential problems associated with improvements in contrast sensitivity resulting from the background retinal illuminance produced by the glare source (de Waard et al, 1992).

The mean stimulus luminance was 49.0cdm^{-2} . Additional luminance levels of 12.3 and 4.9cdm^{-2} were obtained by superimposing neutral density filters in front of the stimulus and its background. After an appropriate choice of starting modulation, a method of increasing contrast was used to measure thresholds. To reduce flicker adaptation effects, flicker was presented in four cycle sequences (lasting 2.14 seconds) separated by 1-second intervals of mean luminance. The contrast of each successive presentation was increased by 0.1 log units. Threshold was recorded as the contrast level at which flicker was first perceived. The final threshold was calculated as the mean of a maximum of four such threshold estimates. The order of measurement was randomized. In addition, to avoid the possibility of observers responding on the basis of time elapsed, a random time delay was inserted at the beginning of each sequence.

A 1,000W tungsten-halogen bulb housed in a projector unit was used. Light from the bulb was projected through a filter centred at 580nm wavelength with a half-height bandwidth of 20nm. The maximum luminous intensity of the glare source was 368cd. The glare source was placed at 6.5° visual angle from the stimulus (Figure 6.1) The illuminance arriving at the eye from the glare source was measured photometrically by a spectrophotometer (4.B.) and was varied between 361 and 22.8lux by means of neutral density filters. Contrast thresholds were measured for each illuminance level (E) for each of the three stimulus luminances (L), giving a total of nine conditions. Five different ratios of L/E were investigated, spanning a range of 1.60 log units.

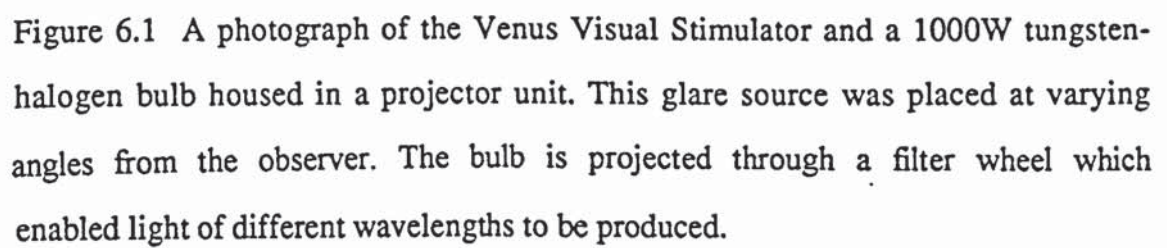
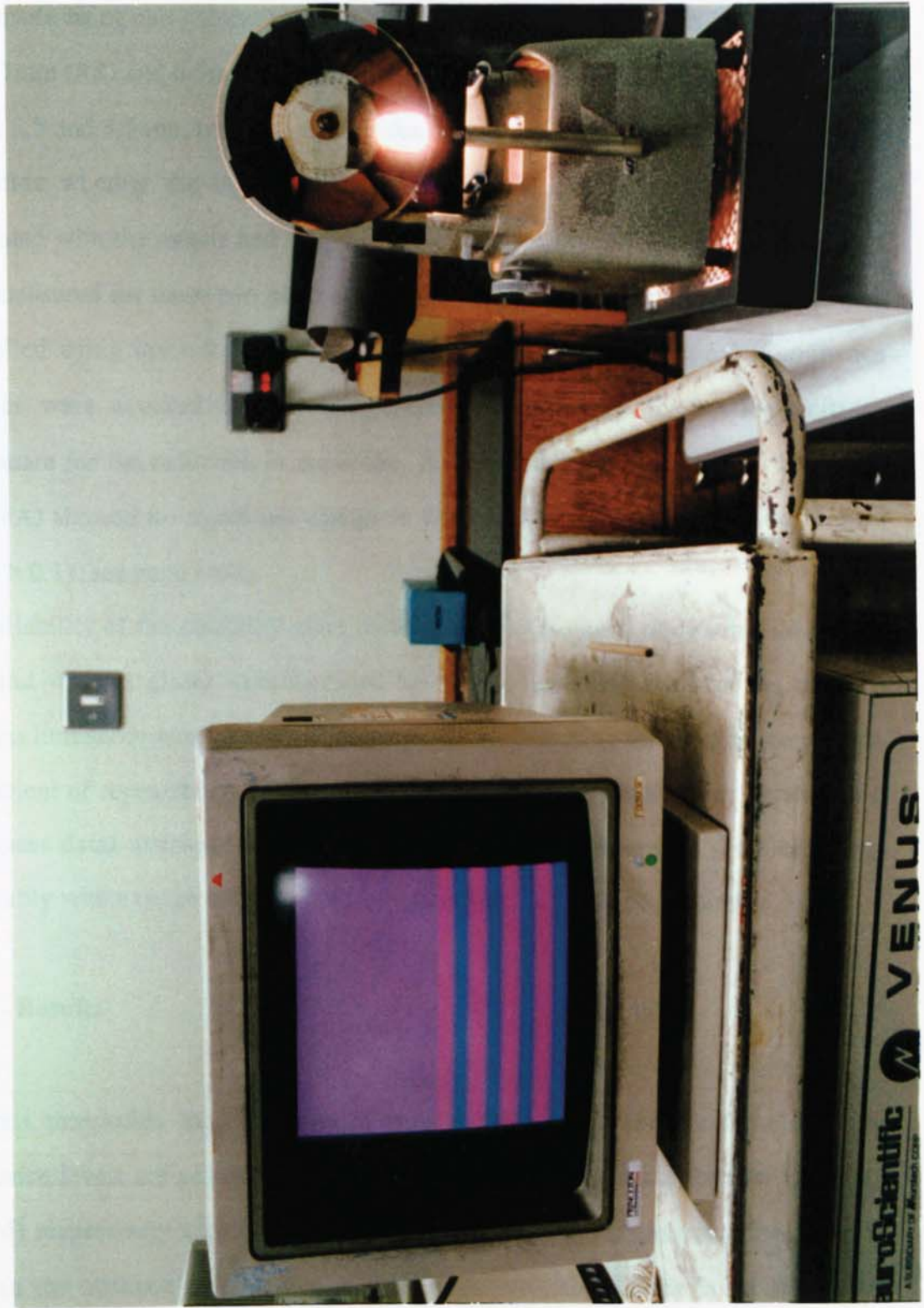
The image area is mostly blank, with a small dark speck visible near the center. The text below describes the equipment shown in the photograph.

Figure 6.1 A photograph of the Venus Visual Stimulator and a 1000W tungsten-halogen bulb housed in a projector unit. This glare source was placed at varying angles from the observer. The bulb is projected through a filter wheel which enabled light of different wavelengths to be produced.



Three experienced observers participated in the study (Age years RS=24, IM=24 and DW=30; Gender M=3). Exclusion criteria are described in 4.B. All observers underwent substantial training in the task before data collection began. Measurements were made using the natural pupil, which varied in diameter from 7mm (observer DW), 7mm (RS) and 6.5mm (IM) for the no-glare, low-stimulus luminance condition to 5.5, 5.5 and 4.5mm, respectively, for the high-glare, high-stimulus luminance. To determine whether the improvement in the optical quality of the retinal image associated with the miosis had a significant effect on contrast thresholds, thresholds were measured for these two pupil size conditions for each observer. Pupil size was controlled using the miotic thymoxamine hydrochloride, and retinal illuminance changes were avoided by increasing stimulus luminance by 0.3 log units to compensate for the reduction in pupil size. A repeated measures analysis of variance (ANOVA) showed no significant change in contrast thresholds as a function of pupil size ($P > 0.1$) (see page 143a).

The reliability of the disability glare measurements (the ratio of contrast thresholds with and without glare) were assessed by taking test-retest data for the medium stimulus luminance at each glare illuminance level (including the no-glare condition). Coefficient of repeatability (95% confidence limits for the discrepancy between test and retest data) averaged 0.15 log units for the three observers. This compares favourably with a range of other disability glare tests (Elliott and Bullimore, 1993).

6.B.2 Results

Contrast thresholds as a function of ocular illuminance for the three stimulus luminance levels are plotted in Figures 6.2, 6.3 and 6.4 for each observer (DW, RS and IM) respectively and shown in Tables 6.1 and 6.2. An illuminance level of zero denotes the absence of glare. In this no-glare condition, there is no significant difference between contrast thresholds for the three stimulus luminances ($P > 0.1$ for all three observers). As glare illuminance increases, however, contrast thresholds for

Others have demonstrated that light scatter in the eye is not uniform over the whole pupil. The peripheral part of the pupil produced more light scatter than the centre, therefore suggesting that light scatter increases with pupil size (Edgar et al, 1995).

the low-stimulus luminance increase dramatically, whereas the increase in contrast thresholds for the high-stimulus luminance is less marked.

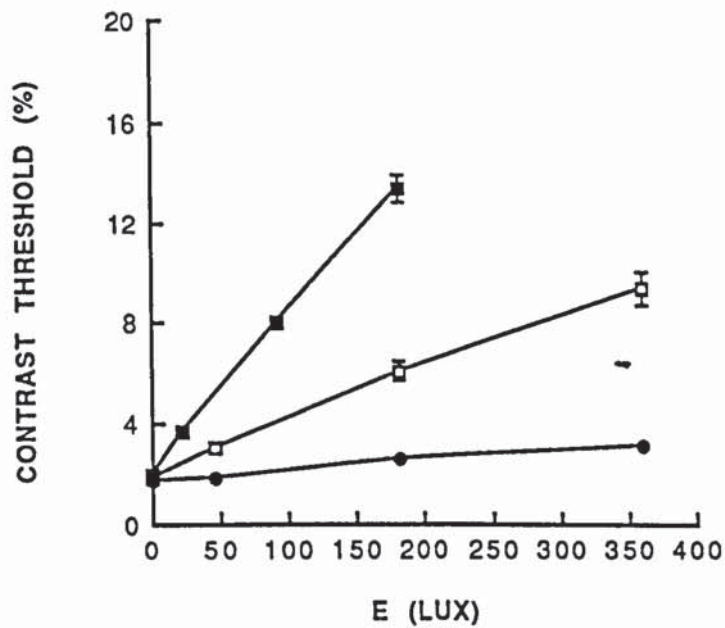


Figure 6.2 Represents data from observer DW. Contrast thresholds as a function of ocular illuminance produced by the glare source are shown. Different symbols represent the three stimulus luminance levels: filled squares, 4.9cdm⁻²; open squares, 12.3cdm⁻² and circles, 49cdm⁻². Data points represent the mean of a maximum of four threshold estimates, and standard error of the estimates are shown.

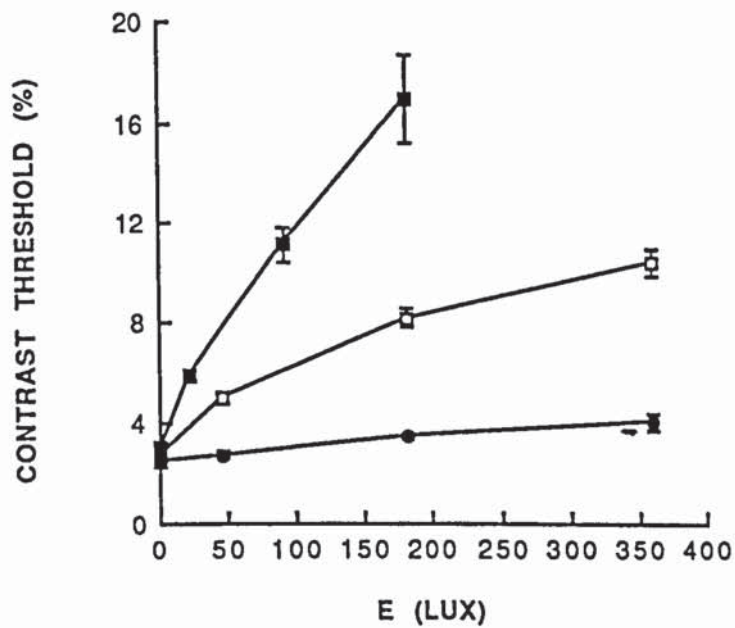


Figure 6.3 Represents data from observer RS. Contrast thresholds as a function of ocular illuminance produced by the glare source are shown. Different symbols represent the three stimulus luminance levels: filled squares, 4.9cdm⁻²; open squares, 12.3cdm⁻² and circles, 49cdm⁻². Data points represent the mean of a maximum of four threshold estimates, and standard error of the estimates are shown.

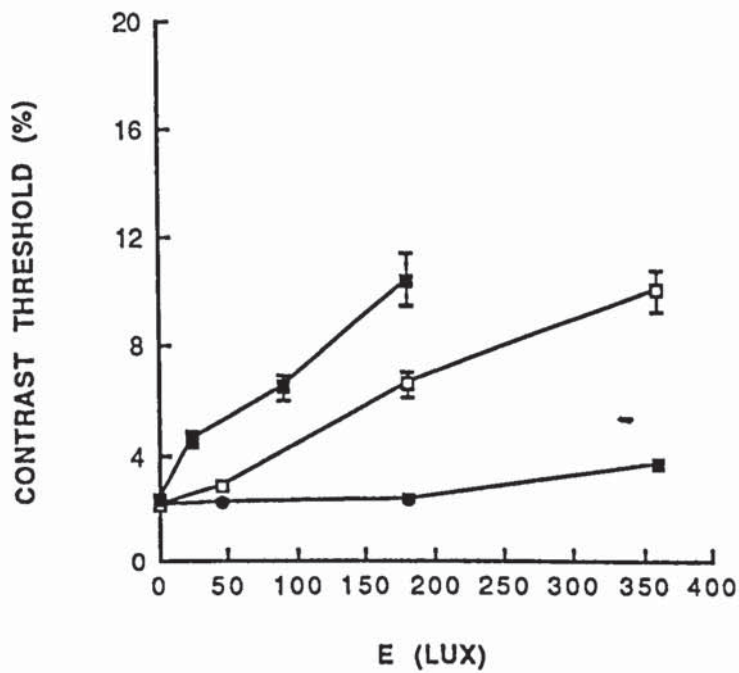


Figure 6.4 Represents data from observer IM. Contrast thresholds as a function of ocular illuminance produced by the glare source are shown. Different symbols represent the three stimulus luminance levels: filled squares, 4.9cdm⁻²; open squares, 12.3cdm⁻² and circles, 49cdm⁻². Data points represent the mean of a maximum of four threshold estimates, and standard error of the estimates are shown.

RS

	Contrast Threshold at 49.0cdm ⁻²	Contrast Threshold at 12.3cdm ⁻²	Contrast Threshold at 4.9cdm ⁻²
E			
0.0	2.50±0.24	2.80±0.26	2.90±0.31
22.8			5.90±0.26
45.4	2.80±0.26	5.00±0.24	
90.1			11.1±0.74
181	3.50±0.12	8.10±0.33	17.0±1.75
361	4.10±0.38	10.4±0.54	

IM

	Contrast Threshold at 49.0cdm ⁻²	Contrast Threshold at 12.3cdm ⁻²	Contrast Threshold at 4.9cdm ⁻²
E			
0.0	2.10±0.17	2.10±0.26	2.40±0.13
22.8			4.60±0.43
45.4	2.30±0.15	2.80±0.13	
90.1			6.50±0.42
181	2.40±0.13	6.60±0.58	10.4±1.09
361	3.70±0.22	10.0±0.81	

Table 6.1 Represents the data from observers RS and IM. Contrast thresholds and standard errors are shown for different stimulus luminance (49.0, 12.3 and 4.9cdm⁻²) and for different ocular illuminance (E) produced by the glare source.

DW

	Contrast Threshold at 49.0cdm ⁻²	Contrast Threshold at 12.3cdm ⁻²	Contrast Threshold at 4.9cdm ⁻²
E			
0.0	1.80±0.15	1.90±0.09	2.00±0.12
22.8			3.80±0.14
45.4	1.90±0.12	3.00±0.05	
90.1			8.00±0.37
181	2.60±0.15	3.00±0.11	13.3±0.53
361	3.20±0.18	9.30±0.75	

Table 6.2 Represents the data from observer DW. Contrast thresholds and standard errors are shown for different stimulus luminance (49.0, 12.3 and 4.9cdm⁻²) and for different ocular illuminance (E) produced by the glare source.

Figures 6.5, 6.6 and 6.7 show the results for each observer (DW, RS and IM) respectively. Each graph shows the ratio of contrast thresholds with and without glare (M_2/M_1) plotted against E/L (Table 6.3). The best-fitting linear regression, weighted according to the inverse variance of each point, is shown. From equation [6.2];

$$M_2/M_1 = 1 + \text{LSF} \cdot E/L$$

If this equation is valid the y-intercept of the linear regression shown in Figures 6.5-6.7 should equal 1, and the data points for different conditions should all lie on the regression line. The actual y-intercepts (± 1 SE) for the three observers were 0.93 ± 0.06 , 1.11 ± 0.14 and 0.99 ± 0.10 (Figures 6.5, 6.6 and 6.7, respectively). R^2 values for each observer exceed 0.95. The gradient of the linear regression predicts the LSF. Values for LSF (± 1 SE) were 0.16 ± 0.01 , 0.11 ± 0.02 and 0.11 ± 0.02 for Figures 6.5, 6.6 and 6.7, respectively. The highest LSF occurred for the oldest subject.

6.B.3 Discussion

The highly linear relationship between M_2/M_1 and E/L and the closeness of the y-intercept to a value of 1 confirm the validity of the Paulsson and Sjöstrand equation (6.2). This conclusion is therefore contradictory to that of Yager et al (1992). Although the method of threshold measurement used in this experiment is criterion-dependent, all three observers were experienced in making these psychophysical measurements, and the test-retest repeatability of scores was good. Unreliability in any part of the methodology is more likely to lead to the conclusion that the relationship between M_2/M_1 and E/L is not linear rather than the reverse.

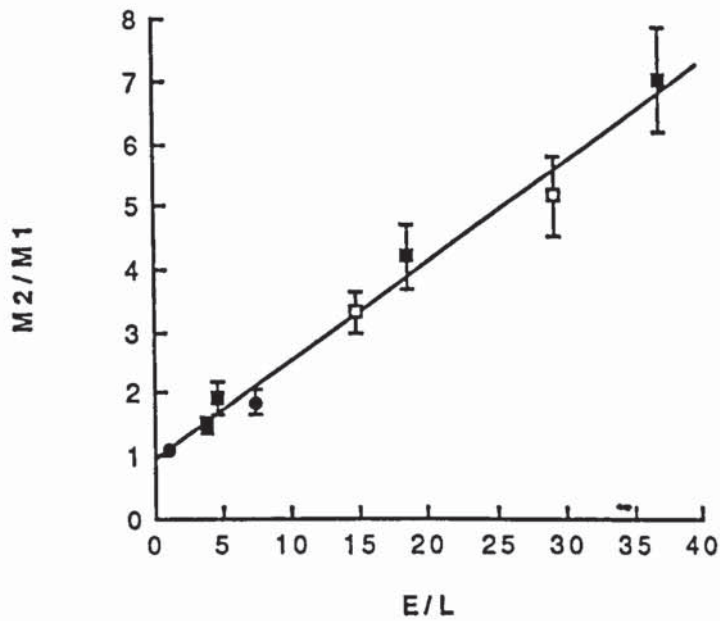


Figure 6.5 Represents data from observer DW. The ratio of contrast thresholds with and without glare (M_2/M_1) against E/L is shown. Different symbols represent the three stimulus luminance levels: filled squares, 4.9cdm^{-2} ; open squares, 12.3cdm^{-2} and circles, 49cdm^{-2} . Standard errors of each data points are shown. The data are fitted with the best-fitting linear regressions weighted according to the inverse variance of each point.

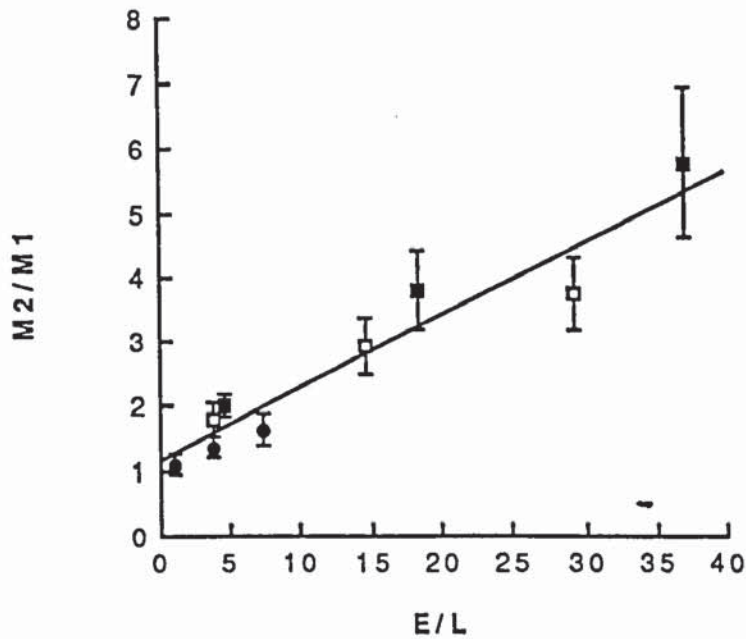


Figure 6.6 Represents data from observer RS. The ratio of contrast thresholds with and without glare (M_2/M_1) against E/L is shown. Different symbols represent the three stimulus luminance levels: filled squares, 4.9cdm^{-2} ; open squares, 12.3cdm^{-2} and circles, 49cdm^{-2} . Standard errors of each data points are shown. The data are fitted with the best-fitting linear regressions weighted according to the inverse variance of each point.

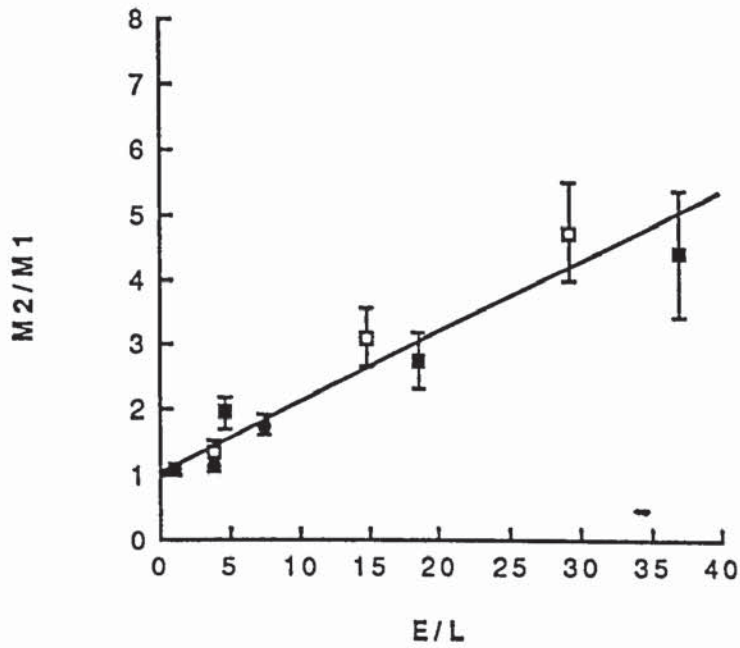


Figure 6.7 Represents data from observer IM. The ratio of contrast thresholds with and without glare (M_2/M_1) against E/L is shown. Different symbols represent the three stimulus luminance levels: filled squares, 4.9cdm^{-2} ; open squares, 12.3cdm^{-2} and circles, 49cdm^{-2} . Standard errors of each data points are shown. The data are fitted with the best-fitting linear regressions weighted according to the inverse variance of each point.

Observers			
	RS	IM	DW
	M_2/M_1	M_2/M_1	M_2/M_1
	49.0cdm ⁻²	49.0cdm ⁻²	49.0cdm ⁻²
E/L			
0.93	1.10±0.23	1.10±0.18	1.10±0.08
3.70	1.40±0.18	1.10±0.13	1.50±0.04
7.37	1.60±0.17	1.80±0.19	1.90±0.19
	12.3cdm ⁻²	12.3cdm ⁻²	12.3cdm ⁻²
3.70	1.80±0.33	1.30±0.23	1.50±0.21
14.72	2.90±0.47	3.10±0.54	3.30±0.33
29.35	3.70±0.58	4.80±0.81	5.20±0.64
	4.9cdm ⁻²	4.9cdm ⁻²	4.9cdm ⁻²
4.65	2.00±0.19	1.90±0.12	1.90±0.29
18.51	3.80±0.56	2.80±0.38	4.20±0.54
36.94	5.80±1.19	4.40±1.01	7.00±0.82

Table 6.3 Shows the data obtained from each observer (RS, IM and DW). The ratio of contrast thresholds with and without glare (M_2/M_1) for each of the three stimulus luminances (49.0cdm⁻², 12.3cdm⁻² and 4.9cdm⁻²) against E/L is shown.

The LSF scores measured in this experiment conform to previously published normative data. LSF is dependent on the angle of the glare source θ . Many formulae have been determined empirically to explain this angular dependency (Vos, 1984). Yager et al (1992) cite the formula of Vos, Walraven and van Meeteren (1976)

$$\text{LSF} = 29/(\theta + 0.13)^{2.8} \quad [6.3]$$

According to this equation, LSF at 6.5° should be 0.15. At an angle of 7° , IJspeert et al (1990) found a mean LSF of 0.12 (95% confidence limits of 0.08 to 0.20) for a group of 20- to 30-year-old subjects. Our three LSF values of 0.16, 0.11, and 0.11 are therefore in good agreement with these values. Using a glare angle of 1.7° , Paulsson and Sjöstrand (1980) found mean LSF scores for five subjects at two E/L values (0.4 and 4) of 4.9 ± 1.9 and 4.5 ± 1.1 , which were not significantly different ($P > 0.1$). Equation [6.3] predicts a LSF at 1.7° of 5.3, which is consistent with Paulsson and Sjöstrand's data (1980).

Yager et al (1992) used a glare source of 3.5° and recorded mean values of LSF for 12 subjects (age range, 22 to 50 years) at two values of E/L (1.87 and 9.26) of 0.26 ± 0.18 (SD) and 0.49 ± 0.34 , respectively. Equation [6.3] predicts a LSF of 0.78. IJspeert et al (1990) give mean values of 3.5° LSF for 20- to 30-year-old subjects and 40- to 50-year-old subjects, respectively, of 0.57 (95% confidence range of 0.38 to 0.89) and 0.67 (95% confidence range from 0.44 to 1.02). Therefore, Yager et al's values appear to be significantly lower than established normal data, particularly at the low E/L condition.

Yager et al's scepticism of the validity of equation [6.2] is in agreement with previous papers concerned with the usefulness of measuring LSF using contrast thresholds with and without glare (de Waard et al, 1992; van den Berg, 1991). The results showed a nonlinear relationship between stray light values measured with the van den Berg

straylightmeter and scores using contrast thresholds measured with and without glare on the Vistech MCT8000 (de Waard et al, 1992). This leads to the important consideration of the optimum stimulus conditions that should be used to determine LSFs when measuring contrast thresholds with and without glare. First, it is essential that the luminance of the stimulus should not be too low and be within the region of Weber's law (where contrast thresholds are independent of luminance). Performance will therefore not be improved by the glare source. In this respect, it is preferable for the stimulus to be of low spatial and temporal frequency content because such stimuli become dependent on retinal illuminance at lower levels than at higher frequencies (van Nes and Bouman, 1967). Second, the stimulus should be surrounded by a field of the same mean luminance. It is well-established that contrast sensitivity is reduced by the presence of a dark border, and de Waard et al (1992) have suggested that, under such conditions, the addition of a veiling luminance on the retina from a glare source could improve sensitivity by brightening the border to the stimulus. Finally, a spatially localized target is preferred because all parts of the stimulus lie at approximately the same visual angle from the glare source, resulting in an even veiling luminance over the entirety. A further point is that neural adaptation effects should be avoided by ensuring that no part of the target is within 1° of the glare source (Vos, 1984).

Abrahamsson and Sjöstrand (1986) updated equation [6.2] to include a correction factor to account for changes in pupil size caused by the glare source. They suggested an empirically determined factor of 1.2. It is questionable whether any correction factor for pupil size is necessary. Equivalent veiling luminance (L_{eq}) is defined as luminance that, when superimposed upon the stimulus (L_s), has the same effect as a veiling retinal illuminance (E_v) upon the retinal illuminance of the stimulus (E_s).

Therefore,

$$E_v / E_s = L_{eq} / L_s$$

because both E_v and E_s depend to the same extent upon pupil size, L_{eq} should remain independent of variations in pupil size. Hence, from equation [6.1], this will also hold true for LSF. The reasoning is that pupil size changes affect retinal illuminance of the stimulus and the glare source equally. Of course, original pupil size is important insofar as it determines retinal illuminance. It should also be noted that the change in pupil size with glare is likely to have a significant effect in cataract. This particularly true for posterior subcapsular cataract in which the decrease in pupil size with glare means that the opacity takes up a much greater proportion of the pupillary area (Yager et al, 1992, de Waard et al, 1992). Obviously, in such cases, the difference between thresholds with and without glare is not simply a measure of light scatter alone but it is, nevertheless, representative of real-life performance. Many patients with posterior subcapsular cataract can see perfectly well under normal levels of luminance but are markedly affected in glare conditions (de Waard et al, 1992).

In conclusion, the results confirm the validity of the Paulsson and Sjöstrand equation (equation [6.2]) for a sample of normal, experienced observers. Correction to the formula to account for pupil size changes are unnecessary. The results confirm the suitability of measuring the LSF using contrast threshold with and without glare, provided that appropriate methods are used.

6.C. Comparison between direct stray light measures and the psychophysical Light Scattering Factor

6.C.1 Introduction

The aim of this study was to establish if the level of stray light can be predicted from disability glare measurements. If this is true the stray light estimates derived from disability glare scores will agree with direct stray light values, which can be conveniently measured with van den Berg's straylightmeter. The method used to derive stray light estimates must obey the proportionality test. The experiment in 6.B. showed that the method used obeyed the proportionality test and that stray light estimates, obtained in 6.B., agreed well with normal age-matched stray light data. What was needed was an investigation that compared direct stray light values with those estimated from appropriately-designed disability glare tests.

6.C.2 Methods

Using the same experimental equipment described in section 6.B. contrast thresholds were measured for different observers both with and without the glare source. For each observer a LSF was calculated using equation [6.2] (see 6.A.) for each glare angle. Four different glare angles were used; 3.25°, 6.5°, 13° and 26° and each LSF for each glare angle was multiplied by the glare angle squared. This value is equivalent to the direct stray light measurements made with van den Berg's straylightmeter (3.B.) These stray light values were averaged over the glare angles used in this technique.

Eight young normal observers (mean age 25.5 years, SD=2.3; Gender M=2, F=6), five elderly subjects (mean age 74.6 years, SD=5.6; Gender M=2, F=2) and four cataract subjects (mean age 79.0 years, SD=7.8; Gender M=2, F=1) were used. The

Lens Opacity Classification System II (LOCS II)(Chylack et al, 1989) was used to classify the type and severity of cataract. Slit-lamp examination of the eye was compared with standard photographs. Two of the cataracts were classified as C I and the other two as either N III or C II, where N refers to nuclear cataract, C to cortical cataract and the number is an estimate of cataract severity.

Measurements were also obtained using the same observers on the van den Berg straylightmeter. The van den Berg straylightmeter measures the amount of stray light using a direct compensation method. In this approach the observer detects when luminance modulation from the scattered light (stray light) and the target luminance modulation are equal. The target or equivalent patch of light and the stray light are both flickered at a frequency which requires high flicker sensitivity. The stray light source is a ring with the equivalent patch in the centre, which is fixated. When the luminance modulation of the equivalent patch is low, flicker due to the stray light source can be detected. This flicker can be cancelled by varying the luminance modulation of the equivalent patch. In this way stray light is directly compensated (3.B.). Three glare angles were used; 3.5°, 10° and 26°. The stray light measurements were averaged over glare angles used in this technique.

6.C.3 Results

Figure 6.8 shows the relationship between stray light estimates derived from the disability glare method described in section 6.C.1 and the direct stray light measurements made with van den Berg's straylightmeter. Stray light values have been averaged over comparable glare angles for both techniques (6.C.1). It is clear that there is an excellent agreement between the stray light estimate and the direct measurement for all but the patients with the most severe cataract (N III and C II).

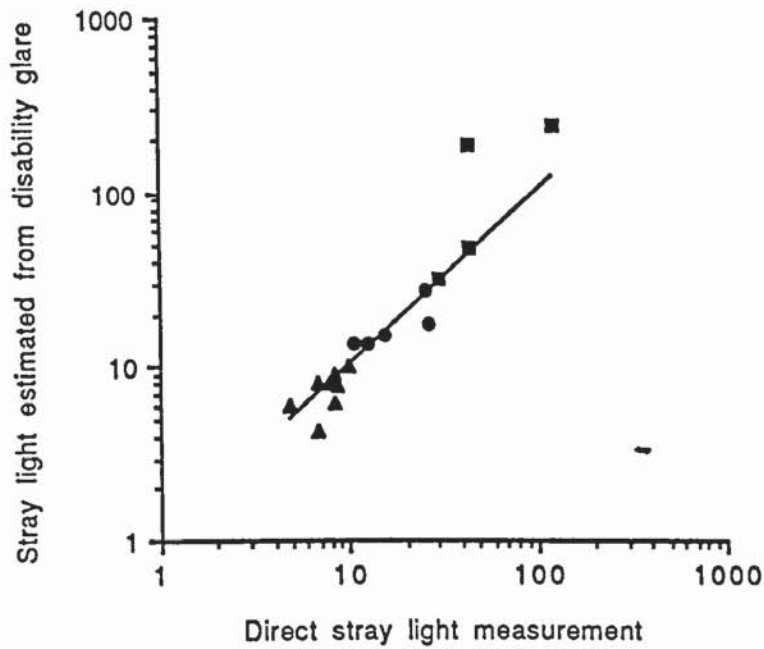


Figure 6.8 Stray light estimated from disability glare measurements plotted against direct stray light measurements using the van den Berg straylightmeter. Triangles represent measurements from normal young observers, circles from normal elderly subjects and squares from patients with cataract. The straight line represents the line of perfect agreement between the two measures.

It remains to be established whether this latter effect is due to overestimation of stray light by disability glare measurements or to underestimation by the straylightmeter.

6.C.4 Discussion

The results shown that there is agreement between direct and estimated measurements of stray light, therefore, it is up to the individual which technique is favoured. Clinicians may well favour the disability glare method because it gives an immediate estimate of the effect of a glare source on visual performance and it is easier for patients to perform. Those wishing to model the optical performance of the eye, for example, are likely to favour a direct method of stray light measurement. Both techniques of stray light estimation are equally valid and, in most cases, can be used interchangeably.

CHAPTER 7 MEASUREMENT OF THE WAVELENGTH DEPENDENCY OF LIGHT SCATTER IN THE NORMAL, ELDERLY AND CATARACTOUS EYE

7.A Introduction

The aim of the study was to investigate wavelength dependent scatter in normal young individuals and in elderly and cataractous eyes. In addition, to take account of any possible angular dependency, light scatter was investigated at several different visual angles.

A localised point source of light within the visual field does not produce an equally well-defined point image on the retina due to the optical imperfections in the ocular media. Instead, a proportion of the light is scattered and this forms the point spread function (PSF). Beyond one degree or so of visual angle from its centre, the PSF declines in amplitude in approximately inverse proportion to the square of the visual angle (see 3.A.1). Whilst there is widespread agreement regarding the angular dependency of stray light (at least beyond one degree of visual angle), much less is known about its spectral composition. Some early studies (Stiles, 1929b; Fry, 1954) assumed the presence of considerable amounts of Rayleigh scatter, in which short wavelength light is scattered preferentially (complete Rayleigh scatter implies that light is scattered in proportion to the reciprocal of its wavelength to the fourth power (see 1.D.)). Ivanoff (1947) demonstrated experimentally the predominance of short wavelengths in stray light. Direct measurement of stray light in enucleated eyes supports the existence of greater scatter of short wavelengths, although not to the same extent as complete Rayleigh scatter (Boettner and Wolter, 1962). Le Grand (1937) suggested that the wavelength dependency of scattered light was itself dependent upon visual angle. At narrow angles, long wavelengths predominated, whilst at greater angles the situation was reversed.

More recent studies deny the existence of significant amounts of wavelength dependent scatter. Vos (1984) points to the important relationship between ocular structure and stray light by noting that, for significant wavelength dependent scatter to exist, the scattering structures themselves must be extremely small (similar to or smaller than the wavelength of light). Whilst protein aggregates of this size do accumulate in the ocular lens with increasing age (Bettleheim, 1985), Vos (1984) and Hemenger (1990, 1992) conclude that the vast majority of forward stray light occurs due to larger scattering structures such as refractive index fluctuations at lens fibre intersections. Wooten and Geri (1987) have demonstrated experimentally the absence of significant wavelength dependent scatter in three normal, young subjects. Van den Berg et al (1991) find a type of wavelength dependency in which red light is scattered more than shorter wavelengths. They attribute this to selective transmission of longer wavelengths through the largely opaque structures of the iris and sclera.

Quantifying the wavelength dependency of stray light is important for several reasons. Firstly, as mentioned above, the phenomenon of wavelength dependency gives important insights into the type and, specifically, the size of ocular structures which give rise to stray light. Second, if significant dependency exists, then the use of filters with appropriate wavelength-selective transmission characteristics may allow selective attenuation of stray light and thus reduce disability glare. The magnitude of this effect is, however, likely to be minimal (see Chapter 5). Third, it may prove to be a relevant parameter for those who wish to model stray light in the human eye as a function of variables such as age, ocular pigmentation and scatter angle (Vos, 1984; IJspeert et al, 1990; IJspeert et al, 1993).

7.B. Methods

Stray light was quantified by measuring the reduction in temporal CS produced by a glare source. Contrast detection thresholds were measured for a spatially uniform 7.5Hz sinusoidal flicker for a 20min.arc circular target on a 2° square background. The stimulus was presented on a CRT at a viewing distance of 2m and was controlled by a Venus Visual Stimulator (4.B.). This localised target was favoured over a stimulus such as a wide-field grating since its visual eccentricity can be accurately specified relative to the glare source. Mean stimulus luminance was 2.71cdm⁻² and was achieved by placing two 0.6ND filters over the CRT. Additional luminance levels of 10.8 and 43.0cdm⁻² were obtained, when required, by removing one or both of the ND filters. Following an appropriate choice of starting modulation, a method of increasing contrast was used to measure threshold. In order to reduce flicker adaptation effects, flicker was presented in two second periods separated by one second intervals of mean luminance. The contrast of each successive presentation was increased by 0.1 log units. Threshold was recorded as the contrast level at which flicker was first perceived. The final threshold was calculated as the mean of four such threshold estimates. In order to avoid the possibility of observers responding on the basis of time elapsed, a random time delay was inserted at the beginning of each sequence.

In the first experiment, two experienced observers (Age years RS=24 and DW=30; Gender M=2) were used and both underwent substantial training in the task before data collection began. The exclusion criteria are described in 4.B. Only two observers were used as the experiment involved quantifying stray light at each wavelength therefore the length of time taken to collect data was long. In a second experiment, only extreme wavelengths (460 and 660nm) were used. In the second experiment five young observers (mean age 24.4 years SD=3.6; Gender M=2, F=3), five elderly observers (mean age 72.4 years SD=7.6; Gender M=2, F=3) and four elderly subjects

with cataract (mean age 79.0 years SD=4.8; Gender M=2, F=2) were used. Details of the cataract patients are shown in Table 7.1. The young sample consisted of 4 subjects with blue/green and one with brown iris colour whilst the elderly all had blue/green irides. The exclusion criteria are described in 4.B. All subjects wore their distance refractive correction where necessary and natural pupils were used throughout.

Subject	Age (years)	LogMAR VA	Cataract Type	Iris Pigmentation
HP	80	0.5	N III	Green
AM	82	0.3	C II	Green
WH	82	0.2	C I	Brown
BJ	72	0.1	C I	Brown

Table 7.1 Classification of the cataract types used in the study. Age, LogMAR visual acuity (VA), cataract type and iris pigmentation are shown. The Lens Opacities Classification System II (LOCS) (Chylack et al, 1989) was used in which slit lamp examination of the eye is compared with standard photographs. N refers to nuclear cataract, C to cortical cataract. The Roman numeral denotes the estimate of cataract severity.

A 1,000W tungsten-halogen bulb housed in a projector unit was used as a glare source. Light from the bulb was projected through a filter wheel which enabled wavelengths of 460nm, 500nm, 540nm, 580nm, 620nm and 660nm to be produced. Half-height bandwidths varied between 22nm and 35nm depending upon the wavelength. At each wavelength, illuminance at the eye was measured with a computer-controlled spectrophotometer (4.B.). Since illuminance at mid-wavelengths far exceeded that at extreme wavelengths, appropriate ND filters were placed over the

filter wheel so that ocular illuminance levels remained approximately constant (within 0.18 log units) across the spectrum. Thus, the mean luminous intensity produced by the glare source, averaged across the wavelength, was 19.44cd.

The glare source was placed at either 3.25°, 6.5°, 13° or 26° visual angle from the stimulus. The distance of the glare source from the observer was halved with each doubling of glare angle. Due to the inverse square law this means that illuminance at the eye increased with the square of the glare angle. Assuming light scatter is approximately inversely proportional to the square of visual angle (Stiles-Holladay relationship), changing the glare source resulted in a veiling retinal illuminance which was approximately constant. Hence, changes in retinal adaptation level were unlikely to have influenced the observed angular dependency of stray light.

Light scatter factors (LSFs) were calculated using the equation derived by Paulsson and Sjöstrand (1980).

$$LSF = (L / E) \cdot ((M_2 / M_1) - 1) \quad [7.1]$$

where L is the stimulus luminance, E the ocular illuminance and M₂ and M₁ are contrast thresholds measured with and without glare respectively (3.A.1). LSF is a quantity that depends only upon scattering angle, and changes in either L or E produce compensating changes in M₂ such that the LSF remains unchanged. The relationship received initial validation (Paulsson and Sjöstrand, 1980), although recent data have been published which question the use of the equation (Yager et al, 1992). However, there has been support for the validity of establishing the LSF by this method, provided appropriate stimulus conditions are used (see Chapter 6).

7.C. Results

Figure 7.1 and 7.2 shows LSFs for two normal subjects (DW and RS respectively) as a function of the wavelength of the glare source. The ages of the subjects are 30 years (DW) and 24 years (RS). Different symbols represent four different angular positions of the glare source which varied between 3.25° and 26°. The data show the expected trend as a function of glare angle, with LSFs being largest for the smaller glare angles. No systematic dependence upon wavelength is evident, although longer wavelengths produce a slight increase in LSF for the 26° data of RS. It is quite clear that the data fail to demonstrate any significant degree of Rayleigh scatter, which preferentially affects shorter wavelengths. Complete Rayleigh scatter would be indicated by a LSF which decreased by 0.63 log units over the wavelength range investigated. If a lesser dependence upon wavelength were present then the expected decrease in LSF would be less (e.g. an exponent of -1 would predict a 0.16 log unit difference between 460nm and 660nm).

Given the absence of a significant wavelength effect in these normal observers, LSFs for different wavelengths were averaged at each different glare angle. In Figure 9.3 these LSFs are plotted as a function of glare angle for both observers, but following the procedure of van den Berg and his co-workers (van den Berg et al, 1991; IJspeert et al, 1990; IJspeert et al, 1993; de Waard et al, 1992; van den Berg and IJspeert, 1992) by multiplying the LSF by glare angle squared. This produces a value known as the “stray light parameter”. Plotted in this way, the Stiles-Holladay approximation ($LSF \propto glare\ angle^{-2}$) would be represented as a horizontal line.

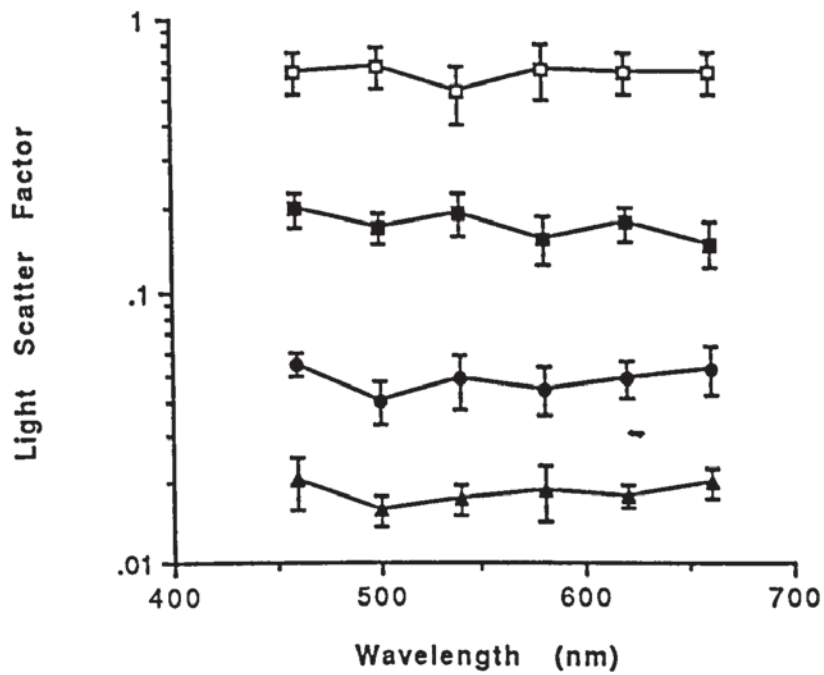


Figure 7.1 Results from observer DW. LSF plotted against wavelength for four different glare angles. Open square, 3.25°; closed square, 6.5°; closed circle, 13°; closed triangle, 26°. One standard error is shown.

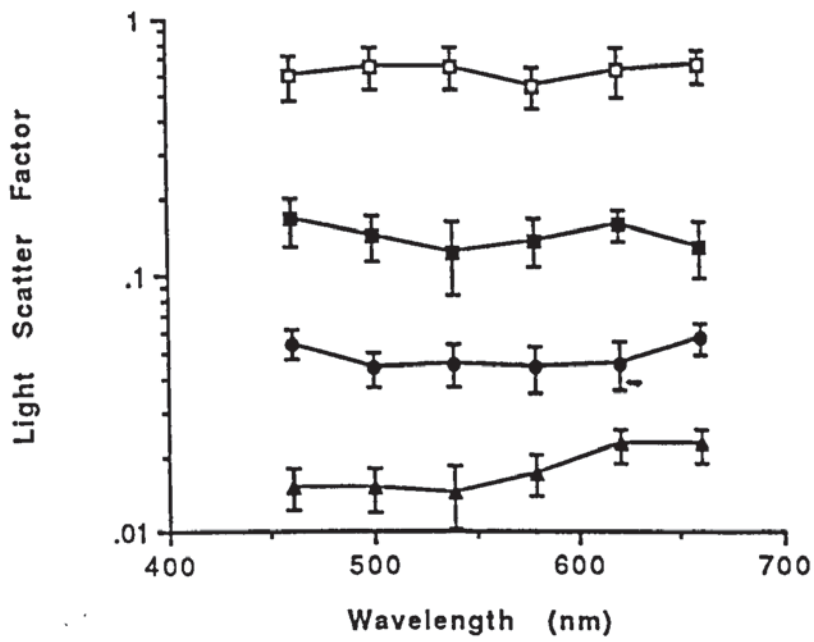


Figure 7.2 Results from observer RS. LSF plotted against wavelength for four different glare angles. Open square, 3.25°; closed square, 6.5°; closed circle, 13°; closed triangle, 26°. One standard error is shown.

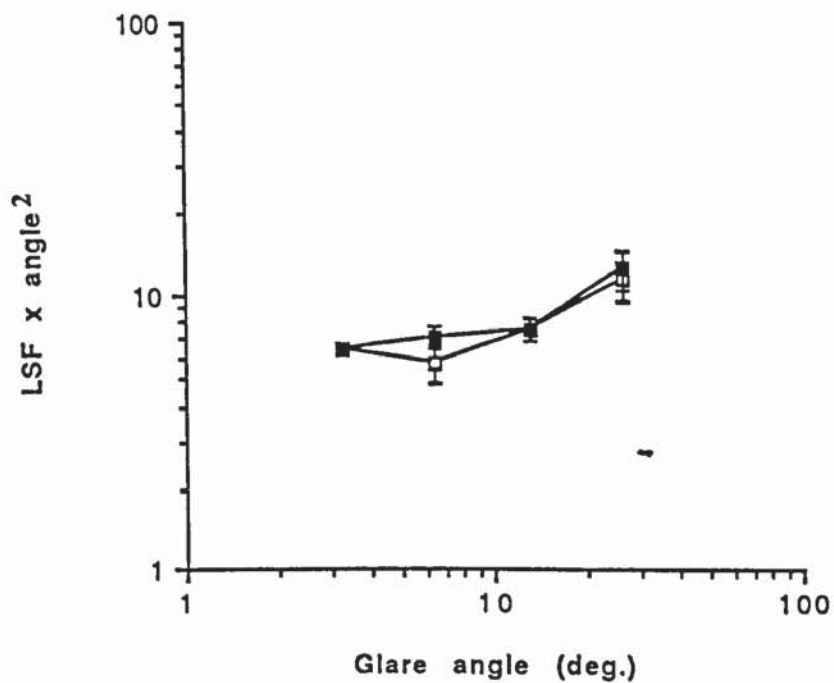


Figure 7.3 Stray light values (light scatter factor multiplied by glare angle squared) plotted against glare angle. Light scatter factors represent data from Figure 7.1 and 7.2 averaged across wavelength. The open square represents data for subject RS; the closed square for subject DW. One standard error is shown.

As can be seen from the figure, the functions are fairly flat at small glare angles but increase steadily as glare angle increases. This means that the exponent relating LSF to the inverse of the glare angle becomes progressively less than 2. This trend, and the absolute values of the stray light parameter, are consistent with the findings of others using young observers (van den Berg et al, 1991; IJspeert et al, 1990).

Stray light values for the young and the older group of subjects are compared in Figure 7.4 and are shown in Tables 7.2 and 7.3 respectively. The data represent the two extreme glare wavelengths (460nm and 660nm), again measured at several different angles. Clearly, the average LSF for the elderly group is much greater than for the younger group. The difference between LSF's in the two groups is fairly constant, averaging 0.41 log units, i.e., a factor of 2.57. In agreement with the findings of IJspeert et al (1990), the young subject with the most ocular pigmentation (brown iris) demonstrated slightly lower LSF values than the other subjects. LSFs at 660nm appear to be slightly less than at 460nm for both groups. For the younger group, two-way repeated measures ANOVA revealed that this difference reached statistical significance ($F_{1,16}=8.77$, $p<0.01$), although the interaction between LSF and glare angle just failed to reach significance ($F_{3,16}=2.96$, $p>0.05$). For the older group, the larger inter-individual variation meant that the difference in LSF between the two wavelengths was not significant ($p>0.1$).

The stray light values for the cataract subjects are illustrated in Figure 7.5 (AM and WH) and 7.6 (HP and BJ) and shown in Table 7.4. It should be noted that the y-axis of both these figures begins 1 log unit higher than the normal data represented in Figure 7.4. This highlights the obvious increase in stray light parameter in the cataract patients compared to the older normals. However, the shape of the functions remains similar to those for normals. Three of the cataract subjects demonstrated slightly higher stray light values for long wavelengths, which is opposite to the slight

wavelength dependence found in young observers. This slight wavelength dependence found in the cataract subjects may be due to the absorption of short wavelength light thus increasing the relative stray light values for long wavelengths. However, as with the normal data this difference was rather small, amounting to less than 0.2 log units.

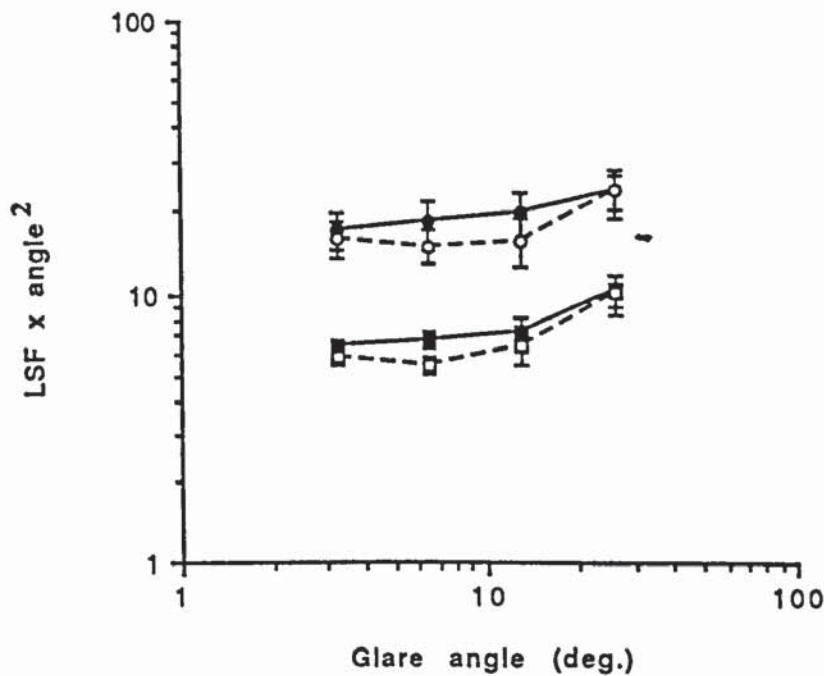


Figure 7.4 Stray light values (light scatter factor multiplied by glare angle squared) for five young (squares) and five older (circles) subjects plotted against glare angle. Filled symbols and solid lines represent data for 460nm glare, whereas open symbols and dashed lines represent data for 660nm. One standard error is shown.

Subject	Iris colour	Age	Glare (years) angle (deg)	LSF x glare angle ²	
				460nm	660nm
JG	Blue	20	3.25	6.76±0.55	5.13±0.50
			6.5	5.66±1.12	4.73±0.47
			13	5.58±0.85	5.34±1.12
			26	9.46±0.68	8.21±1.35
RS	Green	24	3.25	6.33±1.33	6.75±1.00
			6.5	6.51±1.52	4.77±0.97
			13	14.5±2.15	14.0±2.15
			26	10.1±2.03	14.2±2.70
KL	Green	24	3.25	6.46±0.44	5.68±0.50
			6.5	7.10±0.51	6.51±0.63
			13	5.75±0.85	4.73±0.34
			26	8.79±1.35	6.76±0.68
NH	Brown	24	3.25	6.19±0.91	5.04±0.63
			6.5	6.25±1.14	5.11±0.59
			13	6.76±0.85	5.07±0.68
			26	8.11±0.68	7.44±0.68
DW	Blue	30	3.25	6.70±2.40	6.76±2.40
			6.5	8.45±2.50	6.34±2.40
			13	9.30±1.70	8.80±3.55
			26	13.5±6.08	13.5±2.70

Table 7.2 Stray light values (light scatter factor multiplied by glare angle squared) are shown for the five young subjects at different glare angles (3.2°, 6.5°, 13° and 26°) and for the two extreme wavelengths (460nm and 660nm) of the glare source. The age and the iris colour of each subject is also shown.

Subject	Iris colour	Age	Glare (years) angle (deg)	LSF x glare angle ²	
				460nm	660nm
DS	Blue	65	3.25	14.22±2.13	12.35±2.54
			6.5	12.63±1.82	12.84±1.86
			13	13.86±1.69	14.03±2.37
			26	18.93±2.03	16.22±2.70
EM	Green	69	3.25	12.36±3.70	14.67±1.80
			6.5	13.39±2.32	13.94±2.96
			13	16.44±2.87	10.28±2.54
			26	18.86±3.31	15.62±3.04
RS	Blue	70	3.25	20.33±2.29	21.81±5.74
			6.5	23.41±3.04	16.90±2.41
			13	14.03±2.20	13.69±2.20
			26	28.39±8.79	26.36±7.44
SP	Blue	73	3.25	13.56±1.48	9.98±1.13
			6.5	12.89±1.69	8.83±1.01
			13	21.13±3.04	14.37±2.54
			26	18.93±3.38	20.28±2.70
AF	Blue	85	3.25	25.01±2.73	20.94±2.75
			6.5	28.82±5.03	20.28±1.90
			13	32.79±6.25	26.20±3.37
			26	33.12±4.06	39.21±4.06

Table 7.3 Stray light values (light scatter factor multiplied by glare angle squared) are shown for all the elderly subjects at different glare angles (3.25°, 6.5°, 13° and 26°) and for the two extreme wavelengths (460nm and 660nm) of the glare source. The age and the iris colour of each subject is also shown.

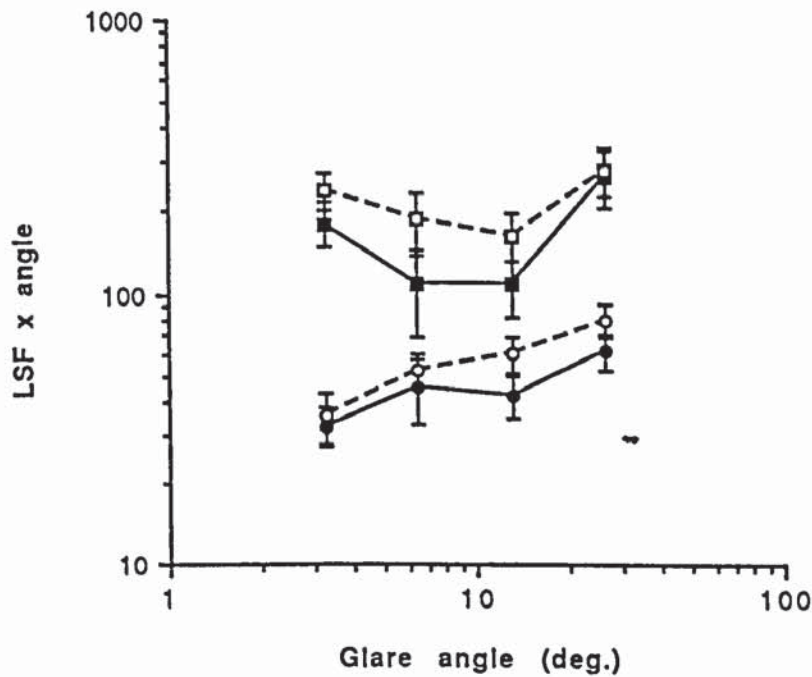


Figure 7.5 Stray light values (light scatter factor multiplied by glare angle squared) plotted against glare angle for two cataract subjects (squares, subject AM; circle, subject WH). Filled symbols and solid lines represent data for 460nm glare, whereas open symbols and dashed lines represent data for 660nm. It should be noted that the y-axis of both these figures begins 1 log unit higher than the normal data represented in Figure 7.4. One standard error is shown.

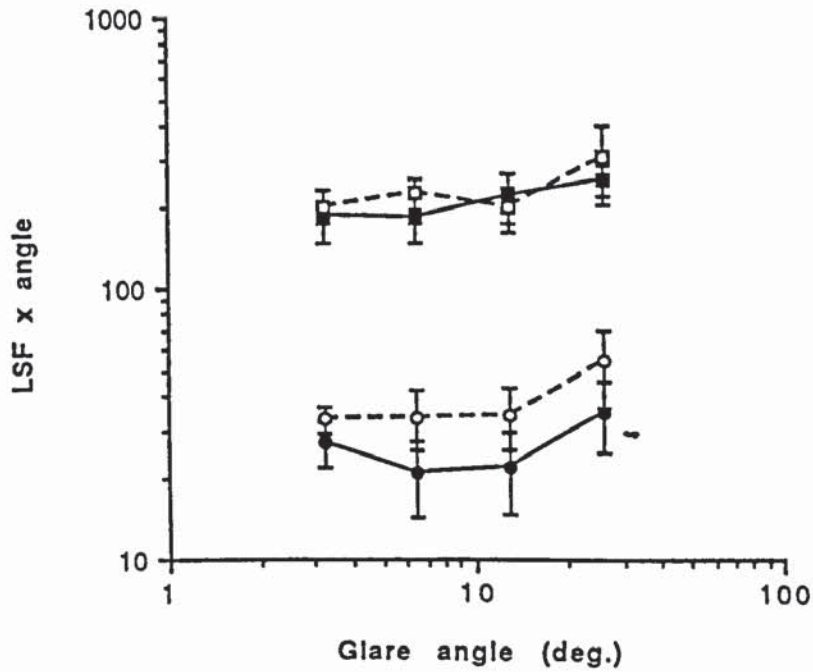


Figure 7.6 Stray light values (light scatter factor multiplied by glare angle squared) plotted against glare angle for two cataract subjects (squares, subject HP; circle, subject BJ). Filled symbols and solid lines represent data for 460nm glare, whereas open symbols and dashed lines represent data for 660nm. It should be noted that the y-axis of both these figures begins 1 log unit higher than the normal data represented in Figure 7.4. One standard error is shown.

Subject	Iris colour	Age (yrs)	Glare angle (deg)	LSF x glare angle ²	
				460nm	660nm
BJ	Brown	72	3.25	27.38±5.40	33.04±3.91
			6.5	20.87±6.68	33.46±8.28
			13	22.14±7.61	34.14±8.79
			26	35.15±10.14	53.40±16.60
WH	Brown	82	3.25	32.58±5.64	35.18±7.49
			6.5	44.62±11.87	52.01±7.44
			13	42.25±7.27	59.49±8.79
			26	61.52±9.47	80.44±10.82
AM	Green	82	3.25	181.47±33.8	239.56±36.7
			6.5	107.61±38.3	187.55±48.3
			13	107.59±25.4	164.27±32.6
			26	269.18±61.5	284.18±54.7
HP	Green	80	3.25	188.51±41.3	200.71±29.0
			6.5	182.10±33.9	223.63±29.5
			13	220.38±45.6	198.91±38.7
			26	252.82±31.1	305.55±100.7

Table 7.4 Stray light values (light scatter factor multiplied by glare angle squared) are shown for all the cataract subjects at different glare angles (3.25°, 6.5°, 13° and 26°) and for the two extreme wavelengths (460nm and 660nm) of the glare source. The age and the iris colour of each subject is also shown.

7.D. Discussion

The stray light values for young observers, and their relationship to glare angle, agree well with recent studies (van den Berg et al, 1991; IJspeert et al, 1990). IJspeert et al (1990) give mean values of LSF for 20- to 30-year-old subjects, at 3.5° and 7° eccentricity of 0.57 (95% confidence range of 0.38 to 0.89) and 0.12 (95% confidence limits of 0.08 to 0.20), respectively, while the results found in this study give mean values of LSF for 20- to 30-year-old subjects, at 3.25° and 6.5° eccentricity of 0.62 (95% confidence range of 0.59 to 0.64) and 0.16 (95% confidence range of 0.13 to 0.19), respectively. The precise value of the exponent relating LSF to glare angle appears to vary depending upon glare angle, becoming less than the Stiles-Holladay relationship would predict as angle increases. The data for the normal elderly observers suggest that the angular dependency changes little, but the amount of stray light increases markedly. This is in agreement with IJspeert et al (1990), although our stray light values for these older normals are slightly higher than their data would predict. The average increase in LSF between our two groups (mean ages 24.4 years and 72.4 years) was a factor of 2.57, whereas recent estimates for age dependency using the straylightmeter (de Waard et al, 1992) would predict a factor of 2.11.

For cataract subjects, some discrepancy appears in the literature regarding stray light values. The most extensive study used the straylightmeter (de Waard et al, 1992) and found maximum stray light factors ($LSF \times \theta^2$) of around 80. Other studies using a portable straylightmeter (van den Berg and IJspeert, 1992) find values of up to 200 (van den Brom et al, 1990; Elliott et al, 1991), and these differences may perhaps be explained by different degrees of lens opacity between the studies. Stray light predictions based upon contrast thresholds with and without glare also show some variation. Elliott et al (1989) found stray light factors between 30 and 180 for a range of cataract types. Paulsson and Sjöstrand (1980) used only subjects with posterior subcapsular cataracts, some of whom demonstrated enormous stray light values

despite relatively good acuities. A similar dramatic effect of glare upon observers with posterior subcapsular cataracts was found by Elliott et al (1989). DeWaard et al (1992) found rather poor agreement between straylightmeter values and contrast sensitivity loss (measured with a Vistech chart) under glare conditions. For substantial lens opacities, the contrast loss produced by a glare source far exceeds that predicted on the basis of stray light measurement. Straylightmeter measurements were performed on the four cataract subjects. Almost perfect agreement in stray light values for the two methods was obtained in the subjects with lesser degrees of cataract (WH and BJ). Values averaged across glare angle were 30 as opposed to 32.4 (BJ) and 46 as opposed to 51.0 (WH) for straylightmeter and contrast loss measurements, respectively. However, equivalent values for the remaining two cataract subjects were markedly different - 120 compared to 229 (HP) and 46 compared to 193 (AM). It is important that further work should account for such discrepancies between stray light measurements and functional loss.

The results indicate that wavelength dependent scatter in normal young, elderly and cataractous eyes is of little or no significance (Figure 9.1-9.6). This is consistent with the finding of Wooten and Geri (1987) for young observers. Neither the data found by Wooten and Geri (1987) nor the data shown here, demonstrate the increase in long wavelength scatter found at large angles by van den Berg et al (1991). This was attributed to preferential transmission of light of these wavelengths through the iris and sclera and amounted to a difference of at least 0.4 log units between red and green scattered light for blue-eyed subjects at a glare angle of 25.4°. However, the possibility cannot be ruled out that this increased long wavelength transmission through ocular structures other than the pupil was negated by predominantly short wavelength scatter produced by the ocular media. What is important from a visual performance aspect, however, is the overall scatter effect. Most of the cataract subjects in this experiment demonstrated a slight tendency for increased stray light

values at long wavelengths. Data from more subjects with cataract are needed to confirm whether this is a common trend.

It has been suggested that long wavelength pass filters should improve visual performance on the basis that they absorb short-wavelength visible light, and that this is preferentially scattered within the eye (Rosenberg, 1984; Leat et al, 1990). The results shown here provide no foundation for this proposal, and indicate that the transmission characteristics of a filter across the visible spectrum are largely irrelevant when considering disability glare. However, UV-induced ocular fluorescence within the lens has been shown to affect visual function (Elliott et al, 1993b). Filters which remove UV radiation are therefore likely to be of significant benefit (Zigman, 1992), although this needs to be established experimentally.

The absence of significant wavelength dependent scatter in the eyes of our three groups has a bearing upon the type and size of scattering structures in the eye. Randomly positioned particles of the order of the wavelength of light or smaller produce significant amounts of Rayleigh scatter, in which blue light is predominantly affected. Furthermore, such small particles cannot explain the value of the exponent relating LSF to glare angle. Small particle scatter would predict a much more isotropic distribution of scattered light rather than the rapid decline which is actually observed (Wesemann, 1987). The obvious conclusion must be that light scatter within the eye is caused by structures which are rather large in comparison to the wavelength of light (Vos, 1984; Wooten and Geri, 1987). The suggestion that particles whose size approximates to the wavelength of light represent a significant cause of scatter in the elderly lens therefore appears to be invalid (Bettelheim, 1985). Hemenger (1990, 1992) suggests that the primary causes of small angle intraocular light scatter are refractive index fluctuations associated with the periodic lens fibre lattice. Alternative sources of intraocular scatter such as retinal scatter, whose wavelength dependence is unknown, should also be taken into account.

It has been suggested that wavelength dependency should be incorporated into mathematical models of intraocular scatter (IJspeert et al, 1993). The results shown here suggest that, in comparison to other variables such as glare angle, age, media quality and ocular pigmentation, wavelength dependency at moderate to large angles is a rather unimportant parameter which may conveniently be ignored.

Retinal factors may also affect the wavelength dependency of scattered light. The Stiles-Crawford effect has been shown to be wavelength dependent, and generally it has been found that the blue or SWS cone type is more directionally sensitive than the MWS or LWS (Enoch and Lakshminarayanan, 1991). This increase in directional sensitivity of the blue cones could counteract any reduction in the amount of blue light due to wavelength dependent scatter.

CHAPTER 8 EFFECT OF ULTRAVIOLET ABSORBING FILTERS ON OUTDOOR VISUAL PERFORMANCE

8.A. Introduction

A further component of intraocular light scatter is lenticular fluorescence. However, whether lenticular fluorescence adversely affects visual performance is equivocal. The only study to date on the role of lenticular fluorescence in visual performance is by Elliott et al (1993b). They measured the visual effect associated with UV-induced lenticular fluorescence for normal observers of varying ages using Regan visual acuity charts at varying levels of contrast. UV radiation was shown to reduce low contrast acuity and this loss increased linearly with age (Elliott et al, 1993b).

Lenticular fluorescence can be attributed to certain compounds associated with lens proteins called fluorophores, which transform UV light into visible light (Le Grand, 1948; Weale, 1985). The fluorescence normally observed is called Stokes fluorescence. This is the emission of less energetic photons which have a longer wavelength than the absorbed photons. If thermal energy is added to an excited state compound then emission at shorter wavelengths than those absorbed occurs and is known as anti-Stokes fluorescence. The lenticular fluorescent emission may be scattered randomly within the globe (Henker, 1924), adding a uniform component to the retinal PSF thus reducing visual performance.

The human lens may contain many fluorophores (Zigman, 1985; Dillon, 1985). The main fluorophore is the amino acid tryptophan, a basic constituent of protein, with an excitation maximum at 290nm and an emission maximum at 340nm (Sato et al, 1973). This was named 'purple' fluorescence. Tryptophan remains at a relatively constant level

throughout life. The cornea strongly absorbs the excitation wavelength of tryptophan. Thus wavelengths which excitate tryptophan do not normally reach the lens (Zuclich et al, 1992) and its fluorescence is of little visual consequence. Other fluorophores in the human lens are believed to result from photo-oxidation reactions involving prolonged exposure of tryptophan to UV radiation (Lerman, 1976). This non-tryptophan fluorescence has been found to increase with age and to correlate with pigmentation and colouration of the crystalline lens (Sato et al, 1973; Spector et al, 1975; Lerman and Borkman, 1976; Occhipinti et al, 1986; Weale, 1991). The non-tryptophan fluorescence can be divided into two fluorophores; blue fluorophores having an excitation waveband of approximately 340-360nm and an emission at 420-440nm, and green fluorophores having an excitation waveband of 420-435nm and an emission at 500-520nm (Lerman et al 1976; Lerman and Borkman, 1978b).

The aim of this study was to determine if the presence of UV light would affect low contrast visual acuity of normal eyes and cataractous eyes.

8.B. Methods

The study was carried out in conjunction with a parallel study at the University of Waterloo, Ontario, Canada. The study at Aston University investigated the effect of UV radiation on visual performance between young and elderly normals and in subjects with cataractous eyes. Forty one subjects were recruited at Aston University; eighteen young normal observers (mean age 24.8 years SD=3.8; Gender M=9, F=9), fifteen elderly normal observers (mean age 73.1 years SD=4.8; Gender M=6, F=9) and eight patients with cataractous eyes (mean age 75.3 years SD=5.2; Gender M=4, F=4).

Visual acuity was measured outside because of the relatively high levels of UV radiation. Ambient levels of UV radiation are affected by many variables, for example,

latitude, time of the year (Johnson et al, 1976), but Rosenthal et al (1985) found that cloud cover did not play a substantial role in sunlight UV exposure. Further, Rosenthal et al (1985) did detect UV exposure variation during daylight hours, but found that the total amount of UV exposure measured between 8-11 a.m. and 11 a.m.-3 p.m. were not significantly different. Measurements taken in this study were all in the same place between June and August and between 11 a.m.- 3 p.m..

The study at the University of Waterloo investigated the effect of age and cataract on visual performance in the presence of UV radiation. Forty six subjects were recruited ; thirty nine normal subjects of age range 22-74 years (mean age 39.8 years SD=13.8; Gender M=13, F=26) and 7 patients with cataractous eyes (mean age 77.1 years SD=7.6; Gender M=5, F=2).

At the University of Waterloo measurements of UV ($\leq 400\text{nm}$) and visible (400nm-780nm) radiation were obtained; a direct measurement into the sun and also a measurement of reflected radiation off the visual acuity chart. The procedure was that as described by Elliott et al (1993b). The mean of the nine recordings showed the amount of UV radiation measured directly was 35Wm^{-2} and indirectly was 4.27Wm^{-2} . The amount of visible light measured directly was 450Wm^{-2} while indirectly it was 54.38Wm^{-2} . These measurements showed that the levels of UV radiation found during the study were high relative to those used in a previous study (Elliott et al, 1993b). The amount of visible light was approximately thirteen times higher than the UV radiation.

Exclusion criteria for both studies were the same as described in 4.B.. All observers wore their distance prescription where necessary and natural pupils were used throughout. Only Caucasian observers were included in the studies to reduce differences in light scatter due to ocular pigmentation (van den Berg et al, 1991).

For both studies low contrast visual acuity was measured outside using two Bailey-Lovie low contrast (10%) logMAR visual acuity charts. The position of the chart remained constant between measurements as did the position of the observer. The charts were placed against a highly reflective background (White card sized 12° square) and the observers viewed the charts with the sun behind the observer. All outside measurements were taken on sunny days with little cloud cover. Visual acuity was measured at 6 metres with best optical correction using full aperture crown glass trial lenses. Crown glass was used as wavelengths above 300nm are not absorbed, therefore the radiation producing the non-tryptophan fluorescence is transmitted through the lens. A by-letter scoring system (0.02 log units per letter) was adopted. To avoid familiarisation with the letters on the charts some subjects were asked to read the letters from right to left.

Low contrast visual acuity measurements were made using two filters. One filter (Schott GG440) reduced the amount of UV light incident on the observer's eye, while the other filter (Schott KG4) transmitted significant levels of UV light. A computer-controlled spectrophotometer was used to analyse the spectral distribution of light emanating from each filter using a standard light source illuminant C which conforms closely to daylight (see Figure 8.1). The luminous transmission of the filters were 87.6% for the GG440 filter and 88.9% for the KG4 filter, therefore the difference in total amount of visible light transmitted was very small. The need for matching the transmission of the filter is important as it is obviously inappropriate to compare directly two filters which transmit different amounts of visible light. If the stimulus has a higher luminance when viewed through one filter compared to the other, a difference in performance when using the two filters would not be surprising.

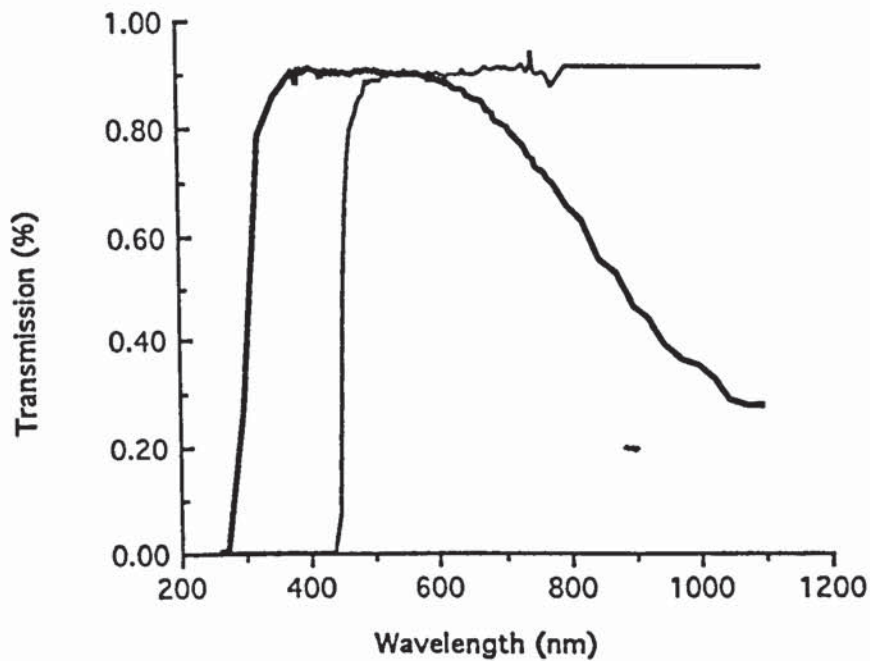


Figure 8.1 The spectral distribution of light emanating from both filters used in the experiment are shown. Wavelength is plotted along the x-axis while the proportion of light transmitted through each filter is plotted on the y-axis. The thick line indicates the KG4 Schott filter (clear). The thin line represents the GG455 Schott filter (UV absorbing).

8.C. Results

Figures 8.2 and Tables 8.1 and 8.2 show the results obtained at Aston University for young normals, elderly normals and for the cataract patients. Visual acuity for the elderly normals was less for the young normals and, as expected, the visual acuities for the cataract group were lower than for the normal observers. The effect of the UV absorbing filter on visual acuity for all three groups of observers (young, elderly and cataract) appears to be small (average difference=0.08 log units) and did not differ between each group. There was no significant difference ($F_{1,39}=1.96, p>0.1$) in visual acuity measured, for all observers, with the clear filter and with the UV absorbing filter.

Figure 8.3 and Tables 8.3 and 8.4 show the outdoor low-contrast visual acuity results obtained at the University of Waterloo for normal observers and the cataract patients. The top graph shows the results obtained using the clear filter (squares represent the clear filter (KG4)) and the bottom graph shows results for the yellow filter (circles represent the UV absorbing filter (GG440)). Normal observers are represented by open squares and open circles, while the cataract patients are shown by closed squares and closed circles. LogMAR visual acuity for the low contrast visual acuity chart is plotted on the y-axis. Age of the subjects is plotted on the x-axis. Lines of regression were plotted through the normal observers results for both graphs and the equations for each line of regression are shown in each graph. Both graphs show that for the normal observers visual acuity decreased with age. The small difference between the two lines of regression indicate that for the normal observers very little change in visual acuity was found between the two filters. Visual acuity of the cataract subjects is poorer than the normal observers. Again very little change in visual acuity was found between the two filters used by the cataract subjects. In fact, an ANOVA showed a slight significant difference between the two filters for the normal and cataract groups combined

($F_{1,44}=4.81$, $p<0.05$). Visual acuity was better through the clear filter, although the average difference was only 0.015 log units. No interaction effect was found.

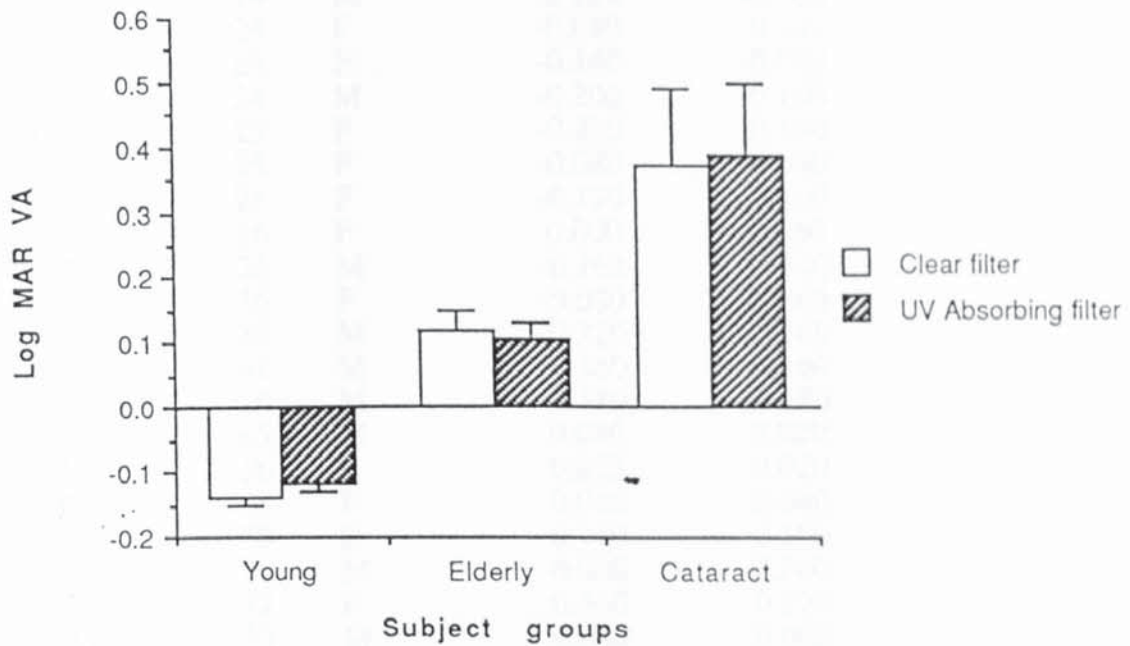


Figure 8.2 The results obtained from Aston University are shown. LogMAR visual acuity is plotted on the y-axis while the subject group (young, elderly and cataract) is plotted on the x-axis. The unshaded columns represent the clear filter (KG4) and the shaded columns represent the UV absorbing filter (GG440).

Normals

Patient	Age	Sex	LogMAR Visual Acuity (Log units)	
	Yrs	M/F	Clear Filter	UV Absorbing Filter
JG	20	F	-0.200	-0.160
AD	20	M	-0.080	-0.080
FT	20	M	-0.140	-0.120
JB	21	M	-0.080	-0.120
MT	22	F	-0.140	-0.140
RS	24	M	-0.220	-0.160
SM	24	F	-0.080	-0.080
KL	24	F	-0.140	-0.080
IM	24	M	-0.200	-0.160
GR	25	F	-0.200	-0.180
NH	25	F	-0.080	-0.080
NE	25	F	-0.120	-0.100
RD	26	F	0.000	0.060
GB	26	M	-0.160	-0.140
AW	26	F	-0.080	-0.060
DW	30	M	-0.220	-0.160
FE	31	M	-0.160	-0.160
PH	34	M	-0.180	-0.180
DS	65	M	0.020	0.020
FS	66	F	0.020	0.020
ML	68	F	0.040	0.040
EP	70	F	0.140	0.100
MS	70	M	0.000	0.000
KP	72	F	0.300	0.320
MM	73	M	0.040	0.000
MD	73	F	0.200	0.160
ES	74	F	-0.020	0.060
HL	74	M	0.200	0.160
TB	76	M	0.020	0.020
OM	78	F	0.100	0.140
BJ	78	F	0.260	0.220
AD	80	M	0.400	0.280
GB	80	F	0.020	0.020

Mean-0.022(SE=0.03) -0.016(SE=0.02)

Table 8.1 The results obtained at Aston University for normal observers are shown. LogMAR visual acuity was recorded for the observers in the presence of the clear filter (KG4) and the UV absorbing filter (GG440).

Cataract Patients

Patient	Age	Sex	LogMAR Visual Acuity (Log units)	
	Yrs	M/F	Clear Filter	UV Absorbing Filter
SD	76	F	0.200	0.220
WE	78	M	0.160	0.220
BJ	78	F	0.180	0.200
BP	80	F	1.140	1.120
FH	82	F	0.220	0.280
DM	82	M	0.220	0.200
SN	83	M	0.640	0.580
MF	80	M	0.200	0.260
			Mean 0.37(SE=0.12)	0.39(SE=0.11)

Table 8.2 The results obtained at Aston University for cataract patients are shown. LogMAR visual acuity was recorded for the observers in the presence of the clear filter (KG4) and the UV absorbing filter (GG440).

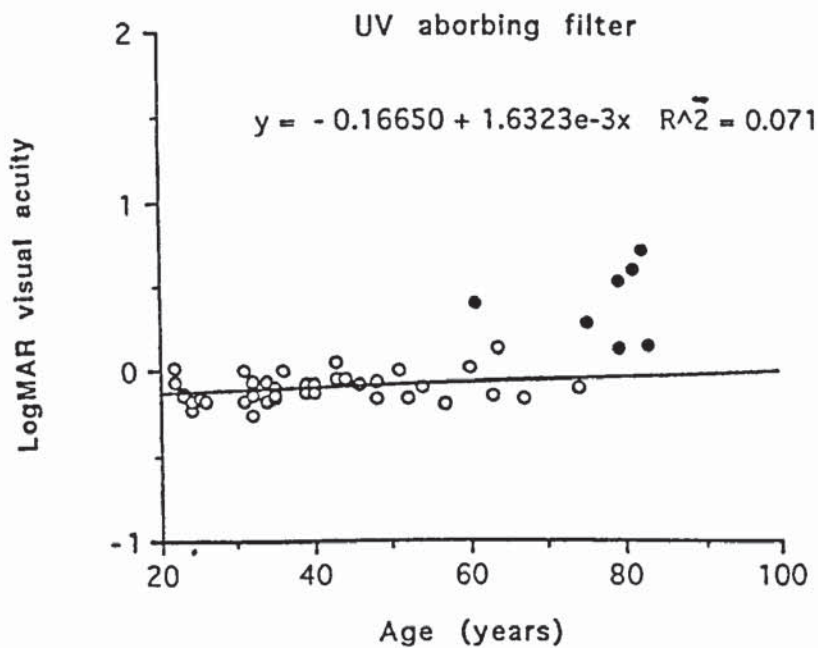
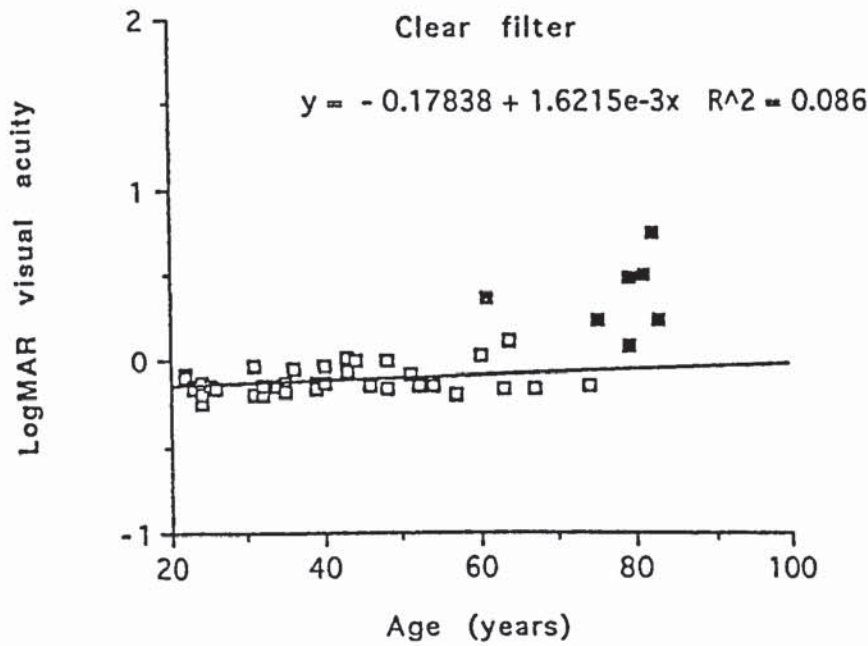


Figure 8.3 The top graph shows the results obtained using the clear filter (Squares represent the clear filter (KG4)) and the bottom graph shows results for the yellow filter (circles represent the UV absorbing filter (GG440)) LogMAR visual acuity is plotted on the y-axis while age of the observers is plotted on the x-axis. Normal observers are represented by open squares and open circles, while the cataract patients are shown by closed squares and closed circles.

Normals

Patient	Age	Sex	LogMAR Visual Acuity (Log units)	
	Yrs	M/F	Clear Filter	UV Absorbing Filter
KC	22	F	-0.080	0.020
LV	22	F	-0.100	-0.060
IB	23	F	-0.140	-0.120
BL	23	F	-0.160	-0.140
MN	24	M	-0.240	-0.220
MP	24	F	-0.120	-0.220
MS	24	M	-0.200	-0.180
JD	25	F	-0.140	-0.160
AR	26	M	-0.160	-0.180
DE	31	M	-0.200	-0.180
PZ	31	M	-0.020	0.000
MS	32	F	-0.160	-0.140
CC	32	F	-0.200	-0.260
LT	32	F	-0.140	-0.060
DC	34	F	-0.140	-0.180
DG	34	F	-0.140	-0.060
MT	35	F	-0.140	-0.160
PM	35	F	-0.120	-0.100
NY	35	F	-0.180	-0.140
BB	36	F	-0.040	0.000
PF	39	M	-0.120	-0.080
NMc	39	F	-0.160	-0.120
SW	40	M	-0.020	-0.080
AW	40	F	-0.120	-0.120
GR	43	F	-0.060	-0.040
PB	43	F	0.020	0.060
LMc	44	F	0.000	-0.040
MC	46	F	-0.140	-0.080
SM	48	F	0.000	-0.060
RJ	48	M	-0.160	-0.160
BH	51	M	-0.080	0.000
JA	52	F	-0.140	-0.160
AS	54	F	-0.140	-0.100
HM	57	F	-0.200	-0.200
GH	60	F	0.040	0.020
ES	63	M	-0.160	-0.140
JM	64	M	0.120	0.140
RP	67	M	-0.160	-0.160
MP	74	M	-0.140	-0.100
		Mean	-0.110 (SE=0.01)	-0.100 (SE=0.01)

Table 8.3 The results obtained at the University of Waterloo for normal observers are shown. LogMAR visual acuity was recorded for the observers in the presence of the clear filter (KG4) and the UV absorbing filter (GG440).

Cataract Patients

Patient	Age	Sex	LogMAR Visual Acuity (Log units)	
	Yrs	M/F	Clear Filter	UV Absorbing Filter
MH	61	M	0.360	0.400
LW	79	M	0.080	0.140
AH	75	M	0.240	0.280
GJ	79	M	0.480	0.540
HR	83	F	0.240	0.160
LS	81	F	0.500	0.600
RC	82	M	0.740	0.720
			Mean 0.380 (SE=0.08)	0.410 (SE=0.08)

Table 8.4 The results obtained at the University of Waterloo for cataract patients are shown. LogMAR visual acuity was recorded for the observers in the presence of the clear filter (KG4) and the UV absorbing filter (GG440).

8.D. Discussion

The surprising finding of the present study was that visual acuity was slightly better when measured through the clear filter. The effect is small and only just reached statistical significance. This therefore suggests that the use of a UV absorbing filter does not improve low contrast visual acuity for the young, elderly or cataract patient. Elliott et al (1993b) showed that forward light scatter due to autofluorescence of the lens is a factor which can affect visual performance. Fluorescent stray light was shown to reduce low contrast visual acuity for older observers by a small amount. This reduction in visual performance may have been small because of the low levels of UV radiation used in the study and a greater reduction might have been found in observers with diabetes or cataract. Patients with diabetes and cataract have been shown to have high levels of autofluorescence (Bleeker et al, 1986; Liang, 1987; Lutze and Bresnick, 1991; Siik et al, 1992).

Zuclich et al (1992) have shown that lenticular fluorescence decreases the amplitude of the visual evoked potential in rhesus monkeys. They projected a 413nm laser onto the lens at 45° to the visual axis while the foveal visual evoked potential was recorded. The visual evoked potential was found to be reduced. If the 413nm wavelength of light was scattered entoptically according to Vos's model (Vos, 1984) the scattering could not explain the reduction, therefore the only other explanation for the reduction in the monkey's visual evoked potentials was the autofluorescence caused by the 413nm excitation wavelength.

Van den Berg (1993) reported that fluorescence could reduce visual function. He found that the total quantal efficiency of fluorescence was between 5% for a 69 year old human lens and 0.4% for 22 year old lens and showed that the forward autofluorescence intensity was less than the backward autofluorescence due to secondary absorption. An increase in veiling luminance due to autofluorescence was

calculated and the total increase in luminous efficiency was by a factor of 3 to 6 at 400nm, and by a factor of 70 to 150 at 380nm. Weale (1985) suggested that there may be certain situations in which lenticular fluorescence may have an impact on vision but predicted that the effects of lenticular fluorescence would be negligible up to 80 years of age.

Protective behaviour such as reducing the palpebral aperture or movement of direction of gaze away from the sun can serve to reduce potential vision loss due to lenticular fluorescence (Sloney, 1983; Rosenthal et al, 1985). The position of the sun during daylight hours means that high levels of UV radiation can be produced by sky light and surface reflection. Therefore, it must be considered that exposure of ultraviolet radiation can be significantly reduced by using broad brimmed hats, spectacles and sunglasses (Sloney, 1983). Most spectacles lenses do absorb some quantity of UV radiation. CR-39 and polycarbonate lenses with an UV absorbing filter transmit very low levels of any ultraviolet radiation. While clear plastic lenses provide reduced protection against ultraviolet radiation, they provide more protection than spectacle crown glass (Pitts, 1990). As the amount of autofluorescence increases with age and high levels of fluorescence can be found in patients with cataract or diabetes these levels could be reduced by incorporating an ultraviolet absorbing filter into glasses or any other optical corrective device (e.g. contact lenses or intraocular lenses).

In this study, the high level of chart luminance outside could have masked any small effect of forward light scatter due to lenticular autofluorescence. The reason for this is that any reduction in visual performance due to stray light is due not only to the amount of light scatter but also depends on the luminance of the stimulus (see equation 5.2). The results shown here indicate that in sunny conditions where UV radiation is high, the effect of autofluorescence is small and is not detectable if stimulus luminance is high, as on a sunny day. If the luminance of the stimulus was

lower while maintaining high levels of UV radiation a reduction in low contrast letter acuity might be found. The conclusion must be that, in normal conditions, UV fluorescence is of little visual importance.

CHAPTER 9 SUMMARY OF RESULTS, CONCLUSIONS AND FUTURE WORK.

9.A. Summary of results and conclusions

The aim of the thesis was to investigate, establish and quantify the relationship between contrast sensitivity, intraocular light scatter and glare, in an attempt to provide a more comprehensive understanding of the visual world of subjects prone to increased light scatter in the eye.

9.A.1 Luminance and colour contrast sensitivity

Having first established a suitable and consistent measurement method for recording contrast threshold, a study was initiated to measure the effect of variable amounts of induced light scatter on the contrast sensitivity function. Subsequent studies investigated the effect of glare on luminance and colour contrast sensitivity for young and elderly subjects. Results showed that without glare the effect of age on sensitivity to both luminance and red-green colour-modulated gratings was small and did not reach statistical significance. However, the reduction in sensitivity for blue-yellow colour modulation with increase in age was highly significant ($p < 0.01$). For both age groups, disability glare was greatest for the red-green stimulus and least for the blue-yellow. Disability glare in the elderly increased relative to the young observers for both red-green and luminance-modulated gratings but not for blue-yellow. The precise effect of a glare source on colour discrimination depends upon a complex interaction between the chromaticity of the glare source and that of the stimulus. In certain circumstances glare can dramatically reduce chromatic discrimination ability by desaturating the component colours.

9.A.2 Effect of filters on glare

The effect of a long wavelength pass (red) and a short wavelength pass (blue) filter on disability glare was examined in the presence of varying amounts of induced wavelength dependent stray light. Disability glare was not significantly different with the red and blue filters, even in the presence of wavelength dependent scatter. Calculation of the veiling luminance transmitted by each filter revealed that the difference in veiling luminance in the two filter conditions was insufficient to result in a measurable difference in disability glare. Filters not only reduce the amount of veiling luminance from the glare source, but they also reduce the luminance of the stimulus, thus contrast is unaffected.

9.A.3 Light Scatter Factor

In 1980, Paulsson and Sjöstrand derived an equation which allowed an intrinsic Light Scatter Factor (LSF) to be determined for any given glare angle. In a recent study the validity of this approach to calculating the LSF was questioned (Yager et al, 1992). The results of the current study obtained confirmed the validity of the Paulsson and Sjöstrand equation for a sample of normal, experienced observers. Corrections to the formula to account for factors such as pupil size changes were found to be unnecessary. The results confirm the suitability of measuring the LSF using contrast threshold with and without glare, provided that appropriate methods are used. To further confirm the validity of the Paulsson and Sjöstrand LSF calculation, a comparison was made between direct stray light values and values obtained using the Paulsson and Sjöstrand LSF calculation for a number of normal young subjects, normal elderly subjects and also subjects with cataract. The results show that there is good agreement between direct and estimated measurements of stray light.

9.A.4 Wavelength dependency of intraocular light scatter

The results indicated that wavelength dependent scatter in normal young, elderly or cataractous eyes is of little or no significance. It has been demonstrated that there is an increase in long wavelength scatter at large glare angles (van den Berg et al, 1991) and it is possible that this increased long wavelength transmission through ocular structures other than the pupil was negated by predominantly short wavelength scatter produced by the ocular media. What is important from a visual performance aspect, however, is the overall scatter effect and the results suggest that wavelength dependency of intraocular light scatter is a rather unimportant parameter relative to other variables. The absence of significant wavelength dependent scatter has a bearing upon the type and size of scattering structures in the eye. The obvious conclusion must be that light scatter within the eye is caused by structures which are rather large in comparison to the wavelength of light.

9.A.5 Ultraviolet radiation

Finally, it seemed desirable to investigate the effect of ultraviolet light has on intraocular light scatter and consequently visual performance. The results indicated that the presence or absence of UV radiation had relatively little effect on visual function for the young, elderly or cataract patient. This can be explained by the fact that high levels of UV light which are necessary to cause significant amounts of autofluorescence are almost always associated with very high levels of visible light. Since it is the ratio of scatter (due to autofluorescence) to visible light which is of importance, no overall effect is found.

9.B. Future Work

9.B.1 Colour contrast sensitivity

The results obtained from the study examining colour contrast sensitivity showed a blue-yellow loss with age. However, evidence for this is equivocal. Some studies provide evidence for significant selective short-wavelength-sensitive (SWS) cone loss with age (Scheffrin et al, 1992; Haegerstrom-Porknoy et al, 1989), whereas in others the effect is slight (Johnson et al, 1988), or even absent in that the sensitivities of all cone types decrease at the same rate as a function of age (Werner and Steele, 1988). Further investigations are needed into this apparent neural loss. The age range of the observers used in this study could be extended to include observers between 30-70 years of age. This could determine the rate of the blue-yellow loss with age and also identify what age this deterioration starts.

Disability glare in the elderly increased for both red-green and luminance modulated gratings, but not for blue-yellow. This means that the reduction in blue-yellow sensitivity produced by the glare source was relatively small. This could be explained on the basis that the veiling luminance from the glare source used in this study altered the colour distribution of the blue-yellow grating, increased SWS cone excitation which thereby improved colour discrimination. Information concerning the effect of varying the colour coordinates of a glare source on colour contrast sensitivity could give validation to this explanation.

9.B.2 Intraocular light scatter

Results confirm the validity of the Paulsson and Sjöstrand equation (equation [6.2]) for a sample of normal, experienced observers. The results also confirm the suitability of measuring the LSF using contrast threshold with and without glare, provided that

appropriate methods are used. Further, the results show that there is agreement between direct and estimated measurements of stray light in the normal and cataractous eye. However, the idea of the interchangeability of both methods is not universal (van den Berg, 1995). The use of an appropriately designed disability glare test which is easy and quick to use should be assessed and estimates of stray light values compared with direct stray light values.

Results showed that some cataract subjects demonstrated slightly higher stray light values for long wavelengths, which was opposite to the slight wavelength dependence found in young observers. The slight wavelength dependence present in the cataract subjects may be due to the absorption of short wavelength light thus increasing the relative stray light values for long wavelengths. Investigations are needed into wavelength dependency of light scatter in cataract patients, as a function of cataract type and severity while compensating for the increased absorption of light. Further investigations would be useful into the amount and wavelength dependency of retinal light scatter. All of these studies will provide more information about the type and size of scattering structures in the eye.

9.B.3. Autofluorescence

The results showed that ultraviolet light has little effect on intraocular light scatter. The high level of chart luminance when outdoors could have masked any small effect of forward light scatter due to autofluorescence of the lens. The results indicated that in sunny conditions where UV radiation is high, the effect of autofluorescence is small and is not detectable if stimulus luminance is high. If the luminance of the stimuli was lower while maintaining high levels of UV radiation, changes in low contrast letter acuity may be found.

REFERENCES

Abrahamsson, M. and Sjöstrand, J. (1986) Impairment of contrast sensitivity function (csf) as a measure of disability glare. *Invest. Ophthalmol. Vis. Sci.* 27, 1131-1136

Adamsons, I., Rubin, G.S., Vitale, S., Taylor, H.R. and Stark, W.J. (1992) The effect of early cataract on glare and contrast sensitivity. A pilot study. *Arch. Ophthalmol.* 110, 1081-86

Allen, M.J. and Vos, J.J. (1967) Ocular scattering light and visual performance as a function of age. *Am. J. Optom.* 44, 717-727

Apple, D., Lichtenstein, S. and Heerlein, K. (1987) Visual aberrations caused by optic components of posterior chamber intraocular lenses. *J. Cataract Refract. Surg.* 13, 431-435

Arden, G.B. (1978) The importance of measuring contrast sensitivity in cases of visual disturbance. *Br. J. Ophthalmol.* 62, 198-209

Bando, M., Nakajima, A. and Satoh, K. (1975) Coloration of the human lens protein. *Exp. Eye Res.* 20, 489-492

Banks, M.S. and Salapatek, P. (1976) Contrast sensitivity function of the infant visual system. *Vision Res.* 16, 867-869

Beems, E.M. and van Best, J.A. (1990) Light transmission of the cornea in whole human eyes. *Exp. Eye Res.* 50, 393-395

Benedek, G.B. (1971) Theory of transparency of the eye. *Appl. Optics* 10, 459-473

Ben-Sira, I., Weinberger, D., Bodenheiner, J. and Yassur, Y. (1980) Clinical method for measurement of light backscattering from the in vivo human lens. *Invest. Ophthalmol.* 19, 435-437

van den Berg, T.J.T.P. (1986) Importance of pathological intraocular scatter for visual disability. *Doc. Ophthalmol.* 61, 327-333

van den Berg, T.J.T.P. (1988) Relation between media disturbances and the visual field. *Doc. Ophthalmol. Proc. Ser.* 49, 33

van den Berg, T.J.T.P. (1991) On the relation between glare and straylight. *Doc. Ophthalmol.* 78, 177-181

van den Berg, T.J.T.P. (1993) Quantal and visual efficiency of fluorescence in the lens of the human eye. *Invest. Ophthalm. Vis. Res.* (in press)

van den Berg, T.J.T.P. (1995) Analysis of intraocular straylight, especially in relation to age. *Optom. Vis. Sci.* 72, 52-59

van den Berg, T.J.T.P. and Boltjes, B. (1988) The point-spread function of the eye from 0° to 100° and the pattern electroretinogram. *Doc. Ophthalmol.* 67, 347

van den Berg, T.J.T.P. and Ijspeert, J.K. (1991) Retinal contrast loss with non-monofocal IOLs. *Doc. Ophthalmol.* 78, 161-167

van den Berg, T.J.T.P. and Ijspeert, J.K. (1992) Clinical assessment of intraocular stray light. *Appl. Opt.* 31, 3694-3696

van den Berg, T.J.T.P. and Spekreijse, H. (1987) Measurement of the straylight function of the eye in cataract and other optical disturbances by means of a direct compensation method. *Invest. Ophthalmol. Vis. Sci. (Suppl.)* 28, 397

van den Berg, T.J.T.P. and Tan, K.E.W.P. (1994) Light transmittance of the human cornea from 320 to 700nm for different ages. *Vision Res.* 34, 1453-1456

van den Berg, T.J.T.P., Ijspeert, J.K. and de Waard, P.W.T. (1991) Dependence of intraocular straylight on pigmentation and light transmission through the ocular wall. *Vision Res.* 31, 1361-1367

van den Berg, T.J.T.P., de Waard, P.W.T., Ijspeert, J.K. and de Jong, P.T.V.M. (1989) Intraocular light scattering assessed quantitatively in age related cataract. *Invest. Ophthalmol. Vis. Sci. (Suppl.)* 30, 499

Bettelheim, F.A. (1975) On the optical anisotropy of lens fibre cells. *Exp. Eye Res.* 21, 231-234

Bettleheim, F.A. (1985) Physical basis of lens transparency. In *The ocular lens*. pp265-300, Maisel, H. (Ed.), Marcel Dekker, New York, USA

Bettelheim, F.A. and Vinciguerra, M.J. (1971) Laser diffraction patterns of highly ordered superstructures in the lenses of bovine eyes. *Ann. N. Y. Acad. Sci.* 172, 429-439

Bettelheim, F.A., Vinciguerra, M.J. and Kaplan, D. (1973) Dynamic laser diffraction of bovine lenses. *Exp. Eye Res.* 15, 149-155

Blakemore, C. and Campbell, F.W. (1969) On the existence of neurons in the human visual system selectively sensitive to orientation and size of retinal images. *J. Physiol.* 203, 237-260

Bleeker, J.C., van Best, J.A. Vrij, L., van der Velde, E.A. and Oosterhuis, J.A. (1986) Autofluorescence of the lens in diabetic and healthy subjects by fluorophotometry. *Invest. Ophthalmol. Vis. Sci.* 27, 791-794

Bodis-Wollner, I. (1980) Detection of visual defects using the contrast sensitivity function. *Int. Ophthalmol. Clinic* 20, 135-155

Bodis-Wollner I. and Camisa, J.M. (1980) Contrast sensitivity measurement in clinical diagnosis. In *Neuro-ophthalmology* Vol 1 pp373-401, Harper and Row publishers, New York, USA.

Boettner, E.A. and Wolter, J.R. (1962) Transmission of the ocular media. *Invest. Ophthalmol.* 1, 776-783

Boynton, R.M. and Clark, F.J.J. (1964) Sources of entopic scatter in the human eye. *J. Opt. Soc. Am.* 54, 110-117

Boynton, R.M. and Kambe, N. (1980) Chromatic difference steps of moderate size measured along theoretically critical axes. *Color Res. Appl.* 5, 13-23.

Brems, R., Apple, D. and Pfeffer, B. (1986) Posterior chamber intraocular lenses in a series of 75 autopsy eyes. 3. Correlation of positioning holes and optic edges with the pupillary aperture and visual axis. *J. Cataract Refract. Surg.* 12, 367-371

- Bron, A.J., Sparrow, J., Brown, N.A.P., Harding, J.J. and Blakyttag, R. (1993) The lens in diabetes. *Eye* 7, 260-275
- van den Brom, H.J.B., Kooijman, A.C. and Blanksma, L.J. (1990) Clinical and physical measurements of the cataractous lens. *Doc. Ophthalmol.* 75, 247-258
- Campbell, F.W. (1979) The transmission of spatial information through the visual system. In *The Neurosciences*. Schmitt, F.O. and Wordon, F.G. (Eds.) M.I.T. Press, Mass., USA.
- Campbell, F.W. and Green, D.G. (1965) Optical and retinal factors affecting visual resolution. *J. Physiol.* 181, 576-593
- Campbell, F.W. and Gubisch, R.W. (1966) Optical quality of the human eye. *J. Physiol.* 186, 558-578
- Campbell, F.W. and Maffei, L. (1974) Contrast and spatial frequency. *Sci. Am.* 231, 106-111
- Campbell, F.W. and Robson, J.G. (1968) Application of Fourier analysis to the visibility of gratings. *J. Physiol.* 197, 551-566
- Carlson, K.H., Bourne, W.M., McLaren, J.W. and Brubaker, R.F. (1988) Variations in human corneal endothelial cell morphology and permeability to fluorescein with age. *Exp. Eye Res.* 47, 27-41
- Carney, L.G. and Jacobs, R.J. (1984) Mechanisms of visual loss in corneal edema. *Arch. Ophthalmol.* 102, 1068-1071
- Chylack, L.T.Jr. (1978) Classification of human cataracts. *Arch. Ophthalmol.* 96, 888-892
- Chylack, L.T.Jr., Leske, M.C., McCarthy, D., Khu, P., Kashiwagi, T. and Sperduto, R. (1989) Lens Opacities Classification System II (LOCS II). *Arch Ophthalmol.* 107, 991-997
- Chylack, L.T.Jr., Wolfe, J.K., Singer, D.M., Leske, M.C., Bullimore, M.A., Bailey, I.L., Friend, J., McCarthy, D. and Wu, S.Y. (1993) The Lens Opacities Classification System III. *Arch. Ophthalmol.* 111, 831-836

- Cinotti, A.A. and Patti, J.C. (1968) Lens abnormalities in an ageing population of nonglaucomatous patients. *Am. J. Ophthalmol.* 66, 25-32
- Claesson, M., Klarén, L., Beckman, C. and Sjöstrand, J. (1994) Glare and contrast sensitivity before and after Nd:YAG laser capsulotomy. *Acta. Ophthalmol.* 72, 27-32
- Clark, B.A.J. (1969) Color in sunglass lenses. *Am. J. Optom. Arch. Am. Acad. Optom.* 46, 825-840
- Cobb, P.W. (1911) The influence of illumination of the eye on visual acuity. *Am. J. Physiol.* 29, 76-99
- Cohen, J.M. and Waiss, B. (1991) An evaluation of horizontally louvered black sunwear for glare reduction in a glare sensitive low vision population. *J. Vis. Rehab.* 5, 61-68
- Coupland, S. and Kirkham, T. (1981) Improved contrast sensitivity with antireflective coated lenses in the presence of glare. *Can. J. Ophthalmol.* 16, 136-140
- Debye, P. (1944) Light scattering in solutions. *J. Appl. Phys.* 15, 338-342
- Demott, D.W. and Boynton, R.M. (1958) Retinal distribution of entopic stray light. *J. Opt. Soc. Am.* 48, 13-30
- Dilley, K.J. and Pirie, A. (1974) Changes to the proteins of the human lens nucleus in cataract. *Exp. Eye Res.* 19, 59-72
- Dillon, J. (1985) Photochemical mechanisms in the lens. In *The ocular lens*. pp349-366, Maisel, H. (Ed.), Marcel Dekker, New York, USA
- Doughty, M.J. and Dilts, D.M. (1994) Identification of topographical variations in the sizes of cells in a monolayer - application to corneal endothelium. *Tissue and Cell* 26, 621-636
- Einstein, A. (1910) Theory of the opalascence of homogenous liquids and liquid in mixtures in the neighbourhood of the critical. *Ann. Phys.* 33, 1275-1298

Elliazy, A.R., Wang, R.H. and Dillon, J. (1994) Model studies on the photochemical production of lenticular fluorophores. *Photochemistry and Photobiology* 59, 479-484

Elliott, D.B. (1987) Contrast sensitivity decline with ageing: A neural or optical phenomenon? *Ophthal. Physiol. Opt.* 7, 415-420

Elliott, D.B. and Bullimore, M.A. (1993) Assessing the reliability, discriminative ability, and validity of disability glare tests. *Invest. Ophthalmol. Vis. Sci.* 34, 108-119

Elliott, D.B., Fonn, D., Flanagan, J. and Doughty, M. (1993a) Relative sensitivity clinical tests to hydrophilic lens-induced corneal thickness changes. *Optom. Vis. Sci.* 70, 1044-1048

Elliott, D.B. Gilchrist, J. and Whitaker, D. (1989) Contrast sensitivity and glare sensitivity changes with three types of cataract morphology: are these techniques necessary in a clinical evaluation of cataract? *Ophthal. Physiol. Opt.* 9, 25-30

Elliott, D.B., Hurst, M.A. and Weatherill, J. (1990a) Comparing clinical tests of visual function in cataract with the patient's perceived visual disability. *Eye* 4, 712-717

Elliott, D.B., Hurst, M.A. and Weatherill, J. (1991) Comparing clinical tests of visual function in cataract patients using a quantification of forward light scatter. *Eye* 5, 601-606

Elliott, D.B., Whitaker, D. and MacVeigh, D. (1990b) Neural contribution to spatiotemporal contrast sensitivity decline in healthy ageing eyes. *Vision Res.* 30, 541-547

Elliott, D.B., Yang, K.C.H., Dumbleton, K. and Cullen, A.P. (1993b) UV-induced lenticular fluorescence: Intraocular straylight affecting visual function. *Vision Res.* 33, 1827-1833

Eppstein, J.A., Kratz, B.J., Callahan, K.M., Wasinger, F., Wang, O. and Bursell, S.E. (1995) Screening for diabetes-mellitus using lens scattering and fluorescence. *Invest. Ophthal. Vis. Sci. (Suppl.)* 36, 819

Fantaguzzi, S., Docchio, F., Guarisco, L. and Branncato, R. (1994) Corneal autofluorescence in diabetic and normal eyes. *International Ophthalmology* 18, 211-214

Farrell, R.A. and McCally, R.L. (1975) On corneal transparency and its loss with swelling. *J. Opt. Soc. Am.* 66: 524-530

Feuk, T. and McQueen, D. (1971) The angular dependence of light scattered from rabbit corneas. *Invest. Ophthalmol.* 10, 294-229

Finkelstein, I.S. (1952) Part II. The biophysics of corneal scatter and diffraction of light induced by contact lenses. *Am. J. Optom. Arch. Am. Acad. Optom.* 29, 231-259

Fry, G.A. (1954) A re-evaluation of the scatter theory of glare. *Illuminating Eng.* 49, 98-102

Fry, G.A. (1965) Distribution of focused and stray light on the retina produced by a point source. *J. Opt. Soc. Am.* 55, 333-334

Ginsburg, A.P. (1984) A new contrast sensitivity test chart. *Am. J. Optom. Physiol. Opt.* 61, 403-407

Goble, R.R., O'Bart, D.P.S., Lohman, C.P., Fitze, F. and Marshall, J. (1994) The role of light scatter in the degradation of visual performance before and after Nd:YAG capsulotomy. *Eye* 8, 530-534

Goldmann, H. (1964) Senile changes of the lens and vitreous. *Am. J. Ophthalmol.* 57, 1-13

Goldman, J.N. and Benedek, G.B. (1967) The relationship between morphology and transparency in the nonswelling corneal stroma of the shark. *Invest. Ophthalmol.* 6, 574-581

Graham, N. and Nachmias, J. (1971) Detection of grating patterns containing two spatial frequencies: A comparison of single-channel and multiple-channel models. *Vision Res.* 11, 251-259

Guth, S.L. (1973) On neural inhibition, contrast effects and visual sensitivity. *Vision Res.* 13, 937-957

- Haegerstrom-Portnoy, G., Hewlett, S.E., and Barr, S.A.N. (1989) S cone loss with aging. In *Colour Vision Deficiencies IX*. Drum B, Verriest G. (Ed.) Kluwer Academic Publishers, Dordrecht, Germany
- Hammer, H., Yap, M. and Weatherill, J. (1986) Visual performance in pseudophakia with standard and ultraviolet-absorbing intraocular lenses: A preliminary report. *Trans. Ophthalmol. Soc. UK* 105, 441-446
- Hard, A-L., Beckman, C. and Sjöstrand, J. (1993) Glare measurements before and after cataract surgery. *Acta. Ophthalmol.* 71, 471-476
- Hart, R.W. and Farrell, R.A. (1969) Light scattering in the cornea. *J. Opt. Soc. Am.* 59, 766-774
- van der Heijde, G.L., Weber, J. and Boukes, R. (1985) Effects of stray light on visual acuity in pseudophakia. *Doc. Ophthalmol.* 59, 81-84
- Heinemann, E.G. (1961) The relation of apparent brightness to the threshold for differences in luminance. *J. Exper. Psychol.* 61, 389-399
- Hemenger, R.P. (1982) Optical density of the crystalline lens. *Am. J. Optom.* 59, 34-42
- Hemenger, R.P. (1990) Light scatter in cataractous lenses. *Ophthal. Physiol. Opt.* 10, 394-396
- Hemenger, R.P. (1992) Sources of intraocular light scatter from inversion of an empirical glare function. *Appl. Opt.* 31, 3687-3693
- Henker, O. (1924) Introduction to the theory of spectacles. pp330. Jena School of Optics, Jena, Germany
- Henning, G.B. (1988) Spatial-frequency tuning as a function of temporal frequency and stimulus motion. *J. Opt. Soc. Am-A* 5, 1362-1373
- Hess, R.F. and Carney, L.G. (1979) Vision through an abnormal cornea; a pilot study of the relationship between visual loss from corneal distortion, corneal edema, keratoconus and some allied corneal pathologies. *Invest. Ophthalmol.* 18, 476-483

- Hess, R.F. and Garner, L.F. (1977) The effect of corneal edema on visual function. *Invest. Ophthalmol.* 16, 5-13
- Hess, R.F. and Woo, G. (1978) Vision through cataracts. *Invest. Ophthalmol.* 17, 428-435
- Hirsch, R.P., Nadler, M.P. and Miller, D. (1984a) Glare measurement as a predictor of outdoor vision among cataract patients. *Annals. Ophthalmol.* 16, 965-968
- Hirsch, R.P., Nadler, M.P. and Miller, D. (1984b) Clinical performance of a disability glare tester. *Arch. Ophthalmol.* 102, 1633-1636
- Hoekstra, J., van der Groot, D.P.A., van der Brink, G. and Bilsen, F.A. (1974) The influence of the number of cycles upon the visual contrast threshold for spatial sine wave patterns. *Vision Res.* 14, 365-368
- Holladay, J.T., Prager, T.C., Trujillo, J. and Ruiz, R.S. (1987) Brightness acuity tester and outdoor visual acuity in cataract patients. *J. Cataract Refract. Surg.* 13, 67-69
- Holladay, L.L. (1926) The fundamentals of glare and visibility. *J. Opt. Soc. Am.* 12, 271-319
- Holladay, L.L. (1927) Action of a light source in the field of view in lowering visibility. *J. Opt. Soc. Am.* 14, 1-15
- IJspeert, J.K., de Waard, P.W.T., van den Berg, T.J.T.P. and de Jong, P.T.V.M. (1990) The intraocular straylight function in 129 healthy volunteers; Dependence on angle, age and pigmentation. *Vision Res.* 30, 699-707
- IJspeert, J.K., van den Berg, T.J.T.P. and Spekreijse, H. (1993) An improved mathematical description of the foveal visual point spread function with parameters for age, pupil size and pigmentation. *Vision Res.* 33, 15-20
- Ivanoff, A. (1947) Contribution a l'etude de la composante inhibitive de l'eblouissement. *Rev. Opt.* 26, 241-266
- Jakus, M.A. (1961) The fine structure of the human cornea. In *The structure of the Eye*. Smelser G.K. (Ed.) Academic Press Inc., New York, USA

- Johnson, C.A., Adams, A.J., Twelker, J.D. and Quigg, J.M. (1988) Age-related changes in the central visual field for short-wavelength-sensitive pathways. *J. Opt. Soc. Am. A.* 5, 2131-2139
- Johnson, C.A., Howard, D.L., Marshall, D. and Shu, H. (1993) A noninvasive video-based method of measuring lens transmission properties of the human eye. *Optom Vis. Sci.* 70, 944-955
- Karbissi, M., Chylack, L.T., Wolfe, J.M. and Mangione, C.M. (1993) Correlation between subjective and objective measures of glare disability in preoperative elderly patients with cataract. *Invest. Ophthalmol. Vis. Sci. (Suppl.)* 34, 1224
- Kelly, D.H. (1975) How many bars makes a grating? *Vision Res.* 15, 625-626
- Kelly, D.H. (1977) Visual contrast sensitivity. *Optica Acta.* 24, 107-129
- Kelly, S.A., Goldberg, S.E. and Bunton, T.A. (1984) Effect of yellow-tinted lenses on contrast sensitivity. *Am. J. Optom. Physiol. Opt.* 61, 657-662
- Kikkawa, Y. (1960) Light scattering studies of the rabbit cornea. *Jap. J. Physiol.* 10, 292-301
- Klang, G. (1948) Measurements and studies of the fluorescence of the human lens in vivo. *Acta. Ophthal. (Suppl.)* 31, 1-152
- Knighton, R., Slomovic, A. and Parrish, A. (1985) Glare measurements before and after neodymium-YAG laser posterior capsulotomy. *Am. J. Ophthalmol.* 100, 708-713
- Knoblauch, K., Saunders, F., Kusuda, M., Hynes, R., Podgor, M., Higgins, K.E. and de Monasterio, F.M. (1987) Age and illuminance effects in the Farnsworth-Munsell 100-hue test. *Applied Opt.* 26, 1441-8
- Koch, D. (1988) The role of glare testing in managing the cataract patient. In *Focal Points 1988. Clinical modules for Ophthalmologists*, American Academy of Ophthalmology, vol. 6, mod. 4. San Francisco, USA
- Koch, D., Emery, J. and Jardeleza, T. (1986) Glare following posterior chamber lens implantation. *J Cataract Refract Surg.* 12, 480-484

- Krauskopf, J. and Farell, B. (1991) Vernier acuity: effects of chromatic content, blur and contrast. *Vision Res.* 31, 735-49
- Kulikowski, J.J. (1971) Some stimulus parameters affecting spatial and temporal resolution of human vision. *Vision Res.* 11, 83-93
- Kurtenbach, W., Sternheim, C.E. and Spillman, L. (1984) Change in hue of spectral colors by dilution with white light (Abney effect). *J. Opt. Soc. Am. A1*, 365-372
- Laing, R.A., Sandstrom, M.M. and Leibowitz, H.M. (1979) Clinical specular microscopy II. Qualitative evaluation of corneal endothelial photomicrographs. *Arch Ophthalmol.* 97, 1720-1725
- Lakowski, R. (1958) Age and colour vision. *Adv. Sci.* 59, 231-236
- Lambert, S.R. and Klyce, S.D. (1981) The origins of Satler's veil. *Am. J. Ophthalmol.* 91, 51-56
- Laming, D. (1991) Contrast sensitivity. In *Vision and Visual Dysfunction. Vol. 5.* Kulikowski, J.J., Walsh, V. and Murray, I.J. (Eds.) The MacMillan Press Ltd., London, UK
- Larsen, M. (1993) Fluorometric assessment of equivalent healthy lens age for people with diabetes. *Invest. Ophthalmol. Vis. Sci. (Suppl.)* 34, 2607
- Lasa, M.S.M., Datiles III, M.B., Podgor, M.J. and Magno, B.V. (1992) Contrast and glare sensitivity. Association with the type and severity of the cataract. *Ophthalmol.* 99, 1045-1049
- Lasa, M.S.M., Podgor, M.J., Datiles III, M.B., Carvso, R.C. and Magno, B.V. (1993) Glare sensitivity in early cataracts. *Br. J. Ophthalmol.* 77, 489-491
- Leat, S.J., North, R.V. and Bryson, H. (1990) Do long wavelength pass filters improve low vision performance? *Ophthal. Physiol. Opt.* 10, 219-224
- Le Claire, J., Nadler, M.P., Weiss, S. and Miller, D. (1982) A new glare tester for clinical testing. *Arch. Ophthalmol.* 100, 153-158

Le Grand, Y. (1937) Recherches sur la diffusion de la lumiere dans l'oeil humain. Rev. Opt. 16, 201-214; 241-266

Le Grand, Y. (1948) Recherches sur la fluoescence des milieux oculaire. Instituto de biofisica Universidade do Brasil.

Leibowitz, H. (1952) The effect of pupil size on visual acuity for photometrically equated test fields at various levels of luminance. J. Opt. Soc. Am. 34, 571-591

Legge, G.E., Mullen K.T. and Woo, G.C. (1987) Tolerance to visual defocus. J. Opt. Soc. Am-A 4, 851-863

Lerman, S. (1976) Lens fluorecence in aging and cataract formation. Doc. Ophthalmol. Proc. Ser. 8, 241-260

Lerman, S. (1980) Human ultraviolet radiation cataracts. Ophthal. Res. 12, 303-314

Lerman, S. and Borkman, R.F. (1976) Spectroscopic evaluation and classification of the normal, aging and cataractous lens. Ophthalmic Res. 8, 335-353

Lerman, S. and Borkman, R.F. (1978a) UV radiation in the aging and cataractous lens. Acta Ophthalmol. 56, 139-149

Lerman, S. and Borkman, R.F. (1978b) Photochemistry and lens aging. In Interdisciplinary topics in gerontology: Gerontological aspects of eye research. pp154-183, von Hahn, H.P. (Ed.), Karger, Basel, Switzerland

Lerman, S., Hockwin, O. and Dragomirescu, V. (1981) UV-visible slit lamp densitography of the human eye. Exp. Eye Res. 33, 587-596

Lerman, S., Kuck, J.F., Borkman, R. and Saker. E. (1976) Induction, acceleration and prevention (in vitro) of an aging parameter in the ocular lens. Ophthalmic Res. 8, 213-226

Lerman, S., Tan, T.T., Louis, D. and Hollander, M. (1970) Anomalous absorptivity of lens proteins due to a fluorogen. Ophthalmic Res. 1, 338-343

- Levi, D.M. and Harworth, R.S. (1977) Spatio-temporal interactions in anisometric and strabismic amblyopia. *Invest. Ophthalmol.* 16, 90-95
- Liang, J.N. (1987) Fluorescence study of the effects of aging and diabetes mellitus on human lens crystallin. *Current Eye Res.* 6, 351-355
- Liang, J.M. (1991) Photooxidation of the nonenzymatic browning products in calf lens alpha-crystallin. *Ophthalmic Research* 23, 259-264
- Liang, J.M., Frey, E. and Chylack, L.T.Jr. (1994) Biochemical and biophysical studies on alpha-crystallin isolated from lens urea-soluble fractions. *Invest. Ophthalmol. Invest. Sci. (Suppl.)* 35, 1743
- Lindstrom, J.I., Feuk, T. and Tengroth, B. (1973) The distribution of light scattering from the rabbit cornea. *Acta. Ophthalmol.* 51, 656-669
- Lovasik, J.V. and Remole, A. (1983) An instrument for mapping corneal light-scattering characteristics. *Ophthalm. Physiol. Opt.* 3, 247-254
- Ludvigh, E. and McCarthy, E.F. (1938) Absorption of visible light by the refractive media of the human eye. *Arch. Ophthalmol.* 20, 37-51
- Lutze, M. and Bresnick, G.H. (1991) Lenses of diabetic patients "yellow" at an accelerated rate similar to older normals. *Invest. Ophthalmol. Vis. Sci.* 32, 194-199
- Magnante, P.C., Noona, C., Wolfe, J.M. and Chylack, L.T.Jr. (1995) Correlation between line spread function and glare disability measurements in patients with early cataract. *Invest. Ophthalmol. Vis. Sci. (Suppl.)* 36, 625
- Malik, N.S., Moss, S.J., Ahmed, N., Furth, A.J., Wall, R.S. and Meek, K.M. (1992) Aging of the human corneal stroma structural and biochemical changes. *Biochimica. et Biophysica. Acta.* 1138, 222-228
- Malina, H.Z. and Martin, X.D. (1995) Deamination of 3-hydroxykynurenine in bovine lenses: a possible mechanism of cataract formation in general. *Graefes Arch. Clin. Exp. Ophthalmol.* 233, 38-44
- Maltzman, B., Horan, C. and Rengel, A. (1988) Penlight test for glare disability of cataracts. *J. Ophthalm. Nurs. Technol.* 7, 137-139

- Mandal, K. and Lerman, S. (1993) Stability of normal and aging lens gamma-crystallins. *Ophthalmic Res.* 25, 295-301
- Maurice, D.M. (1957) The structure and transparency of the cornea. *J. Physiol.* 136, 263-286
- Maurice, D.M. (1962) Distribution and movement of plasma protein in the cornea. *J. Physiol.* 162, 2P
- Mie, G. (1908) Optics of turbid media. *Ann. Phys.* 25, 377-445
- Miller, D. and Benedek, G. (1978) *Intraocular light scattering.* Thomas, C.C., Springfield, IL, USA
- Miller, D. and Lazenby, G. (1977) Glare sensitivity in corrected aphakes. *Ophthalmic Surg.* 8, 54-57
- Miller, D., Brooks, S.M. and Wolf, E. (1976) The effect of the honeycomb on glare function. *Arch. Ophthalmol.* 94, 451-454
- Miller, D., Jernigan, M.E., Molnar, S., Wolf, E. and Newman, J. (1972) Laboratory evaluation of a clinical glare tester. *Arch Ophthalmol.* 87, 324-332
- Mitchell, D.E. and Wilkinson, F. (1974) The effect of early astigmatism on the visual resolution of gratings. *J. Physiol.* 243, 739-756
- Mitchell, E.S. and Hurst, M.A. (1993) The relationship between forward light scatter and cataract. *Invest. Ophthalmol. and Vis. Sci. (Suppl.)* 34, 1414
- Miyahara, E., Smith, V.C. and Pokorny, J. (1993) How surrounds affect chromaticity discrimination. *J. Opt. Soc. Am. A.* 10, 545-53.
- Moon, P. and Spencer, D.E. (1943) The specification of foveal adaption. *J. Opt. Soc. Am.* 33, 444-456
- Moreland, J.D. (1971) The effect of inert ocular pigments on anomaloscope matches and its reduction. *Mod. Probl. Ophthalmol.* 11, 12-8

- Mota, M.C., Carvalho, P., Ramolho, J.S., Cardoso, E., Gaspar, A.M. and Abren, G. (1994) Protein glycation and in-vivo distribution of human lens fluorescence. *International Ophthalmology* 18, 187-193
- Mota, M.C., Ramolho, J.S., Carvalho, P., Quadrado, T. and Daltar, A.S. (1992) Monitoring in-vivo lens changes - A comparative study with biochemical analysis of protein aggregation. *Doc. Ophthalmologica* 82, 287-296
- Mullen, K.T. (1985) The contrast sensitivity of human colour vision to red-green and blue-yellow chromatic gratings. *J. Physiol.* 359, 381-400
- McCally, R.L. and Farrell, R.A. (1976) The depth dependence of light scattering from the normal rabbit cornea. *Exp. Eye Res.* 23, 69-81
- Nadler, D.J., Jaffe, N.S., Clayman, H.M., Jaffe, M.S. and Luscombe, S.M. (1984) Glare disability in eyes with intraocular lenses. *Am. J. Ophthalmol.* 97, 43-47
- Nagy, A.L., Eskew, R.T. and Boynton, R.M. (1987) Analysis of color-matching ellipses in a cone-excitation space. *J. Opt. Soc. Am. A.* 4, 756-768
- van Nes, F.L. and Bouman, M.A. (1967) Spatial modulation transfer in the human eye. *J. Opt. Soc. Am.* 57, 401-406
- Neumann, A., McCarty, G., Steedle, T. (1988) The relationship between cataract type and glare disability as measured by the Miller-Nadler glare tester. *J. Cataract Refract Surg.* 14, 40-45
- Occhipinti, J.R., Mosier, M.A. and Burstein, N.L. (1986) Autofluorescence and light transmission in the aging crystalline lens. *Ophthalmologica* 192, 203-209
- Olsen, T. (1982) Light scattering from the human cornea. *Invest. Ophthalmol.* 23, 81-86
- Olzat, L. and Thomas, J.P. (1981) Why frequency discrimination is sometimes better than detection. *J. Opt. Soc. Am.* 71, 64-70
- Ortwerth, B.J. and Olesen, P.R. (1994) UVA photolysis using the protein-bound sensitizers present in human lenses. *Photochemistry and Photobiology* 60, 53-60

- Pau, M. (1955) Die doppelbrechung van sklera und cornea. *Klin. Monatsbl. Augenheilkd.* 131, 610-615
- Pau, H., Degen, J. and Hans-Herbert, S. (1993) Different regional changes of fluorescence spectra of clear human lenses and nuclear cataracts. *Graefe's Arch. Clin. Exp. Ophthalmol.* 231, 656-661.
- Paulsson, L.E. and Sjöstrand, J. (1980) Contrast sensitivity in the presence of a glare light. *Invest. Ophthalmol.* 19, 401-406
- Pfaff, D.S. and Werner, J.S. (1994) Effect on cataract surgery on contrast sensitivity and glare in patients with 20/50 or better Snellen acuity. *J. cataract Refract. Surg.* 20, 620-625
- Philipson, B. (1973) Changes in the lens related to the reduction of transparency. *Exp. Eye Res.* 16, 29-39
- Phillips, A.F. and McDonnell, P.J. (1994) Laser-induced fluorescence spectra of rabbit and human cornea. *Invest. Ophthalmol. Vis. Sci. (Suppl.)* 35, 2011
- Pitts, D.G. (1990) Ultraviolet absorbing spectacle lenses contact lenses and intraocular lenses. *Optom. Vis. Sci.* 67, 435-440
- Polse, K.A., Brand, R.J., Cohen, S.R. and Gullon, M. (1990) Hypoxic effects on corneal morphology and function. *Invest. Ophthalmol. Vis. Sci.* 31, 1542-1554
- Porkorny, J., Smith, V.C. and Lutze, M. (1989) Heterochromatic modulation photometry. *J. Opt. Soc. Am. A6*, 1618-1623
- Reeves, B.C., Wood, J.M. and Hill, A.R. (1991) Vistech VCTS 6500 charts - within- and between-session reliability. *Optom. Vis. Sci.* 68, 728-737
- Regan, D., Giaschi, D.E. and Fresco, B.B. (1993) Measurement of glare sensitivity in cataract patients using low-contrast letter charts. *Ophthalm. Physiol. Opt.* 13, 115-123
- Remole, A. (1981) Effect of saline solution immersion on corneal scattering characteristics. *Am. J. Optom. Phys. Opt.* 58, 435-444

- Rieger, G. (1992) Improvement of contrast sensitivity with yellow filter glasses. *Can. J. Ophthalmol.* 27, 137-138
- Robson, J.G. (1966) Spatial and temporal contrast sensitivity functions of the visual system. *J. Opt. Soc. Am.* 56, 1141-1142
- Rosenberg, R. (1984) Light, Glare and Contrast in Low Vision Care. In *Clinical Low Vision 2nd Edition* p 197-212, Faye, E.E. (Ed.) Little Brown & Co., Boston, USA
- Rosenthal, F.S., Safran, M. and Taylor, H.R. (1985) The ocular dose of ultraviolet radiation from sunlight exposure. *Photochemistry and Photobiology*, 42,163-171
- Rovamo, J. and Virsu, V. (1979) An estimation and application of the human cortical magnification factors. *Exp. Brain Res.* 37, 495-510
- Rovamo, J., Virsu, V. and Nasenen, R. (1978) Cortical magnification factor predicts the photopic contrast sensitivity. *Nature* 271, 54-56
- Ruddock, K.H. (1965) The effect of age upon colour vision. II. Changes with age in light transmission of the ocular media. *Vision Res.* 5, 47-58
- Rubin, G.S. Adamsons, I.A. and Stark, W.J. (1993) Comparison of acuity, contrast sensitivity and disability glare before and after cataract surgery. *Arch. Ophthalmol.* 111, 56-61
- Rutkowsky, W.F. (1987) Light filtering lenses as an alternative to cataract surgery. *J. Am. Optom. Assoc.* 58, 640-641
- Said, F.S. and Weale, R.A. (1959) The variation with age of the spectral transmissivity of the living human crystalline lens. *Gerontologia* 3, 213-231
- Sanders, B. and Larsen, M. (1994) Photochemical bleaching of fluorescent glycosylation products. *International Ophthalmology* 18, 195-198
- Satoh, K., Brando, M. and Nakajima, A. (1973) Fluorescence in human lens. *Exp. Eye Res.* 16, 167-172

- Savage, G.L., Haegerstrom-Portnoy, G., Adams, A.J. and Hewlett, S.E. (1993) Age-changes in the optical-density of human ocular media. *Clinical Vision Sciences* 8, 97-108
- Savoy, R.L. and McCann, J.J. (1975) Visibility of low-spatial-frequency sine wave targets: Dependence on number of cycles. *J. Opt. Soc. Am.* 65, 343-350
- Schade, O.H. (1956) Optical and photoelectric analog of the eye. *J. Opt. Soc. Am.* 46, 721-739
- Scheffrin, B.E., Werner, J.S., Plach, M., Utlaut, N. and Switkes, E. (1992) Sites of age-related sensitivity loss in a short-wave cone pathway. *J. Opt. Soc. Am. A.* 9, 355-363
- Sen, A.C., Veno, N. and Chakrabarti, B. (1992) Studies on human lens. 1 Origin and development of fluorescent pigments. *Photochemistry and Photobiology* 55, 753-764
- Sigelman, J., Trokel, S.L. and Spector, A. (1974) Quantitative biomicroscopy of lens light back scatter: Changes in aging and opacification. *Arch Ophthalmol.* 92, 437-442
- Siik, S., Airaksinen, P.J. and Tuulonen, A. (1992) Light scatter in aging and cataractous human lens. *Acta. Ophthalmol.* 70, 383-388
- Siik, S., Airaksinen, P.J., Tuulonen, A. and Nieminen, H. (1993) Autofluorescence in cataractous human lens and its relationship to light scatter. *Acta Ophthalmol.* 71, 388-392
- Simpson, G.C. (1953) Ocular haloes and coronas. *Br. J. Ophthalmol.* 37, 450-486
- Sjöstrand, J. (1978) Contrast sensitivity in amblyopia; a preliminary report. *Metabol. Ophthalmol.* 2, 135-137
- Skalka, H. (1981) Arden grating test in evaluating "early" posterior subcapsular cataracts. *South Med. J.* 74, 1368-1370
- Sliney, D.H. (1983) Eye protective techniques for bright light. *Ophthalmology* 90, 937-944
- Smith, P., Pratzler, K., Webster, N. and Miller, D. (1987) A clinical comparison of two methods of glare testing. *Ophthalmic Surg.* 18, 680-682

- Sparrow, J.M., Bron, A.J., Phelps Brown, N.A., Aycliffe, W. and Hill, A.R. (1986) The Oxford clinical cataract classification and grading system. *International Ophthalmology* 9, 207-225
- Sparrow, J.M., Bron, A.J. Phelps Brown, N.A. and Neil, H.A.W. (1992) Autofluorescence of the crystalline lens in early and late onset diabetes. *Br. J. Ophthalmol.* 76, 25-31
- Spector, A., Roy, D. and Stauffer, J. (1975) Isolation and characterization of an age-dependent polypeptide from human lens with non-tryptophan fluorescence. *Exp. Eye Res.* 21, 9-24
- Sperling, G. (1964) Linear theory and the psychophysics of flicker. *Proc. Symp. Physiology of flicker. Doc. Ophthalmol.* 18, 3-15
- Stevenson, R., Vaja, N. and Jackson, J. (1983) Corneal transparency changes resulting from osmotic stress. *Ophthalm. Physiol. Opt.* 3, 33-39
- Stiles, W.S. (1929a) The effect of glare on the brightness difference threshold. *Proceedings of the Royal Society* 104B, 322-355
- Stiles, W.S. (1929b) The scattering theory of the effect of glare on the brightness difference threshold. *Proc. Roy. Soc.* 105, 131-141
- Stiles, W.S. and Crawford, B.H. (1937) The effect of glaring light source on extrafoveal vision. *Proceedings of the Royal Society* 122B, 255-280
- Stocker, F.W. and Moore, L.W. (1975) Detecting changes in the cornea that come with age. *Geriatrics* 30, 57-69
- Strong, N.P., Hess, R.F. and Losada, M.A. (1992) Quantifying the effect of intraocular light scatter in posterior subcapsular cataract. *Invest. Ophthalmol. Vis. Sci. (Suppl.)* 33, 965
- Sunderraj, P., Villada, J.R., Joyce, P.W. and Watson, A. (1992) Glare testing in pseudophakes with posterior capsule opacification. *Eye* 6, 411-413

- Thibos, L.N., Bradley, A., Still, D.L., Zhang, X. and Howarth, P.A. (1990) Theory and measurement of ocular chromatic aberration. *Vision Res.* 30, 33-49
- Thomas, J. (1978) Normal and amblyopic contrast sensitivity functions in central and peripheral retinas. *Invest. Ophthalmol.* 17, 746-753
- Trokel, S.L. (1962) The physical basis for transparency of the crystalline lens. *Invest. Ophthalmol.* 1, 493-501
- Tupper, B., Miller, D. and Miller, R. (1985) The effect of a 550nm cutoff filter on the vision of cataract patients. *Ann. Ophthalmol.* 17, 67-72
- Twersky, V. (1975) Transparency of pair correlated, random distributions of small scatterers, with applications to the cornea. *J. Opt. Soc. Am.* 65, 524-530
- Verriest, G.J. (1963) Further studies on acquired deficiency of color discrimination. *J. Opt. Soc. Am.* 53, 183-195
- Vinciguerra, M.J. and Bettelheim, F.A. (1971) Packing and orientation of fiber cells. *Exp. Eye Res.* 11, 214-219
- Vos, J.J. (1962) On mechanisms of glare. Institute for perception RVO-TNO, Soesterberg, Netherlands
- Vos, J.J. (1984) Disability glare - a state of the art report. *Commission International de l'Eclairage Journal* 3, 39-53
- Vos, J.J. and Boogard, J. (1963) Contributions of the cornea to entopic scatter. *J. Opt. Soc. Am.* 53, 864-873
- Vos, J.J. and Bouman, M.A. (1964) Contribution of the retina to entopic scatter. *J. Opt. Soc. Am.* 54, 95-100
- Vos, J.J., Walraven, J. and van Meeteren, A. (1976) Light profiles of the foveal image of a point source. *Vision Res.* 16, 215-219
- de Waard, P.W.T., IJspeert, J.K., van den Berg, T.J.T.P. and de Jong, P.T.V.M. (1992) Intraocular light scattering in age-related cataracts. *Invest. Ophthalmol. Vis. Sci.* 33, 618-625

- Wald, G. (1952) Alleged effects of the near ultraviolet on human vision. *J. Opt. Soc. Am.* 42, 171-177
- Walls, G.L. and Judd, H.D. (1933) Intra-ocular colour filters of vertebrates. *Br. J. Ophthalmol.* 17, 641-705
- Walraven, J. (1973) Spatial characteristics of chromatic induction. *Vision Res.* 13, 1739-1753
- Watson, A.B. and Robson, J.G. (1981) Discrimination at threshold: Labelled detectors in human vision. *Vision Res.* 15, 115-1122
- Weale, R.A. (1982) *A biography of the eye.* Lewis, H.K. and Co. Ltd, London, UK.
- Weale, R.A. (1985) Human lenticular fluorescence and transmissivity, and their effects on vision. *Exp. Eye Res.* 41, 457-473
- Weale, R.A. (1987) Age and the transmittance of the human crystalline lens. *J. Physiol.* 395, 577-587
- Weale, R.A. (1988) Age and the transmittance of the human crystalline lens. *J. Physiol. (Lond.)* 395, 577-587
- Weale, R.A. (1991) The lenticular nucleus, light and the retina. *Exp. Eye Res.* 53, 213-218
- Weatherill, J. and Yap, M. (1986) Contrast sensitivity in pseudophakia and aphakia. *Ophthalm. Physiol. Optics* 6, 297-301
- Webster, M.A., De Valois, K.K. and Switkes, E. (1990) Orientation and spatial frequency discrimination for luminance and chromatic gratings. *J. Opt. Soc. Am.* A7, 1034-1049
- Wellsknecht, M.C., Huggins, T.G., Dyer, D.G., Thorpe, S.R. and Baynes, J.W. (1993) Oxidized amino-acids in lens protein with age - measurement of O-tyrosine and ditryosine in the aging human lens. *J. Biological Chemistry.* 268, 12348-12352

- Werner, J.S. and Steele, V.G. (1988) Sensitivity of human foveal color mechanisms throughout the life span. *J. Opt. Soc. Am. A.* 5, 2122-2130.
- Wesemann, W. (1987) Incoherent image formation in the presence of scattering eye media. *J. Opt. Soc. Am. A.* 4, 1439-1447
- Westheimer, G. (1964) Pupil size and visual resolution. *Vision Res.* 4, 39-45
- Westheimer, G. (1979) The spatial sense of the eye. *Invest. Ophthalmol. Vis. Sci.* 18, 893-912
- Wiegand, W., Thaer, A.A., Kroll, P. Geyer, O.C. and Garcia, A.J. (1995) Optical sectioning of the cornea with a new confocal in-vivo slit-scanning videomicroscope. *Ophthalmology* 102, 568-575
- Williamson, T.H., Strong, N.P., Sparrow, J., Aggarwal, R.K. and Harrad, R. (1992) Contrast sensitivity and glare in cataract using the Pelli-Robson chart. *Br. J. Ophthalmol.* 76, 719-722
- Wilson, H.R., McFarlane, D.K. and Phillips, G.C. (1983) Spatial frequency tuning of orientation selective units estimated by oblique masking. *Vision Res.* 23, 873-882
- Wolf, E. and Gardiner, J.S. (1965) Studies on the scatter of light in the dioptric media of the eye as a basis of visual glare. *Arch. Ophthalmol.* 74, 338-345
- Wolfe, J.M. (1990) An introduction to contrast sensitivity testing. In *Glare and contrast sensitivity for clinicians*. Nadler, M.P., Miller, D. and Nadler, D.J. (Eds.) Springer-Verlag, New York, USA
- Wolfe, J.M. (1992) A new psychophysical method to assess ocular light scatter. In: *Noninvasive Assessment of the Visual System Technical Digest*. Washington DC: Optical Society of America 1, 175-178
- Wooten, B.R. and Geri, G.A. (1987) Psychophysical determination of intraocular light scatter as a function of wavelength. *Vision Res.* 27, 1291-1298
- Wyzecki, G. (1956) Theoretical investigation of colored lenses for snow goggles. *J. Opt. Soc. Am.* 46, 1071-1074

- Yager, D., Yuan, R. and Mathews, S. (1992) What is the utility of the psychophysical 'light scattering factor'? *Invest. Ophthalmol. Vis. Sci.* 33, 618-625
- Yap, M. (1982) The effect of a yellow filter on contrast sensitivity. *Ophthalm. Physiol. Opt.* 4, 227-232
- Yappert, M.C., Borchman, D. and Byrdwell, W.C. (1993) Comparison of specific blue and green fluorescence in cataractous versus normal human lens fractions. *Invest. Ophthalmol. Vis. Sci.* 34, 630-636
- Yappert, M.C., Lal, S. and Borchman, D. (1992) Age dependence and distribution of green and blue fluorophores in human lens homogenates. *Invest. Ophthalmol. Vis. Sci.* 33, 3555-3560
- Yeh, T., Pokorny, J. and Smith, V.C. (1993) Chromatic discrimination with variation in chromaticity and luminance: data and theory. *Vision Res.* 33, 1835-1845
- Yuan, R., Mathews, S. and Yager, D. (1993) Controlling unwanted sources of threshold change in disability glare studies. *Optom. Vis. Sci.* 70, 976-981
- Zaret, M.M., Snyder, W.Z. and Birenbaum, L. (1976) Cataract after exposure to non-ionizing radiant energy. *Br. J. Ophthalmol.* 60, 632-637
- Zemon, V., Gutowski, W. and Horton, T. (1983) Orientational anisotropy in the human visual system: An evoked potential and psychophysical study. *Int. J. Neurosci.* 19, 259-286
- Zigman, S. (1971) Eye lens colour formation and function. *Science* 171, 807-809
- Zigman S. (1985) Photobiology of the lens. In *The ocular lens*. pp301-347, Maisel, H. (Ed.) Marcel Dekker, New York, USA.
- Zigman, S. (1990) Vision enhancement using a short wavelength light-absorbing filter. *Optom. Vis. Sci.* 67, 100-104
- Zigman, S. (1992) Light filters to improve vision. *Optom. Vis. Sci.* 69, 325-328
- Zigman, S., Datiles, M. and Torczynski, E. (1979) Sunlight and human cataracts. *Invest. Ophthalmol.* 18, 462-467

Zigman, S., Groff, J., Yulo, T. and Griess, G. (1976) Light extinction and protein in the lens. *Exp. Eye Res.* 23, 555-567

Zuckerman, J.L., Miller, D., Dyes, W. and Keller, M. (1973) Degradation of vision through a simulated cataract. *Invest. Ophthalmol.* 12, 213-224

Zuclich, J.A., Glickman, R.D. and Menendez, A.R. (1992) In situ measurements of lens fluorescence and its interference with visual function. *Invest. Ophthalmol. Vis. Res.* 33, 410-415

Finlay, D. and Wilkinson, J. (1984) The effects of glare on the contrast sensitivity function. *Human Factors* 24, 283-287

Edgar, F.D., Barbur, J.L. and Woodward, E.G. (1995) Pupil size measurements in relation to light scatter in the eye. *Invest. Ophthalmol. Vis. Sci.* 36, S938

Johnson, F.S., Mo, T. and Green, A.E.S. (1976) Average latitudinal variation in ultraviolet radiation at the earth's surface. *Photochemistry and Photobiology* 23, 170-188

Enoch, J.M. and Lakshminarayanan, V. (1991) Retinal fibre optics. In *Visual optics instrumentation* pp280-309, Charman, W.N. (Ed.), Macmillan Press, London

Berman, S.M., Bullimore, M.A., Jacobs, R.J., Bailey, I.L. and Gandhi, N. (1994) An objective measure of discomfort glare. *J. Illuminating Engineering Soc.* 23, 40-48

Ruddock, K.H. (1972) Light transmission through the ocular media and macular pigment and its significance for psychophysical investigation. In *Handbook of sensory physiology, Vol. VIII/4 Visual Psychophysics*, Jameson, D. and Hurvich, L.M. (Eds.), Springer, Berlin

Werner, J.S., Donnelly, S.K. and Kliegl, R. (1987) Aging and human macular pigment density. Appended with translations from the work of Max Schultze and Ewald Hering. *Vision Res.* 27, 257-268

APPENDICES

1.A. Supporting publications

Steen, R., Whitaker, D. and Wild, J.M. and Elliott, D.B. (1993) Reduction of luminance and colour contrast sensitivity due to disability glare. *Ophthal. Physiol. Opt.* 13, 107

Steen, R., Whitaker, D., Elliott, D.B. and Wild, J.M. (1993) Effect of filters on disability glare. *Ophthal. Physiol. Opt.* 13, 371-376

Steen, R., Whitaker, D., Wild, J.M. and Elliott, D.B. (1993) Effect of filters on disability glare in the presence of wavelength dependent scatter. *Invest. Ophthalmol. Vis. Sci. (Suppl.)* 34, 1414

Steen, R., Whitaker, D., Elliott, D.B. and Wild, J.M. (1994) Age-related effects of glare on luminance and color contrast sensitivity. *Optom. Vis. Sci.* 71, 792-796

Steen, R., Whitaker, D. Elliott, D.B. and Wild, J.M. (1994) Effect of glare on luminance and colour contrast sensitivity as a function of age. *Invest. Ophthalmol. Vis. Sci. (Suppl.)* 35, 1952

Whitaker, D., Steen, R. and Elliott, D.B. (1993) Light scatter in normal young, elderly, and cataractous eye demonstrates little wavelength dependency. *Optom. Vis. Sci.* 70, 963-968

Whitaker, D., Elliott, D.B. and Steen, R. (1994) Confirmation of the validity of the psychophysical light scattering factor. *Invest. Ophthalmol. Vis. Sci.* 35, 317-321

Whitaker, D., Elliott, D.B. and Steen, R. (1994) Disability glare and straylight: Two sides of the same coin? *Invest. Ophthalmol. Vis. Sci.* 35, 2660-2661

Pages removed for copyright restrictions.